

N⁰ d'ordre...../FS/UMBB/2025

People's Democratic Republic of Algeria
Ministry of Higher Education and Scientific Research
University M'Hamed Bougara of Boumerdes



Faculty of Sciences

Doctoral Thesis

Presented by:

Abdelbaki BENAYAD

Submitted for the Fulfilment of the Requirements of the
DOCTORAT-LMD degree in

Field: Computer Science

Option: Artificial intelligence and its applications

Use of Artificial Intelligence (AI) methods for improving visible light communications in modern wireless networks

In front of a jury composed of:

Pr. Dalila ACHELI	Professor	UMBB	President
Pr. Yassine MERAIHI	Professor	UMBB	Supervisor
Dr. Amel BOUSTIL	MCA	UMBB	Co-Supervisor
Pr. Mohamed Amine RIAHLA	Professor	UMBB	Examiner
Dr. Saida ISHAK BOUSHAKI	MCA	UMBB	Examiner
Pr. Abdelfettah HENTOUT	Professor	ENSTA Alger	Examiner

Academic Year: 2024/2025

ACKNOWLEDGEMENTS

I would like to express my sincere and heartfelt gratitude to my thesis advisor, Professor Yassine Meraihi, for his invaluable guidance, unwavering support, and continuous encouragement throughout this research journey. His profound expertise and insightful feedback have been instrumental in shaping both the direction and the outcome of this work. I deeply appreciate his time, dedication, and constructive suggestions, all of which have significantly enhanced the quality of my thesis. This research would not have been possible without his mentorship and support.

I am also profoundly grateful to Dr. Boustil, whose constant support and encouragement have been a driving force throughout my academic journey. Her invaluable advice and insightful perspectives have played a crucial role in my growth as a researcher. I sincerely appreciate her mentorship, which has provided me with numerous opportunities for both personal and professional development.

With deep appreciation and gratitude, I dedicate this work to Dr. Yahia salma, Dr. Makhmoukh Sylia, Dr. Refas Ikram, Dr. Ait Saadi Amylia, and Dr. El-Taani Rachda. Your unwavering support, insightful guidance, and continuous encouragement have been an invaluable source of strength throughout my academic journey. Your dedication to research and your passion for knowledge have inspired me in countless ways. I am truly fortunate to have had the opportunity to work alongside such brilliant and supportive colleagues. This thesis is a testament to the collaborative spirit, intellectual growth, and friendship that we have shared. Thank you for your encouragement, your belief in my abilities, and the countless moments of motivation that have made this journey meaningful.

I am also sincerely thankful to the esteemed members of my thesis committee: Professor Mohamed Amine Riahla, Professor Dalila Acheli, Dr. Saida Ishak Boushaki, and Professor Abdelfettah Hentout, for their valuable time, constructive feedback, and insightful suggestions. Their contributions have significantly enriched the depth and quality of my research.

My deepest appreciation goes to my parents for their unconditional love, unwavering support, and constant encouragement, which have been my greatest source of motivation and inspiration. Their belief in me has been the foundation of my perseverance. I am equally grateful to my brothers for their steadfast support and encouragement.

Finally, I extend my heartfelt thanks to my colleagues and friends for their support, companionship, and motivation throughout my studies. Their presence has made this journey not only fulfilling but also truly meaningful.

Visible Light Communication (VLC) has emerged as a promising wireless technology that utilizes Light Emitting Diodes (LEDs) for simultaneous illumination and high-speed data transmission. Compared to traditional Radio Frequency (RF) systems, VLC offers advantages such as higher data rates, enhanced security, and reduced electromagnetic interference. However, optimal LED placement remains a significant challenge, as it directly impacts coverage, data throughput, and energy efficiency. Given the NP-hard nature of this problem, conventional optimization methods are computationally infeasible for large-scale deployments.

This research focuses on developing and enhancing meta-heuristic optimization algorithms to efficiently address the LED placement challenge in VLC networks. We propose and evaluate three advanced techniques: Enhanced Whale Optimization Algorithm (EWOA), Hybrid Coronavirus Herd Immunity Optimize with Firefly Algorithm (ICHIO-FA), and a Multi-Objective Puma Optimizer (MOPO). These approaches integrate chaotic maps, Opposition-Based Learning (OBL), non-dominated sorting, and crowding distance mechanisms to improve search efficiency, convergence speed, and solution quality.

Extensive benchmarking against state-of-the-art meta-heuristics demonstrates that our proposed methods significantly outperform existing algorithms in solution quality, robustness, and computational efficiency. The findings of this research contribute to advancing optimization techniques in VLC systems, providing scalable and efficient solutions, to deployment in next-generation communication networks.

Keywords: Visible light communication (VLC); Light emitting diode (LED); Optimization methods; meta-heuristic.

La communication par lumière visible (VLC) est une technologie sans fil prometteuse qui exploite les diodes électroluminescentes (LEDs) pour assurer simultanément éclairage et la transmission de données à haute vitesse. Comparée aux systèmes traditionnels à radiofréquence (RF), la VLC offre plusieurs avantages, notamment des débits de transmission plus élevés, une sécurité renforcée et une réduction des interférences électromagnétiques. Cependant, le placement optimal des LEDs demeure un défi majeur, influençant directement la couverture, le débit de transmission et l'efficacité énergétique. Étant donné la complexité NP-difficile de ce problème, les méthodes d'optimisation classiques deviennent inapplicables pour les déploiements à grande échelle.

Cette recherche vise à développer et améliorer des algorithmes d'optimisation méta-heuristiques pour résoudre efficacement le problème de placement des LEDs dans les réseaux VLC. Nous proposons et évaluons trois techniques avancées : Enhanced Whale Optimization Algorithm (EWOA), Hybrid Coronavirus Herd Immunity Optimizer avec Firefly Algorithm (ICHIO-FA), et un Optimiseur Puma Multi-Objectif (MOPO). Ces approches intègrent des mécanismes tels que les cartes chaotiques, l'apprentissage par opposition (OBL), le tri non-dominé et la distance de encombrement, afin d'améliorer l'efficacité de la recherche, la vitesse de convergence et la qualité des solutions.

Une évaluation approfondie par rapport aux méta-heuristiques de pointe montre que nos méthodes surpassent significativement les algorithmes existants en termes de qualité des solutions, robustesse et efficacité computationnelle. Les résultats de cette recherche contribuent à l'avancement des techniques d'optimisation dans les systèmes VLC, offrant des solutions scalables et performantes pour les déploiements réels et les réseaux de communication de nouvelle génération.

Mots clés: Communication par lumière visible (VLC); Diode électroluminescente (LED); les méthodes d'optimization; les méta-heuristique.

برزت الاتصالات بالضوء المرئي (VLC) كإحدى التقنيات اللاسلكية الواعدة، حيث تعتمد على الصمامات الثنائية الباعثة للضوء (LEDs) لتوفير الإضاءة ونقل البيانات عالية السرعة في آن واحد. وبالمقارنة مع أنظمة الترددات الراديوية (RF) التقليدية، توفر تقنية VLC مزايا متعددة مثل معدلات نقل بيانات أعلى، وأمان محسن، وتقليل التداخل الكهرومغناطيسي. ومع ذلك، لا يزال التحديد الأمثل لمواقع الـ LEDs يشكل تحديًا كبيرًا، نظرًا لتأثيره المباشر على نطاق التغطية، ومعدل نقل البيانات، وكفاءة استهلاك الطاقة. وبالنظر إلى أن هذه المشكلة تُصنف ضمن فئة المشكلات المعقدة من نوع NP-Hard، فإن طرق التحسين التقليدية غير عملية من الناحية الحسابية عند التعامل مع أنظمة واسعة النطاق.

تركز هذه الدراسة على تطوير وتحسين خوارزميات التحسين الميتا-إرشادية لمعالجة تحدي توزيع الـ LEDs في شبكات VLC بكفاءة. نقترح ونقيّم ثلاث تقنيات متقدمة هي: خوارزمية تحسين الحوت المحسنة (EWOA)، الخوارزمية الهجينة لمناعة القطيع للفيروس التاجي مع خوارزمية اليراعات (ICHIO-FA)، وخوارزمية بوما متعددة الأهداف (MOPO). تدمج هذه الخوارزميات عناصر مثل الخرائط الفوضوية، والتعلم القائم على المعارضة (OBL)، وفرز الحلول غير المهيمن عليها، وآليات مسافة التزاح بهدف تحسين كفاءة البحث، وسرعة التقارب، وجودة الحلول.

أظهرت تجارب مقارنة موسّعة مع أحدث الخوارزميات الميتا-إرشادية أن الأساليب المقترحة تتفوق بشكل كبير على الخوارزميات الموجودة من حيث جودة الحلول، والموثوقية، والكفاءة الحسابية. وتُساهم نتائج هذا البحث في تطوير تقنيات التحسين في أنظمة VLC، مما يوفر حلولاً قابلة للتوسعة وفعالة لنشرها في شبكات الاتصال من الجيل القادم.

الكلمات المفتاحية: الاتصالات بالضوء المرئي (VLC)؛ الصمامات الثنائية الباعثة للضوء (LED)؛ أساليب التحسين؛ الخوارزميات الميتا-إرشادية.

General Introduction		17
1 State of the art in visible light communication		20
1.1	Introduction	20
1.2	VLC History	21
1.3	What is VLC technology ?	23
1.4	VLC Architecture	25
1.4.1	VLC Communication Layers	26
1.4.1.1	The MAC Layer (Medium Access Control)	26
1.4.1.1.1	Role of the MAC Layer:	27
1.4.1.1.2	Services from the MAC Layer to Upper Layers:	27
1.4.1.1.3	Services from the Physical Layer to the MAC Layer:	27
1.4.1.2	Physical Layer (PHY)	27
1.4.1.2.1	PHY I (Outdoor)	28
1.4.1.2.2	PHY II (Indoor)	28
1.4.1.2.3	PHY III (Multiple Optical Transceivers)	28
1.4.2	The IEEE 802.15.7 Standard for VLC	29
1.5	Modulation Techniques in VLC	29
1.5.1	Intensity Modulation (IM)	29
1.5.2	Amplitude Shift Keying (ASK)	29
1.5.3	Frequency Shift Keying (FSK)	30
1.5.4	Phase Shift Keying (PSK)	30
1.5.5	On-Off Keying (OOK)	31
1.5.6	Pulse Width Modulation (PWM)	31
1.5.7	Orthogonal Frequency Division Multiplexing (OFDM)	31
1.6	Balancing Advantages and Challenges of VLC	32
1.6.1	Advantages of VLC	32

1.6.2	Challenges and Limitations of VLC	33
1.7	VLC Applications	34
1.7.1	Indoor Applications	34
1.7.2	Outdoor Applications	35
1.8	Conclusion	37
2	Optimization algorithms	39
2.1	Introduction	39
2.2	Optimization Problem	40
2.2.1	Objective Function	40
2.3	Classification of Optimization Problems	41
2.3.1	Classification Based on Decision Variable Type	41
2.3.1.1	Quantitative Variables	41
2.3.1.2	Qualitative Variables	42
2.3.1.3	Mixed Variables	42
2.3.2	Classification Based on the Number of Objectives	43
2.3.2.1	Single-Objective Optimization	43
2.3.2.2	Multi-Objective Optimization	43
2.3.3	Classification Based on Constraints	43
2.3.3.1	Unconstrained Optimization	43
2.3.3.2	Constrained Optimization	43
2.3.4	Classification Based on Computational Complexity	44
2.3.4.1	P Problems	44
2.3.4.2	NP Problems	44
2.3.4.3	NP-Hard Problems	44
2.3.4.4	NP-Complete Problems	44
2.4	Main methods for tackling optimization Problems	44
2.4.1	Enumerative Methods	46
2.4.2	Deterministic Methods	46
2.4.3	Stochastic Methods	47
2.5	Optimization Problem Algorithms	47
2.5.1	Classical Algorithms (Exact Approaches)	47
2.5.2	Artificial Intelligence Algorithms	50
2.5.2.1	Heuristic Algorithms	50
2.5.2.2	Meta-Heuristic Algorithms	50
2.6	Multi-Objective Optimization Problems (MOPs)	53
2.6.1	Objective function space	53
2.6.2	Pareto-Optimality in MOPs	54
2.6.3	Characteristics of Pareto Fronts	55

2.6.4	Essential Aspects of Multi-Objective Optimization	55
2.7	Key Approaches to Multi-Objective Problems	56
2.7.1	No Preference Methods	56
2.7.1.1	Global Criterion Method	56
2.7.2	A Priori Preference Methods	57
2.7.2.1	Lexicographic Method	57
2.7.2.2	Goal Programming	57
2.7.3	Interactive Preference Methods	57
2.7.4	A Posteriori Preference Methods	57
2.7.4.1	Weighting Method	58
2.7.4.2	ϵ -Constraint Method	58
2.7.4.3	Normal Boundary Intersection (NBI)	58
2.7.4.4	TOPSIS	58
2.8	Multi-Objective Optimization Algorithms	59
2.8.1	Evolutionary Algorithms	59
2.8.2	Swarm-Based Algorithms	59
2.8.3	Trajectory-Based Algorithms	60
2.8.4	Immune-Inspired Algorithms	60
2.8.5	Nature-Inspired Algorithms	60
2.8.6	Deterministic Approaches	60
2.9	Conclusion	61
3	An improved approach for solving the LEDs Placement Problem in In-	
	door VLC System	64
3.1	Introduction	64
3.2	LEDs Placement Problem in Indoor VLC System	65
3.2.1	System Model	65
3.2.1.1	Channel Model	66
3.2.2	Mathematical Model	68
3.2.2.1	The objective function Formulation	68
3.3	PRELIMINARIES	68
3.3.1	Whale Optimizer Algorithm (WOA)	68
3.3.1.1	Encircling Prey	69
3.3.1.2	Bubble-Net Attacking Mechanism	69
3.3.1.3	Search for Prey	70
3.3.1.4	Whale Optimizer Algorithm Pseudocode	70
3.3.2	Chaotic Map	70
3.3.3	Opposition-Based Learning	72
3.4	The Proposed EWOA for Solving the LEDs Placement Problem	73

3.4.1	Simulation Results	76
3.4.2	Discussion and Analysis	76
3.5	Conclusion	77
4	A hybrid approach for solving the LEDs Placement Problem in Indoor VLC System	79
4.1	Introduction	79
4.1.1	Coronavirus Herd Immunity Optimizer (CHIO)	80
4.1.1.1	CHIO Algorithm Pseudocode	82
4.1.2	Firefly Optimization Algorithm (FA)	82
4.1.2.1	Initialization	84
4.1.2.2	Attractiveness and Movement Mechanism	84
4.1.2.3	Position Update Mechanism	85
4.2	Hybrid Coronavirus Herd Immunity Optimizer (ICHIO-FA)	86
4.2.1	The Proposed ICHIO-FA Algorithm for Solving the LEDs Placement Problem	86
4.2.2	Simulation Results and Analysis	90
4.2.2.1	Impact of the Control Parameter λ	90
4.2.2.2	Impact of Varying the Number of LEDs	92
4.2.2.3	Impact of Varying the Number of Users	94
4.2.2.4	Impact of Varying the Area of Photo detectors (PDs)	95
4.2.3	Statistical Analysis	95
4.2.4	Convergence Analysis	97
4.3	Conclusion	100
5	A Multi-Objective approach for solving the LEDs Placement Problem in Indoor VLC System	111
5.1	Introduction	111
5.2	Puma Optimizer (PO)	113
5.2.1	Mathematical Model	113
5.2.1.1	Phase Selection Mechanism	113
5.2.1.2	Exploration Phase	114
5.2.1.3	Exploitation Phase	114
5.2.2	Algorithm Workflow	114
5.2.3	Computational Complexity Analysis	115
5.3	Mathematical Definition of Multi-Objective Optimization Problems	116
5.3.1	Pareto Dominance	116
5.3.2	Pareto Optimality and Crowding Distance Mechanism	116
5.4	Multi-objective LED's placement problem	117

- 5.5 Multi-Objective Puma Optimizer (MOPO) for solving LEDs Placement in indoor VLC System 117
 - 5.5.1 Implementation procedure of MOPO algorithm 118
 - 5.5.2 Simulation results and performance evaluation 120
- 5.6 Conclusion 122

General Introduction **126**

LIST OF FIGURES

1.1	Fire communication system used in ancient Greece [1].	22
1.2	Alexander Graham Bell's method of transmitting sound using sunlight [2].	22
1.3	Light spectrum wavelength [3].	24
1.4	VLC Architecture diagram [4].	25
1.5	Topologies supported by MAC in the IEEE 802.15.7 standard [5].	27
1.6	MAC frame structure [6].	28
1.7	PHY frame structure [6].	28
1.8	FSK, ASK, and PSK modulation techniques [7].	30
1.9	On-Off Keying modulation [8].	31
1.10	Li-Fi Architecture [9].	34
1.11	Underwater VLC applications [10].	36
1.12	Vehicular VLC (V-VLC) applications [11].	36
1.13	Visible Light Communications Applications [12].	37
2.1	Classification of optimization problems	42
2.2	Classification of optimization problems based on computational complexity.	45
2.3	Classification of Optimization Algorithms	48
2.4	Regions of a design problem with two-variable and two objective functions [13]	54
2.5	Non-dominated solutions and True Pareto front [13]	55
3.1	Indoor VLC Room Model	66
3.2	Channel model of visible light transmission	67
3.3	Chaotic value distributions over 200 iterations	72
3.4	The point Pmo and its corresponding opposite in a one-dimensional search space.	72
3.5	Illustration of the point Pmo and its opposite in a two-dimensional search space.	73
3.6	Flowchart of EWOA	75

3.7	Coverage (a), Throughput (b) and Fitness (c) under various numbers of LEDs	77
3.8	Coverage (a), Throughput (b) and Fitness (c) under various numbers of Users	78
4.1	Flowchart of ICHO-FA	89
4.2	Coverage, Throughput and Fitness under various values of Lambda	91
4.3	Coverage (a), Throughput (b) and Fitness (c) under various numbers of LEDs	93
4.4	Coverage (a), Throughput (b) and Fitness (c) under various number of Users	94
4.5	Coverage (a), Throughput (b) and Fitness (c) under various values of Photo-Detector Area	96
4.6	Scenario 1	99
4.7	Scenario 2	99
4.8	The convergence analysis according the fitness value and number of iteration under different scenarios	99
5.1	Flowchart of MOPO	121
5.2	100 iterations	124
5.3	200 iterations	124
5.4	300 iterations	124
5.5	400 iterations	124
5.6	500 iterations	124
5.7	600 iterations	124
5.8	Pareto fronts obtained by the proposed MOPO compared with NSGA-II, MOWOA and the True PF under different iterations.	124
5.9	700 iterations	125
5.10	800 iterations	125
5.11	900 iterations	125
5.12	1000 iterations	125
5.13	Pareto fronts obtained by the proposed MOPO compared with NSGA-II, MOWOA and the True PF under different iterations.	125

LIST OF TABLES

2.1	Classical Optimization Algorithms	49
2.2	Heuristic Algorithms	50
2.3	Single-Solution-Based Meta-Heuristics	51
2.4	Population-Based Meta-Heuristic Algorithms	52
2.5	Classification of MOO Approaches Based on Preference Timing	58
2.6	Multi-Objective Optimization Algorithms	62
2.7	Multi-Objective Optimization Algorithms	63
2.8	Comparison of Multi-Objective Optimization Algorithms	63
3.1	Coverage, mean throughput, and fitness under various values of number of LEDs and Users	76
4.5	Simulation parameters of VLC System	92
4.1	The main notations used in this paper	101
4.2	Parameter values of the algorithms considered in our simulations	102
4.3	Scenarios settings	103
4.4	Coverage, mean throughput, and fitness under various values of the parameter λ and the Area of the Photo-Detector	103
4.6	Coverage, mean throughput, and fitness under various values of number of LEDs and Users	104
4.7	Convergence analyses scenarios	104
4.8	The Friedman test of the Coverage under parameter various of number of LEDs	104
4.9	The Friedman test of the Mean Throughput under parameter various of number of LEDs	104
4.10	The Friedman test of the Fitness value under parameter various of number of LEDs	105

4.11	The Friedman test of the Coverage under parameter various of number of users	105
4.12	The Friedman test of the Mean Throughput under parameter various of number of users	105
4.13	The Friedman test of The Fitness Value under parameter various of number of users	105
4.14	The Friedman test of the Coverage under various of Lambda	105
4.15	The Friedman test of the Mean Throughput under parameter various of Lambda	106
4.16	The Friedman test of Fitness value under parameter various of Lambda	106
4.17	The Friedman test of the Coverage under parameter various of Area of the Photo-Detector A	106
4.18	The Friedman test of the Mean Throughput per under parameter various of Area of the Photo-Detector A	106
4.19	The Friedman test of the Fitness value under parameter various of Area of the Photo-Detector A	106
4.20	The Post-Hoc test of the Coverage for each algorithm under various values of Lambda	107
4.21	The Post-Hoc test of the Throughput for each algorithm under various values of Lambda	107
4.22	The Post-Hoc test of the Fitness for each algorithm under various values of Lambda	107
4.23	The Post-Hoc test of the Coverage for each algorithm under various numbers of LEDs	108
4.24	The Post-Hoc test of the Throughput for each algorithm under various numbers of LEDs	108
4.25	The Post-Hoc test of the Fitness value for each algorithm under various numbers of LEDs	108
4.26	The Post-Hoc test of the Coverage for each algorithm under various number of Users	109
4.27	The Post-Hoc test of the Throughput for each algorithm under various number of Users	109
4.28	The Post-Hoc test of the Fitness value for each algorithm under various number of Users	109
4.29	The Post-Hoc test of the Coverage for each algorithm under various of photo-detector Area	110
4.30	The Post-Hoc test of the Throughput for each algorithm under various of photo-detector Area	110

4.31 The Post-Hoc test of the Fitness value for each algorithm under various of
photo-detector Area 110

Wireless communication technologies are fundamental to modern society, driving progress in telecommunications, transportation, and healthcare [14]. Their widespread adoption enables seamless access to information, improved productivity, and increased convenience [15].

Most existing wireless systems rely on radio frequency (RF) technology for data transmission. However, the growing demand for bandwidth driven by broadband services such as mobile video, high-speed internet, and video conferencing has led to increased congestion in the RF spectrum. According to the International Telecommunication Union (ITU), more than 4.5 billion people used the internet in 2019 [16], intensifying pressure on available RF resources and raising concerns about their ability to meet future communication needs. These limitations have encouraged the exploration of alternative wireless technologies, including optical wireless communication (OWC).

OWC, which uses visible or infrared light to transmit data through free space, has emerged as a promising complement to RF-based systems [17]. It offers advantages such as higher data rates, increased security, and immunity to electromagnetic interference. OWC is suitable for a wide range of applications, including satellite communication, high-speed data transfer, mobile connectivity, and the Internet of Things (IoT).

A prominent subset of OWC is visible light communication (VLC), which operates in the visible spectrum (380 THz–790 THz) [18]. VLC transmits data by modulating the intensity of light-emitting diodes (LEDs), enabling simultaneous illumination and communication [19, 20]. LEDs are energy-efficient, long-lasting, and capable of rapid switching [21, 22], making them well-suited for VLC. Due to its low power consumption, high security, and resistance to RF interference, VLC is especially useful in environments where RF communication is limited or undesirable. It can be seamlessly integrated into existing lighting infrastructure for use in indoor networking [23], automotive and aerospace systems [24, 25], healthcare environments [26], and underwater communication [27].

A typical VLC system consists of LEDs serving as transmitters and photodetectors

(PDs) acting as receivers. One of the key technical challenges is determining the optimal placement of LEDs to maximize system performance. This problem is computationally complex and classified as NP-hard [28]. To address it, researchers have employed meta-heuristic optimization algorithms to find efficient solutions for LED deployment while meeting illumination and communication requirements.

Numerous meta-heuristic algorithms including evolutionary algorithms (EA), particle swarm optimization (PSO), and hybrid methods have been proposed to tackle this problem. Ding et al. [29] used an EA to optimize LED placement in a $5\text{ m} \times 5\text{ m} \times 3\text{ m}$ room, successfully reducing signal loss. Wang et al. [30] extended this work by optimizing for maximum signal-to-noise ratio (SNR). Sharma et al. [31] proposed HypEA, which outperformed PSO. Stefan and Haas [32] used a genetic algorithm (GA) in a $2.5\text{ m} \times 5\text{ m} \times 3\text{ m}$ space, improving area spectral efficiency.

Other studies explored PSO-based strategies to minimize signal outage [33], hybrid SA-PSO algorithms for improved positioning accuracy [34], and enhanced Cuckoo Search algorithms [35, 36]. The Whale Optimization Algorithm (WOA) has also shown promise; Kumawat et al. [28] applied it for optimizing LED panels, and Meng et al. [37] improved it using elite opposition-based learning and Lévy flight, resulting in IWOA.

Additional contributions include the Modified Artificial Fish Swarm Algorithm (MAFSA), which achieved high precision in a $4\text{ m} \times 4\text{ m} \times 6\text{ m}$ room [38], and the Manta Rays Foraging Optimization (MRFO) algorithm, which outperformed several state-of-the-art methods [39]. Multi-objective optimization has also been explored; for example, Costa et al. [40] used NSGA-II to balance transmitted power and spectral efficiency.

While many existing studies have applied meta-heuristic algorithms to optimize specific performance metrics such as maximizing the signal-to-noise ratio (SNR), minimizing positioning error, or reducing power consumption, these approaches typically focus on single-objective formulations and simplified scenarios. Most of the current work targets only one aspect of system performance, such as SNR, received power, accuracy, or error rates. In contrast, our research addresses a more complex and practical scenario: optimizing the placement of multiple LEDs to serve multiple users in an indoor VLC environment. We aim to jointly optimize both user coverage and throughput, providing a more comprehensive solution that accounts for spatial distribution and communication quality. Furthermore, this thesis advances the state of the art by introducing enhanced, hybrid, and multi-objective meta-heuristic algorithms specifically designed to solve the LED placement problem more effectively and efficiently.

Building on the growing interest in LED placement optimization for indoor VLC systems, this thesis presents four major contributions aimed at addressing key challenges in this domain:

1. **Problem Formulation:** We develop a system and mathematical model for LED deployment that supports varying numbers of LEDs and users, using throughput

and user coverage as performance metrics.

2. **Improved Optimization Algorithm:** We propose the Enhanced Whale Optimization Algorithm (EWOA) [41], which integrates sine chaotic mapping and opposition-based learning to improve solution diversity and convergence.
3. **Hybrid Meta-Heuristic Approach:** We introduce ICHIO-FA [42], a hybrid method combining an improved Coronavirus Herd Immunity Optimizer and Firefly Algorithm to enhance optimization performance.
4. **Multi-Objective Optimization:** We develop MOPO (Multi-Objective Puma Optimizer), which applies non-dominated sorting and crowding distance mechanisms to effectively balance competing objectives in LED placement.

This thesis is organized into five chapters, each addressing different aspects of LED placement optimization in VLC systems:

- **Chapter 1** presents a comprehensive overview of VLC technology, including its architecture, modulation schemes, strengths, limitations, and real-world applications. It identifies key research challenges such as user mobility, shadowing, and illumination constraints and reviews existing optimization strategies.
- **Chapter 2** discusses optimization methodologies, with a focus on classical, heuristic, and meta-heuristic algorithms. It covers their mathematical foundations, classification, and complexity, and compares single-objective versus multi-objective approaches, emphasizing bio-inspired algorithms for NP-hard problems like LED placement.
- **Chapter 3** introduces EWOA, an enhanced meta-heuristic that integrates chaotic maps and opposition-based learning. Simulations show that EWOA outperforms conventional algorithms in maximizing throughput and coverage.
- **Chapter 4** presents the hybrid ICHIO-FA algorithm, which overcomes limitations of standalone methods by combining chaotic strategies and OBL. It demonstrates improved accuracy and convergence speed in optimizing LED placement.
- **Chapter 5** describes MOPO, a multi-objective optimization algorithm designed to balance throughput and coverage. It uses ranking, crowding distance, and non-dominated sorting to achieve a diverse set of Pareto-optimal solutions. Results show that MOPO outperforms NSGA-II and MOWOA in both diversity and convergence rate.

Finally, the thesis concludes with a summary of key findings and outlines potential directions for future research.

CHAPTER 1

STATE OF THE ART IN VISIBLE LIGHT COMMUNICATION

graphicx

1.1 Introduction

The global proliferation of mobile and wireless-enabled devices such as smartphones, tablets, and IoT technologies has grown at an unprecedented pace in recent years. While Radio Frequency (RF) communication remains the most widely used wireless technology due to its maturity and infrastructure readiness, it faces critical limitations, including bandwidth saturation, electromagnetic interference, and security vulnerabilities.

In parallel, significant advances in semiconductor lighting technologies, particularly Light Emitting Diodes (LEDs), have revolutionized the lighting industry [43]. LEDs are now favored for their superior energy efficiency, durability, and extended lifespan compared to traditional lighting systems. With their widespread adoption across residential, commercial, and industrial applications, it is anticipated that LEDs will eventually replace all conventional light sources.

What sets LEDs apart is their ability to support high-frequency switching, enabling them to function not only as illumination devices but also as data transmitters. This dual-purpose capability has paved the way for the development of Visible Light Communication (VLC), a branch of optical wireless communication that utilizes the visible light spectrum (380-780 THz) for data transmission [44]. In a typical VLC setup, LEDs act as transmitters, while photodetectors (PDs) are used to receive modulated light signals and decode information.

The core idea behind VLC is to repurpose existing indoor lighting infrastructure for high-speed wireless communication, offering a secure, cost-effective, and interference-free

alternative to RF systems. Although the concept of optical wireless communication dates back to Alexander Graham Bells photophone in 1880, VLC has only recently gained attention due to the advancements in LED technology and growing data demand. Modern VLC systems can now achieve gigabit-per-second (Gbps) transmission rates, progressing from 80 Mbit/s in 2008 to 3000 Mbit/s by 2014, highlighting its promise for future communication systems.

This chapter presents a comprehensive overview of Visible Light Communication systems, covering both foundational concepts and advanced applications. The content is structured as follows:

- **VLC History:** A brief account of the historical development of VLC, tracing its roots and technological evolution.
- **What is VLC Technology?** An in-depth explanation of VLC as a communication technology and how it leverages visible light for data transmission.
- **VLC Architecture:** A description of the components, structure, and communication flow in a typical VLC system.
- **Modulation Techniques in VLC:** An overview of the modulation schemes used to encode and transmit data via light sources.
- **Balancing Advantages and Challenges of VLC:** A critical analysis of VLCs strengths, such as bandwidth and security, and its limitations, such as line-of-sight dependency.
- **VLC Applications:** Exploration of current and emerging applications of VLC across sectors such as healthcare, transportation, industry, and smart homes.
- **Conclusion:** A summary of the key points and an outlook on future research directions in VLC.

Through this structured exploration, the chapter aims to provide both a foundational understanding and an up-to-date review of VLC technology, laying the groundwork for subsequent chapters that delve into optimization techniques and practical implementations.

1.2 VLC History

Although VLC has gained significant traction in recent years, the concept of utilizing light for communication dates back centuries. Various civilizations have historically employed light-based signaling techniques to exchange information efficiently across distances [45],



Figure 1.1: Fire communication system used in ancient Greece [1].

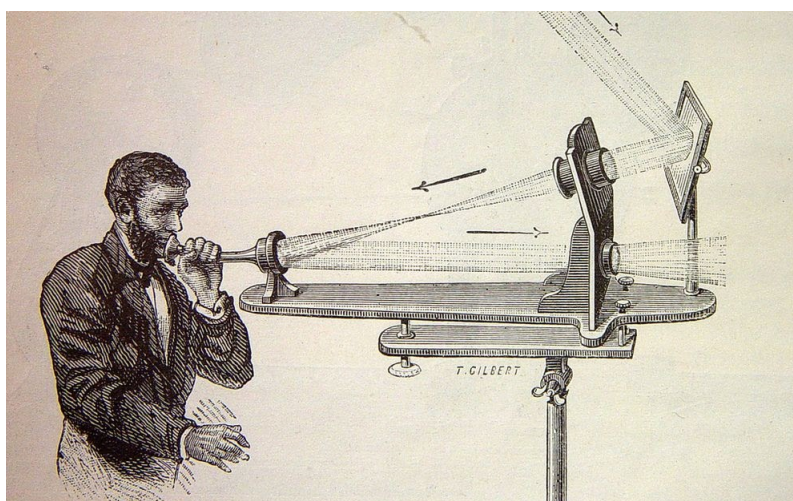


Figure 1.2: Alexander Graham Bell's method of transmitting sound using sunlight [2].

[1] 1.1. Notable examples include the use of smoke signals by Native American tribes and the transmission of light signals between naval vessels. These historical methods highlight the long-standing effectiveness of optical communication for conveying crucial messages.

The modern evolution of optical wireless communication began in 1880 with Alexander Graham Bell's photophone, a revolutionary invention that laid the foundation for contemporary VLC systems [2] 1.2. This device functioned similarly to a telephone but used a flexible mirror system to modulate voice signals. By varying the frequency of the modulated light, the photophone encoded audio signals onto sunlight reflections. At the receiving end, selenium cells in conjunction with a concentrator mirror facilitated the decoding of transmitted signals, enabling successful communication over distances exceeding 200 meters.

Despite the photophone's early success, its widespread adoption was hindered by the emergence of RF communication. In 1894, Guglielmo Marconi's invention of the radio telegraph significantly expanded wireless communication capabilities by enabling long-

range transmission via RF signals. As a result, RF-based communication rapidly outpaced optical wireless systems, shifting technological focus toward radio waves.

Interest in light-based communication re-surfed in the early 2000s, driven by advancements in Light Emitting Diodes (LEDs) and their potential application in VLC systems. In a pioneering experiment, a white LED was successfully used for both illumination and data transmission in an indoor setting, achieving impressive throughput rates of up to 400 Mbps [46]. This breakthrough sparked further research into advanced modulation techniques and LED technology improvements, solidifying VLC as a viable alternative to RF communication.

A significant turning point in VLC development occurred in 2011 [47], when researchers achieved major progress in the field. Today, VLC continues to attract considerable attention from leading research institutions and major corporations such as NASA, Disney, and Philips, all of which are actively engaged in developing products and conducting studies to expand its practical applications [48]. These ongoing efforts underscore VLCs growing significance as a next-generation communication technology .

1.3 What is VLC technology ?

Visible Light Communication (VLC) is an advanced wireless communication technology that operates within the visible light spectrum (400-800 nm) [3]. As a key branch of optical wireless communication, VLC enables high-speed data transmission by modulating light sourceswitching them on and off at speeds imperceptible to the human eye. One of its distinguishing advantages is its resistance to electromagnetic interference, making it particularly suitable for environments where traditional Radio Frequency (RF) communication is restricted.

The emergence of VLC technology stems from the need to address several fundamental limitations associated with RF-based wireless communication [49]. These limitations can be categorized into three main challenges:

- **Electromagnetic Spectrum Saturation** The rapid increase in data traffic has led to congestion within the RF spectrum, causing bandwidth limitations and performance degradation. VLC offers an effective alternative by utilizing the untapped visible light spectrum, thereby reducing the dependency on RF-based channels and alleviating spectrum scarcity.
- **Dual Functionality: Lighting and Communication** Unlike RF systems, which are solely designed for data transmission, VLC provides a dual-purpose functionality, serving both as a lighting system and a data communication medium. This feature makes VLC highly adaptable for indoor environments, smart homes, offices,

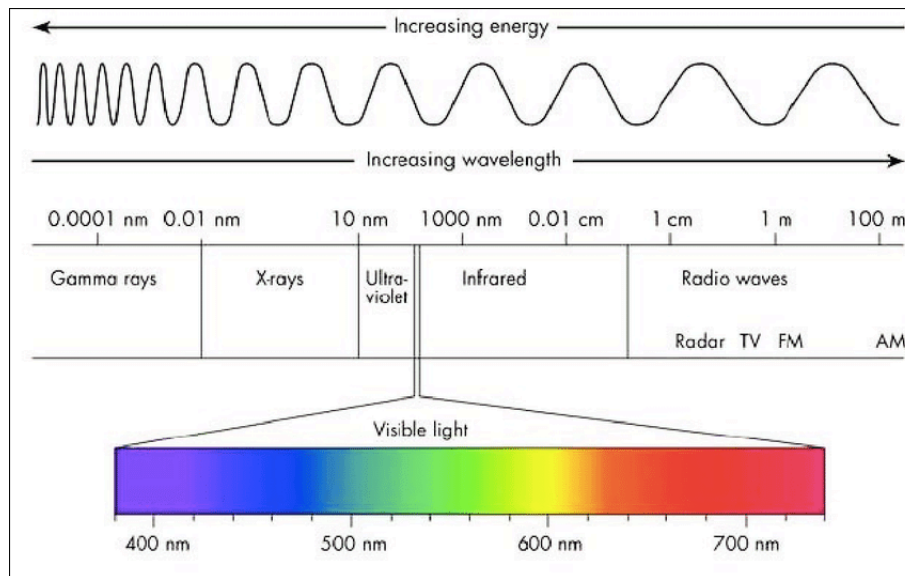


Figure 1.3: Light spectrum wavelength [3].

and vehicular communication systems, where illumination and data transfer can be seamlessly integrated.

- **Health and Safety Considerations** The potential health risks associated with prolonged exposure to RF electromagnetic waves have raised concerns, particularly in densely populated areas. VLC, which relies on visible light waves, is considered a safer alternative, as it does not emit harmful radiation and poses no known biological risks to humans.

At the core of VLC systems is a photosensitive receiver, which captures data signals emitted from optical light sources. Among the various light sources used, Light-Emitting Diodes (LEDs) play a crucial role as the primary medium for data transmission, display, and illumination [50]. White LEDs have emerged as the preferred light source in VLC due to their superior characteristics, including:

- **High Modulation Bandwidth:** Enables faster data transmission rates.
- **Enhanced Sensitivity:** Improves signal detection accuracy.
- **Long Lifespan:** Increases operational efficiency and reduces maintenance costs.
- **Improved Brightness:** Provides better illumination while supporting communication.
- **Compact and Lightweight:** Facilitates easy integration into smart lighting systems.
- **Energy Efficiency:** Consumes significantly less power than traditional light sources.
- **Low Cost and User-Friendliness:** Ensures affordability and ease of deployment.

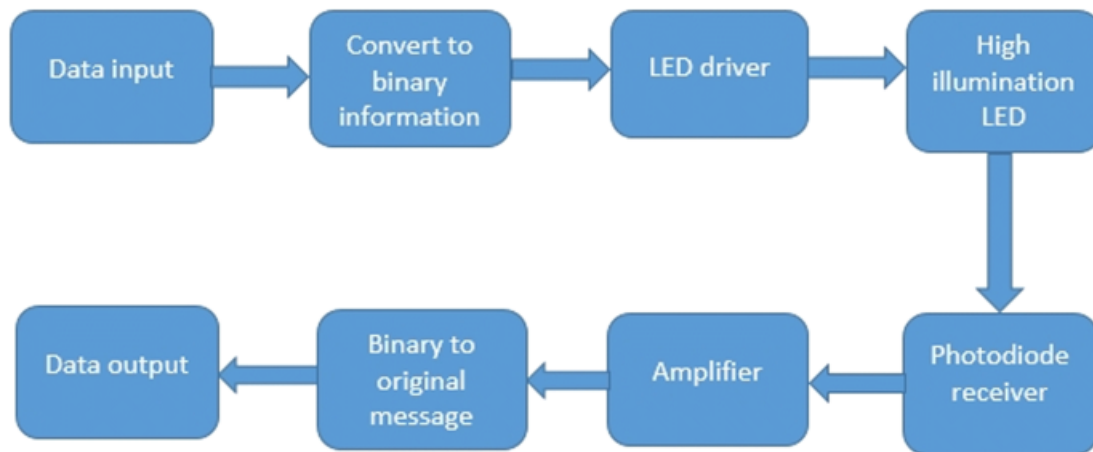


Figure 1.4: VLC Architecture diagram [4].

By leveraging the unique properties of LEDs, VLC technology enhances data transmission efficiency while simultaneously fulfilling illumination requirements. This strategic integration of lighting and wireless communication makes VLC a promising field with broad applications in smart infrastructure, healthcare, automotive communication, and high-speed indoor networking.

1.4 VLC Architecture

Visible Light Communication (VLC) systems are structured into three main components: a transmitter, a communication channel, and a receiver. These elements work together to facilitate data transmission using optical signals instead of conventional radio frequency waves [4]. VLC employs light-emitting diodes (LEDs) as transmitters and photodetectors as receivers, allowing for high-speed and secure wireless communication.

1. Transmitter:

The transmitter plays a crucial role in encoding and sending optical signals. As shown in Figure 1.5, data from the source is first converted into a digital bit stream using a source encoder. To enhance data reliability and minimize errors caused by channel distortions, a channel encoder introduces redundancy.

The encoded data is then modulated to control the intensity of the emitted optical signal. While intensity modulation is the most commonly used approach, other modulation techniques can also be implemented. A conductive circuit regulates the current passing through the LED, adjusting its brightness accordingly.

LEDs are widely used as VLC transmitters due to their advantages, including low power consumption, durability, cost efficiency, and rapid switching speeds, making them suitable for both lighting and communication purposes [51].

2. VLC Channel:

The VLC channel serves as the medium through which the optical signal propagates. During transmission, the signal experiences attenuation, noise, and interference, which can affect overall system performance. Additionally, light rays may undergo reflection, refraction, or scattering, leading to multipath propagation.

VLC channels are classified into two primary types:

- Line-of-Sight (LOS) Channel: The optical signal reaches the receiver directly without obstruction. Signal attenuation depends on factors such as distance and environmental conditions in outdoor applications.
- Non-Line-of-Sight (NLOS) Channel: The optical signal is reflected or scattered before reaching the receiver, resulting in potential interference and signal distortion [52].

3. Receiver:

The receiver captures, filters, and processes the optical signal to extract transmitted data. It consists of multiple components, including an optical filter, concentrator, photodiode, amplifier, demodulator, and decoder.

The optical concentrator focuses the received signal onto the photodiode, optimizing light capture. To minimize interference from ambient light sources, an optical filter is applied before conversion into an electrical current by the photodiode. This current is then amplified, demodulated, and decoded to reconstruct the original transmitted data [53].

Commonly used photodetectors in VLC systems include PIN diodes and avalanche photodiodes (APDs), valued for their high sensitivity, compact size, and fast response times.

1.4.1 VLC Communication Layers

The VLC system operates based on two primary communication layers:

- Medium Access Control (MAC) Layer
- Physical (PHY) Layer

Each layer has specific functions that contribute to efficient VLC communication.

1.4.1.1 The MAC Layer (Medium Access Control)

The MAC layer manages data transmission and network coordination in VLC systems, supporting multiple topologies such as peer-to-peer, broadcast, and star configurations [5]. It regulates access control, ensures mobility, enhances security, and prevents flicker while managing network connections.

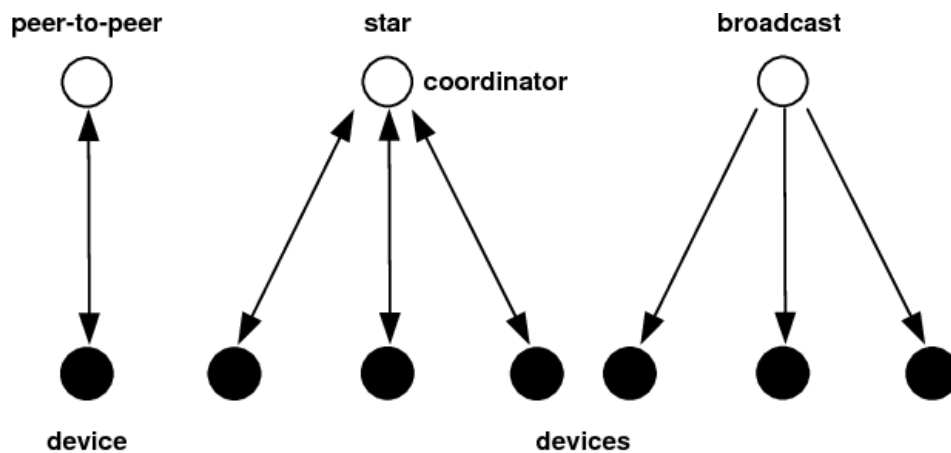


Figure 1.5: Topologies supported by MAC in the IEEE 802.15.7 standard [5].

1.4.1.1.1 Role of the MAC Layer: The MAC layer is responsible for:

- Managing mobility to ensure uninterrupted communication.
- Implementing security protocols for data protection.
- Controlling access to the VLC channel.
- Mitigating flicker caused by rapid LED switching.
- Handling network association and dissociation of devices.

1.4.1.1.2 Services from the MAC Layer to Upper Layers: The MAC layer provides two key services:

- MCPS-SAP Data Service, which facilitates data exchange.
- MLME-SAP Management Service, which oversees network and transmission management.

1.4.1.1.3 Services from the Physical Layer to the MAC Layer: The physical layer interacts with the MAC layer through:

- PD-SAP Data Service, responsible for efficient data transmission.
- PLME-SAP Management Service, which manages physical layer operations.

1.4.1.2 Physical Layer (PHY)

The physical layer defines the specifications for VLC communication devices and modulation techniques. According to the IEEE 802.15.7 standard, VLC PHY is classified into three categories based on application requirements [6].

Frame Control	Sequence Number	Dest.VPAN Identifier	Addressing Fields	Auxiliary Security Header	Frame Payload	FCS
MHR					MSDU	MFR

Figure 1.6: MAC frame structure [6].

Preamble	PHY header	HCS (CRC)	Optional fields	PSDU
SHR	PHR			PHY payload

Figure 1.7: PHY frame structure [6].

1.4.1.2.1 PHY I (Outdoor)

- Designed for outdoor environments.
- Supports data rates from 11.67 to 266.6 kbps.
- Utilizes convolutional and Reed-Solomon (RS) coding.

1.4.1.2.2 PHY II (Indoor)

- Optimized for indoor environments.
- Supports data rates from 1.25 to 96 Mbps.
- Uses Run-Length Limited (RLL) coding to maintain signal integrity.

1.4.1.2.3 PHY III (Multiple Optical Transceivers)

- Suitable for multiple transceiver systems.
- Achieves speeds between 12 to 96 Mbps.
- Employs Color Shift Keying (CSK) modulation for better performance.

1.4.2 The IEEE 802.15.7 Standard for VLC

The IEEE 802.15.7 standard, introduced in 2011, regulates short-range wireless optical communication through visible light. It enables intensity modulation of LED-based transmitters while ensuring flicker-free operation [54].

This standard defines three access topologies: peer-to-peer, star, and broadcast. It also specifies addressing schemes, modulation techniques such as On-Off Keying (OOK) and Variable Pulse Position Modulation (VPPM), and error correction methods to optimize performance in different environments [55].

To support dimming functionality, the standard includes mechanisms like OOK and VPPM [56, 57]. It also establishes different Forward Error Correction (FEC) codes for indoor and outdoor applications, considering factors like path loss and interference.

The IEEE 802.15.7 standard continues to evolve, integrating advancements such as parallel transmission techniques and vehicular VLC applications, further enhancing its role in wireless optical communication.

1.5 Modulation Techniques in VLC

The performance and efficiency of Visible Light Communication (VLC) systems are significantly influenced by the choice of modulation techniques. Proper modulation ensures reliable data transmission via light waves while mitigating signal degradation caused by external factors. This section explores various modulation schemes utilized in VLC, highlighting their characteristics, advantages, and applications.

1.5.1 Intensity Modulation (IM)

Intensity Modulation (IM) is the fundamental modulation technique in VLC, encoding data by altering the intensity of light emissions [7]. In this scheme, binary data variations translate into fluctuations in light intensity, enabling straightforward implementation. However, IM is susceptible to ambient light interference and environmental conditions that can affect signal quality. Despite its simplicity, it necessitates interference mitigation strategies to ensure reliable data transmission in practical VLC applications.

1.5.2 Amplitude Shift Keying (ASK)

Amplitude Shift Keying (ASK) conveys digital information by modulating the amplitude of the optical carrier signal [7]. Although ASK is simple to implement, it is highly vulnerable to noise and exhibits a limited modulation index, restricting its performance in noisy environments. To enhance robustness, researchers are exploring advanced ASK variants

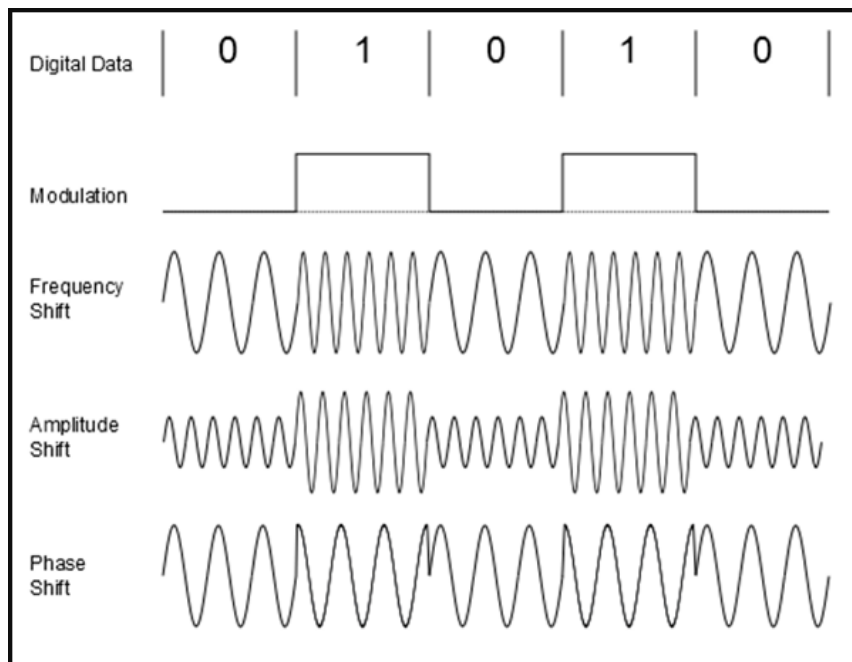


Figure 1.8: FSK, ASK, and PSK modulation techniques [7].

incorporating error correction mechanisms, expanding its potential applications in VLC systems.

1.5.3 Frequency Shift Keying (FSK)

Frequency Shift Keying (FSK) encodes data by varying the frequency of the light signal based on the transmitted information [7]. One key advantage of FSK is its resistance to amplitude-related disturbances. However, achieving high data rates with FSK can be challenging due to the inherently high frequency of light carriers. To optimize FSK for high-speed data transmission, advanced modulation index techniques and adaptive frequency shifts are being investigated.

1.5.4 Phase Shift Keying (PSK)

Phase Shift Keying (PSK) modifies the phase of the optical carrier signal to represent digital information [7]. PSK is well-suited for high-speed data transmission, offering efficient bandwidth utilization and enhanced resistance to certain types of environmental interference. Ongoing research focuses on developing adaptive algorithms that improve PSKs robustness against environmental distortions, ensuring stable VLC performance across different conditions.

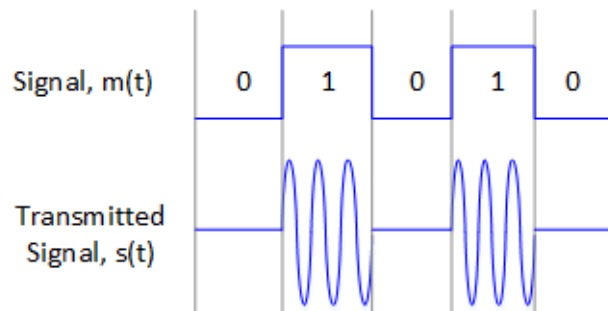


Figure 1.9: On-Off Keying modulation [8].

1.5.5 On-Off Keying (OOK)

On-Off Keying (OOK) is a straightforward form of intensity modulation, where the light source is switched on and off according to the binary data stream. While easy to implement, OOK has limitations in achieving high data rates and maintaining signal quality in environments with strong ambient light. Despite these challenges, OOK remains a viable choice for specific VLC applications. Recent research aims to enhance OOK by employing adaptive pulse width strategies to improve data rates and counteract interference from background light sources [8].

1.5.6 Pulse Width Modulation (PWM)

Pulse Width Modulation (PWM) encodes data by altering the duration of emitted light pulses. This technique provides a balance between simplicity and data rate efficiency, making it suitable for moderate- to high-speed VLC applications. Current advancements in PWM focus on refining pulse width control mechanisms, incorporating adaptive algorithms to dynamically adjust pulse durations based on environmental conditions for optimal data transmission.

1.5.7 Orthogonal Frequency Division Multiplexing (OFDM)

Orthogonal Frequency Division Multiplexing (OFDM) is a sophisticated modulation technique widely adopted in VLC systems to support high-speed data transmission. By dividing the data into multiple orthogonal subcarriers, OFDM enables parallel data transmission, mitigating channel fading effects and enhancing system resilience. Ongoing research is directed toward optimizing subcarrier allocation strategies and improving synchronization mechanisms to adapt OFDM to dynamic VLC environments, thereby increasing its robustness and adaptability.

1.6 Balancing Advantages and Challenges of VLC

VLC is emerging as a cutting-edge wireless communication technology, presenting a host of benefits alongside certain inherent challenges. This section provides an in-depth examination of both the advantages and limitations of VLC, offering a comprehensive understanding of its potential and areas requiring further refinement.

1.6.1 Advantages of VLC

VLC offers several key advantages, including:

- **Extensive Bandwidth Availability:**

By utilizing the vast visible light spectrum, which spans from 380 to 780 THz, VLC provides nearly 400 THz of available bandwidth [44]. This bandwidth is significantly larger than that of traditional Radio Frequency (RF) communication, making VLC an unregulated, globally accessible, and practically limitless solution for high-speed data transmission.

- **Health and Safety Compliance:**

Unlike RF-based communication, which has raised concerns regarding potential health risks, VLC relies solely on visible light, posing no known hazards to human health. The use of LEDs for signal transmission enables high-power communication without adverse biological effects, making it a safe and viable alternative to RF systems [55].

- **Interference-Free Operation in Sensitive Environments:**

VLC is well-suited for deployment in settings where RF signals may interfere with critical electronic systems, such as hospitals, aircraft, and industrial automation. Since VLC does not generate electromagnetic interference, it can be safely integrated into environments that are traditionally restricted for RF-based communications.

- **Enhanced Security Against Eavesdropping:**

A distinctive security feature of VLC stems from its reliance on visible light, which cannot penetrate walls or opaque objects. This physical limitation naturally prevents unauthorized interception of signals, making VLC particularly suitable for applications that demand high-security data transmission.

- **Cost-Effective Implementation:**

The affordability of VLC arises from its ability to leverage existing LED lighting infrastructure. Since VLC transceivers primarily consist of LED emitters and photo-diode receivers, system implementation costs are significantly lower compared

to other wireless technologies. Furthermore, VLC operates within the unlicensed spectrum, eliminating regulatory expenses.

- **Eco-Friendly and Energy-Efficient Communication:**

VLC aligns with global sustainability efforts by utilizing energy-efficient LED lighting for both illumination and data transmission. By re-purposing existing lighting infrastructure, VLC reduces additional power consumption, contributing to energy conservation and lower carbon emissions.

1.6.2 Challenges and Limitations of VLC

Despite its numerous benefits, VLC is subject to several limitations that must be addressed to ensure widespread adoption and reliability [58], [59]:

- **Interference and Background Noise:**

The presence of ambient light sources, including sunlight and artificial illumination, introduces interference and noise, which can degrade VLC performance. Effective interference mitigation techniques are crucial to maintaining a high Signal-to-Interference-plus-Noise Ratio (SINR) at the receiver.

- **Limitations on Optical Power:**

To comply with safety regulations, VLC systems must adhere to optical power constraints within the visible spectrum. Unlike infrared or ultraviolet light, which have stricter power limitations, visible light emissions must also consider human comfort, preventing excessive glare and ensuring acceptable illumination levels.

- **Flicker and Human Perception Issues:**

VLC systems that rely on intensity modulation may introduce flickering effects, which can cause visual discomfort or nausea in extreme cases. Advanced modulation techniques are required to smooth signal transitions and prevent noticeable flickering, ensuring user comfort.

- **Line-of-Sight (LOS) Dependency and Blockage Issues:**

Since visible light cannot penetrate opaque objects, VLC performance is highly dependent on maintaining a clear line-of-sight (LOS) between the transmitter and receiver. Any obstruction between the communicating devices can lead to signal degradation or complete transmission failure. Addressing this challenge requires the integration of Non-Line-of-Sight (NLOS) techniques, such as optical reflections or relay systems.

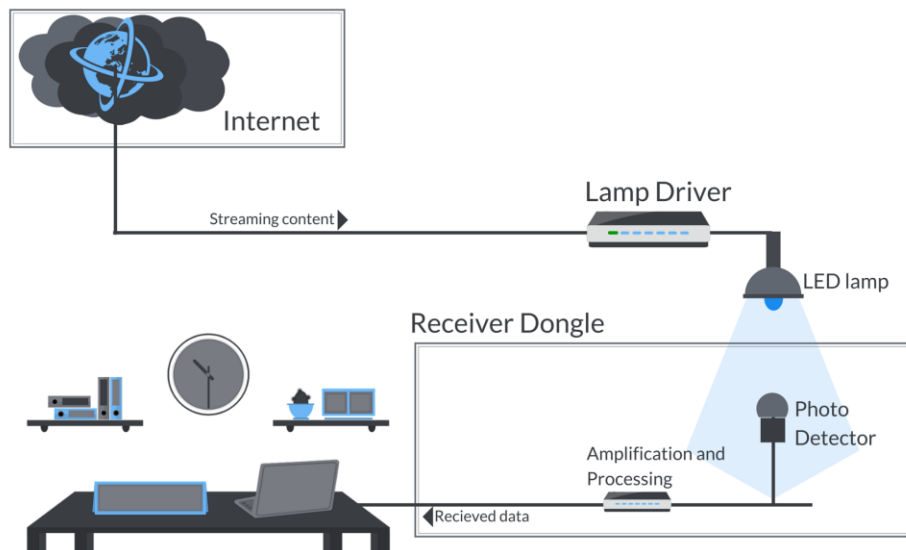


Figure 1.10: Li-Fi Architecture [9].

While VLC presents significant opportunities for high-speed, secure, and cost-effective wireless communication, overcoming these challenges is essential for its broader implementation across various applications. Continuous advancements in interference mitigation, modulation techniques, and hybrid communication strategies will further enhance VLCs feasibility and efficiency in real-world scenarios.

1.7 VLC Applications

VLC is a revolutionary technology with diverse applications across various domains. Its ability to provide high-speed, secure, and interference-free wireless communication makes it a promising alternative to traditional RF-based systems. This section explores the major indoor and outdoor applications of VLC, highlighting its advantages in different scenarios.

1.7.1 Indoor Applications

- **Li-Fi (Light Fidelity) Optical Wi-Fi:**

Li-Fi, a key application of VLC, utilizes visible light for high-speed wireless communication, serving as an alternative to traditional Wi-Fi. By modulating light frequencies from standard LED fixtures, Li-Fi enables multi-Gb/s data transmission to mobile terminals within short distances [9]. This innovation enhances data security and reduces congestion in RF-based networks.

- **Indoor Positioning and Navigation:**

VLC offers high-precision indoor localization, overcoming the limitations of GPS

in enclosed spaces such as shopping malls, airports, and hospitals. By leveraging techniques such as received signal strength (RSS), time of flight (ToF), and triangulation, VLC can achieve centimeter-level accuracy, making it highly valuable for navigation in complex indoor environments [60].

- **RF Spectrum Offloading:**

The growing demand for wireless connectivity often leads to RF spectrum congestion. VLC provides a complementary solution by offloading high-data-rate transmissions from traditional RF networks. Hybrid VLC-RF systems can efficiently distribute data, reducing overall network load and improving performance in high-density areas [49].

- **Healthcare and Aviation Communication:**

VLC's electromagnetic interference-free (EMI-free) nature makes it ideal for environments where RF signals can disrupt sensitive electronic equipment. In hospitals, VLC can facilitate wireless communication for medical devices without interfering with critical healthcare equipment. Similarly, in aviation, VLC reduces cabling complexity and weight, improving efficiency in aircraft communication systems [11].

- **Hazardous and Industrial Environments:**

In industrial settings such as petrochemical plants, mining operations, and military applications, VLC provides a safe and reliable communication alternative. Unlike RF, which can pose explosion risks in flammable environments, VLC ensures secure data transmission using existing lighting infrastructure, making it a preferred choice for such high-risk areas [11].

1.7.2 Outdoor Applications

VLC also demonstrates strong potential in outdoor environments, where RF communication may struggle due to interference, limited spectrum, or high attenuation.

- **Underwater Optical Communication:**

Traditional RF signals experience severe attenuation underwater, limiting their range. VLC presents a viable alternative by utilizing visible light for short-range, high-speed underwater communication. It enables communication between divers, remotely operated underwater vehicles (ROVs), and underwater base stations, significantly enhancing data transmission in marine applications [10].

- **Smart City Infrastructure and IoT Connectivity:**

VLC can play a crucial role in the development of smart cities by integrating with public lighting systems. Streetlights equipped with VLC transmitters can function

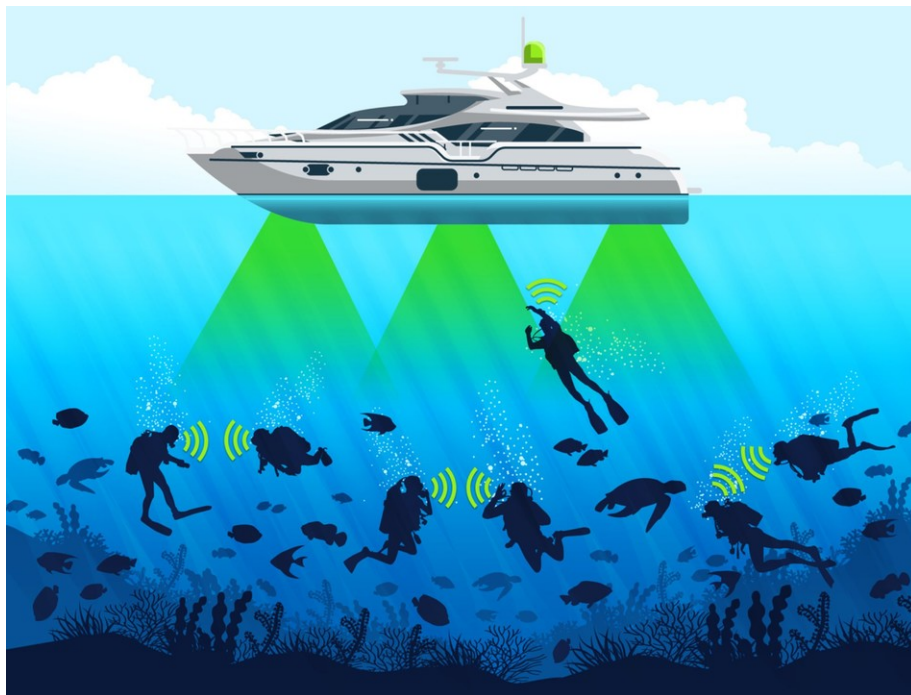


Figure 1.11: Underwater VLC applications [10].

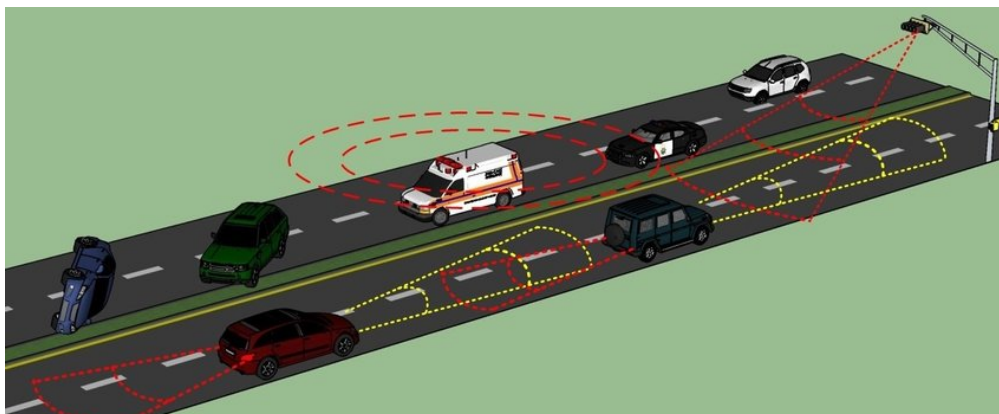


Figure 1.12: Vehicular VLC (V-VLC) applications [11].

as data access points, providing public Wi-Fi, real-time environmental monitoring, and intelligent traffic management. This integration enhances sustainability, energy efficiency, and smart city connectivity [61].

- **Intelligent Transportation Systems (ITS):**

VLC contributes to vehicle-to-vehicle (V2V) and vehicle-to-infrastructure (V2I) communication, improving road safety and traffic management. VLC-based ITS applications enable features such as collision avoidance, adaptive traffic signals, and pedestrian safety assistance. By leveraging traffic lights and vehicle headlights as VLC transmitters, data exchange in real-time enhances driving conditions and reduces accidents [62].

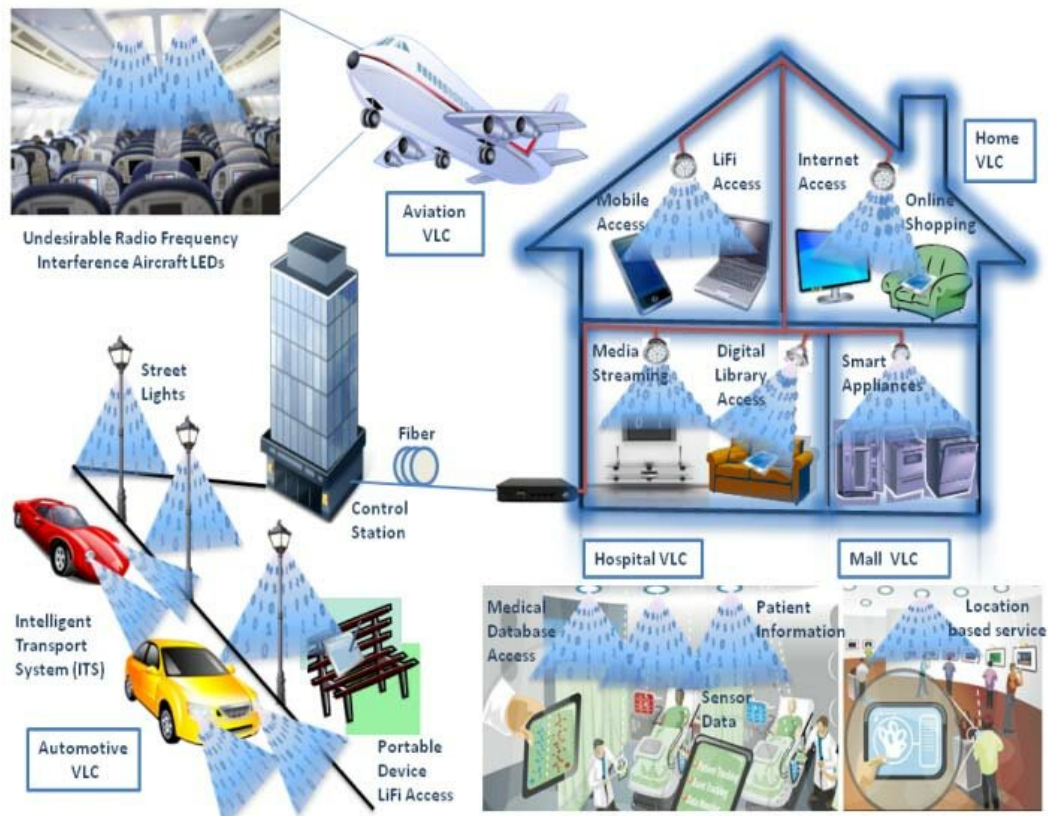


Figure 1.13: Visible Light Communications Applications [12].

The broad spectrum of VLC applications highlights its potential as a next-generation wireless communication technology. Whether in controlled indoor settings or challenging outdoor environments, VLC offers enhanced security, high-speed data transmission, and interference-free connectivity. As research and development progress, VLC is expected to revolutionize communication systems across various domains, driving the advancement of smart cities, intelligent transportation, and industrial automation.

1.8 Conclusion

In this chapter, we provided a comprehensive overview of Visible Light Communication (VLC), an emerging wireless communication technology that utilizes Light Emitting Diodes (LEDs) for data transmission. We discussed the key advantages of VLC over traditional Radio Frequency (RF) communication, including its extensive bandwidth availability, improved security, energy efficiency, and immunity to electromagnetic interference.

We explored the historical progression of light-based communication, tracing its origins from early optical signaling techniques to the invention of Alexander Graham Bells photo-phone. Despite the initial challenges faced by optical communication technologies, modern advancements in LED technology have reignited interest in VLC, enabling significant improvements in data transmission rates, modulation techniques, and real-world

applications.

Furthermore, we examined the architecture of VLC systems, detailing the roles of transmitters, receivers, and the optical wireless channel. Special emphasis was placed on modulation techniques such as On-Off Keying (OOK), Pulse Width Modulation (PWM), and Orthogonal Frequency Division Multiplexing (OFDM), each offering distinct advantages for various VLC applications.

This chapter serves as the foundation for the subsequent sections of this thesis. The following chapters will delve into the proposed optimization methodologies, their implementation, and performance evaluation. By addressing the challenges associated with LED placement in VLC systems, this research aims to contribute to the development of more efficient, scalable, and practical VLC deployment strategies for future wireless communication networks.

2.1 Introduction

Optimization is a fundamental discipline with applications spanning various fields, including research, mathematics, computer science, management, and industrial engineering. It is concerned with systematically identifying the most effective and efficient solution from a range of feasible options for a given problem. As technological advancements continue to introduce increasingly complex challenges, the demand for robust and efficient optimization methods has grown significantly.

Optimization problems can be classified based on multiple criteria, including the nature of decision variables, the presence of constraints, the number of objectives, and computational complexity. These problems are typically categorized as continuous or discrete, constrained or unconstrained, single-objective or multi-objective, and deterministic or stochastic. Given this diversity, different optimization techniques have been developed to address specific problem domains effectively.

A wide range of optimization algorithms has been proposed to tackle these challenges, broadly classified into classical methods and Artificial Intelligence (AI)-based techniques. Classical methods, such as gradient descent, linear programming, and quadratic programming, have been widely used for structured optimization problems. However, their efficiency tends to decline when dealing with highly complex, high-dimensional, or non-convex problems. To address these limitations, AI-driven approaches such as genetic algorithms, particle swarm optimization, ant colony optimization, and neural networks have emerged as powerful alternatives. These techniques offer adaptive, flexible, and scalable solutions, particularly in real-world applications where traditional methods may struggle.

In certain cases, hybrid optimization approaches that integrate classical and AI techniques can further enhance performance by leveraging the strengths of both paradigms. These hybrid models improve convergence speed, robustness, and accuracy, making them

highly effective for solving large-scale and multi-objective optimization problems.

Given the critical role of optimization across various domains, this chapter provides a comprehensive overview of optimization problems and their classification criteria. We examine different types of optimization problems based on decision variables, objectives, constraints, and computational complexity. Additionally, we explore various solution methodologies, categorizing them into classical algorithms and AI-based techniques. A clear understanding of these methodologies enables researchers and practitioners to make informed decisions when selecting the most suitable optimization approach for their specific problem domains.

2.2 Optimization Problem

An optimization problem in computer science is defined as a task that requires solving through specialized algorithms known as optimization algorithms. These algorithms evaluate various potential solutions within a defined search space and return the best possible solution based on predefined criteria. Fundamentally, an optimization problem consists of three key components: the search space, the objective function, and constraints. Mathematically, an optimization problem is represented as follows [63]:

$$P = (D, f, C) \tag{2.1}$$

where P denotes the optimization problem, D represents the search space of the problem domain, f is the objective function, and C refers to the problem's constraints.

The search space D consists of a set of decision variables that define the domain of possible solutions. It is expressed as:

$$D = \{X_1, X_2, \dots, X_n\} \tag{2.2}$$

where n represents the dimensionality of the problem domain.

2.2.1 Objective Function

The objective function is a mathematical representation of one or more objectives that need to be optimized. Depending on the nature of the problem, these objectives may be subject to constraints C . The objective function evaluates the quality of a given solution and attempts to produce an optimal output based on the relationship between decision variables in D . It is defined as follows [63]:

$$\begin{aligned} f : D &\longrightarrow \mathbb{R} \\ \forall d \in D, \quad f(d) &= \text{fitness}(\mathbb{R}) \end{aligned} \tag{2.3}$$

The objective function serves two primary purposes: first, to evaluate the quality of potential solutions using Eq. (2.2), and second, to guide the search process towards promising regions of the search space [64]. In the literature, optimization problems are categorized into two types based on their objective functions:

1. **Minimization Problem:**

In a minimization problem, the objective function seeks to find the global minimum solution, where the lowest fitness value corresponds to the best performance. It is mathematically defined as follows:

$$\begin{aligned} & \text{Minimize } f \\ \forall d \in D, \quad & f(\bar{d}) \leq f(d) \end{aligned} \tag{2.4}$$

2. **Maximization Problem:**

In a maximization problem, the goal is to find the global maximum solution, where the highest fitness value represents the best performance. It is defined as follows:

$$\begin{aligned} & \text{Maximize } f \\ \forall d \in D, \quad & f(\bar{d}) \geq f(d) \end{aligned} \tag{2.5}$$

2.3 Classification of Optimization Problems

Optimization problems can be categorized based on various factors, including the type of decision variables, the number of objectives, the presence of constraints, and computational complexity. This classification aids in selecting the most appropriate optimization technique for solving a given problem effectively.

2.3.1 Classification Based on Decision Variable Type

In an optimization problem, decision variables represent a set of unknown and controllable parameters that belong to a defined domain. Optimization algorithms adjust these variables to achieve the best possible outcome for the objective function. Based on their nature, decision variables can be classified into three types:

2.3.1.1 Quantitative Variables

Quantitative variables are numerical in nature and can be further divided into:

1. **Continuous numerical variables:** These variables can take any value within a given range in the real number domain \mathbb{R} , forming an uncountable set of values.
2. **Discrete numerical variables:** Discrete variables have a countable set of possible values, typically taking on integer values within a defined range.

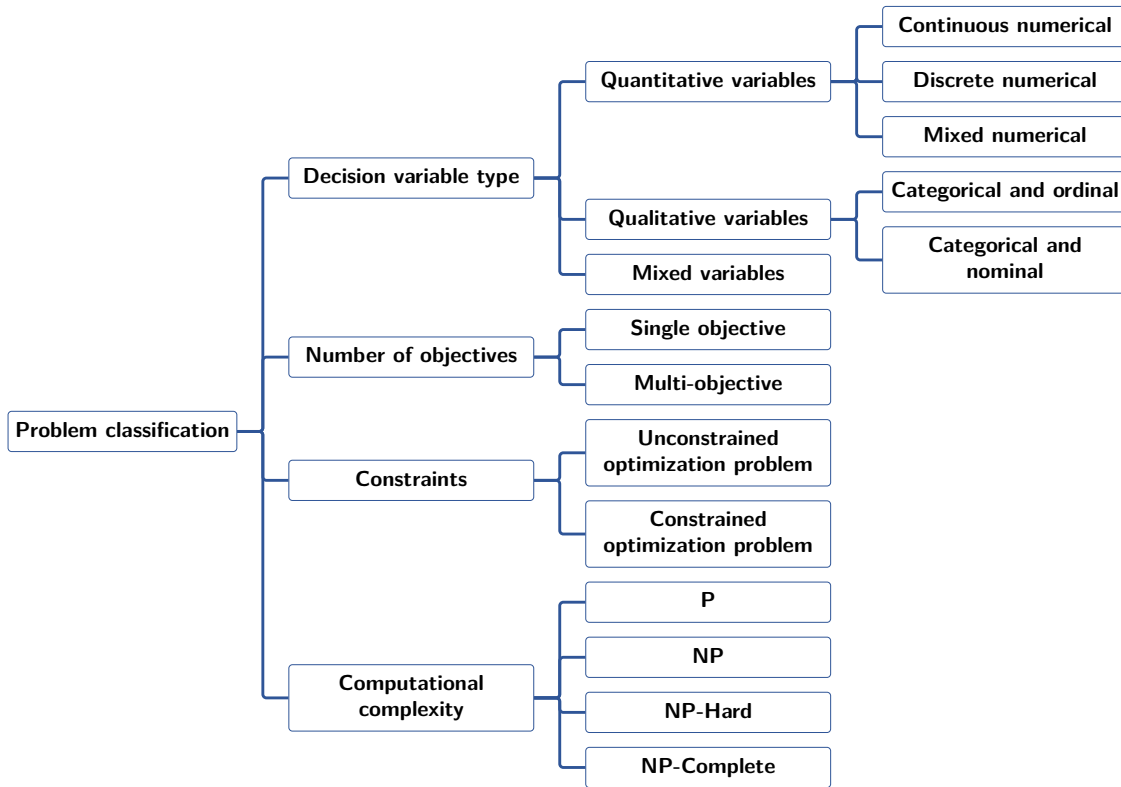


Figure 2.1: Classification of optimization problems

3. **Mixed numerical variables:** These variables combine both continuous and discrete numerical values, often used in hybrid optimization problems.

2.3.1.2 Qualitative Variables

Qualitative variables, unlike quantitative ones, do not take numerical values. Instead, they are represented by labels or categories. They can be classified into:

1. **Categorical and ordinal variables:** These variables have an inherent order among their categories, meaning the sequence of values holds significance.
2. **Categorical and nominal variables:** In contrast, nominal categorical variables lack any meaningful order or hierarchy among their values.

2.3.1.3 Mixed Variables

Mixed (or hybrid) variables contain both quantitative and qualitative components. They are commonly encountered in real-world optimization problems such as the Traveling Salesman Problem (TSP), where both numerical and categorical decision-making is required.

2.3.2 Classification Based on the Number of Objectives

Depending on the number of objectives to be optimized, an optimization problem can be classified into one of two categories:

2.3.2.1 Single-Objective Optimization

A single-objective optimization (SO) problem focuses on optimizing a single criterion or an aggregate function that combines multiple criteria into one. This type of optimization is straightforward in terms of determining the best solution, as it is simply the one with the most favorable fitness value. However, SO problems often fail to provide trade-off solutions for competing objectives.

2.3.2.2 Multi-Objective Optimization

Multi-objective optimization (MO) involves optimizing two or more conflicting objectives simultaneously [65]. Unlike SO problems, MO problems do not yield a single best solution but instead produce a set of trade-off solutions known as Pareto-optimal solutions. These solutions represent the best possible compromises among conflicting objectives.

2.3.3 Classification Based on Constraints

Constraints define the limitations and feasibility conditions of an optimization problem. Based on the presence and nature of constraints, optimization problems can be categorized into:

2.3.3.1 Unconstrained Optimization

Unconstrained optimization involves optimizing an objective function without any restrictions on the variables. In some cases, constrained optimization problems are transformed into unconstrained problems by incorporating penalty terms into the objective function. This technique allows constrained problems to be solved using unconstrained optimization methods.

2.3.3.2 Constrained Optimization

In constrained optimization, the objective function is optimized while satisfying a set of predefined constraints. These constraints can be classified as:

- **Hard constraints:** Constraints that must be strictly satisfied. If a solution violates a hard constraint, it is discarded.

- **Soft constraints:** Constraints that are desirable but not mandatory. If a solution does not satisfy a soft constraint, it is still accepted but may result in suboptimal performance.

2.3.4 Classification Based on Computational Complexity

Another criterion for classifying optimization problems is computational complexity, which refers to the time and resources required by an algorithm to find a solution. It also reflects the difficulty of solving the problem. Based on complexity, optimization problems can be categorized into the following classes:

2.3.4.1 P Problems

Polynomial-time (P) problems are those that can be efficiently solved using deterministic algorithms within polynomial time. These problems are considered tractable.

2.3.4.2 NP Problems

Non-deterministic Polynomial-time (NP) problems form a larger class that includes problems for which a solution can be verified in polynomial time, even if finding the solution may not necessarily be efficient.

2.3.4.3 NP-Hard Problems

NP-hard problems are problems as difficult as the hardest NP problems. A problem is classified as NP-hard if an NP-complete problem can be reduced to it in polynomial time. Some NP-hard problems can be solved in polynomial time, but in general, they are computationally challenging.

2.3.4.4 NP-Complete Problems

NP-complete problems belong to both the NP and NP-hard categories. These problems are among the most difficult in the NP class, as no polynomial-time algorithm has been found to solve them efficiently. However, their solutions can still be verified in polynomial time.

2.4 Main methods for tackling optimization Problems

The main methods for tackling optimization problems can be categorized based on their search techniques into three main groups: **Enumerative, Deterministic, and Stochas-**

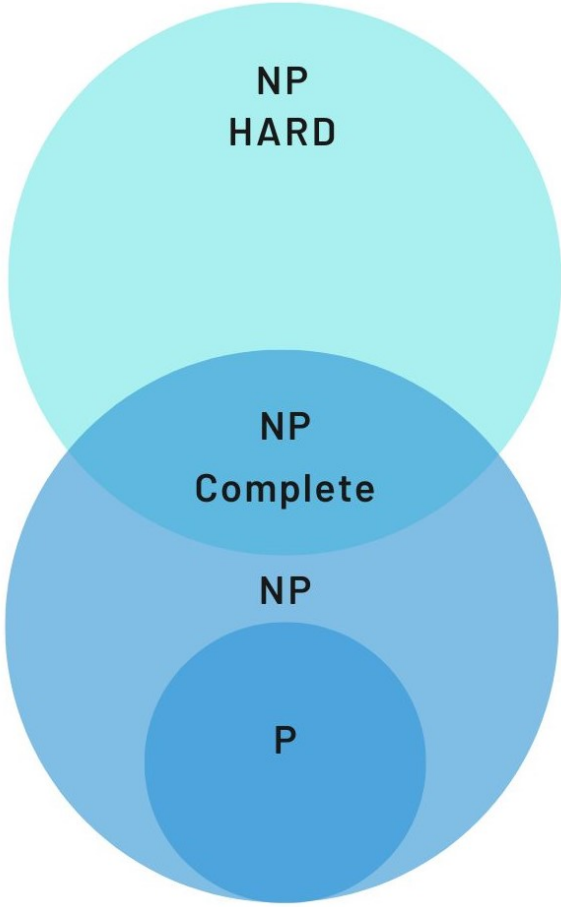


Figure 2.2: Classification of optimization problems based on computational complexity.

tic Methods.

2.4.1 Enumerative Methods

Enumerative methods systematically evaluate all possible solutions within the search space. While this approach ensures that the optimal solution is identified, it is computationally expensive and impractical for large-scale problems due to the exponential growth of the search space [66].

2.4.2 Deterministic Methods

Deterministic methods rely on gradients or derivatives to guide the optimization process. Some widely used deterministic techniques include:

- Greedy algorithms
- Hill Climbing methods
- Branch and Bound
- Depth-First Search (DFS) and Breadth-First Search (BFS)
- Best-First Search
- Calculation-based approaches [67, 68].

However, as highlighted by Parkinson et al. [66] and Coello et al. [69], deterministic methods struggle with the following types of optimization problems:

- Problems with discrete decision variables.
- High-dimensional search spaces.
- Presence of multiple local optima (multimodal functions).
- Non-differentiable objective functions and constraints.
- Discontinuous functions or fragmented feasible regions.
- Cases where evaluation programs may crash for some design configurations.

Given these limitations, both enumerative and deterministic approaches are generally unsuitable for solving real-world and engineering-related MOPs. Consequently, they will not be further discussed in this thesis.

2.4.3 Stochastic Methods

Stochastic optimization techniques have demonstrated significant success in solving complex MOPs, primarily due to advancements in computational power and processing capabilities. These methods initiate the optimization process with a randomly generated set of candidate solutions and iteratively refine them over multiple iterations [70].

Most stochastic algorithms used for multi-objective optimization are inspired by natural phenomena and are commonly referred to as **meta-heuristics**. These algorithms are typically classified into four categories based on their source of inspiration:

- Evolutionary-based algorithms.
- Physics-based algorithms.
- Human behavior-inspired algorithms.
- Swarm intelligence-based algorithms [71].

Yang [72] further categorizes meta-heuristics based on their search strategies into trajectory-based and population-based approaches.

While numerous meta-heuristics exist for solving single-objective optimization problems, only a subset of them have been successfully adapted to handle multi-objective optimization problems.

2.5 Optimization Problem Algorithms

Over the years, numerous algorithms have been developed to tackle optimization problems efficiently. These algorithms differ in their approaches to searching for optimal solutions, and based on their nature and methodology, they can be broadly categorized into two main groups: **classical algorithms** and **Artificial Intelligence (AI) based approaches**, as illustrated in Figure 2.3.

2.5.1 Classical Algorithms (Exact Approaches)

Classical algorithms represent the earliest methods introduced in the literature for solving optimization problems. Also known as exact approaches, these algorithms are highly efficient in finding precise solutions. However, when applied to large-scale or complex problems, classical methods can become computationally expensive, often requiring excessive processing time to reach an optimal solution. Table 2.1 presents a summary of well-known classical optimization algorithms along with their classifications.

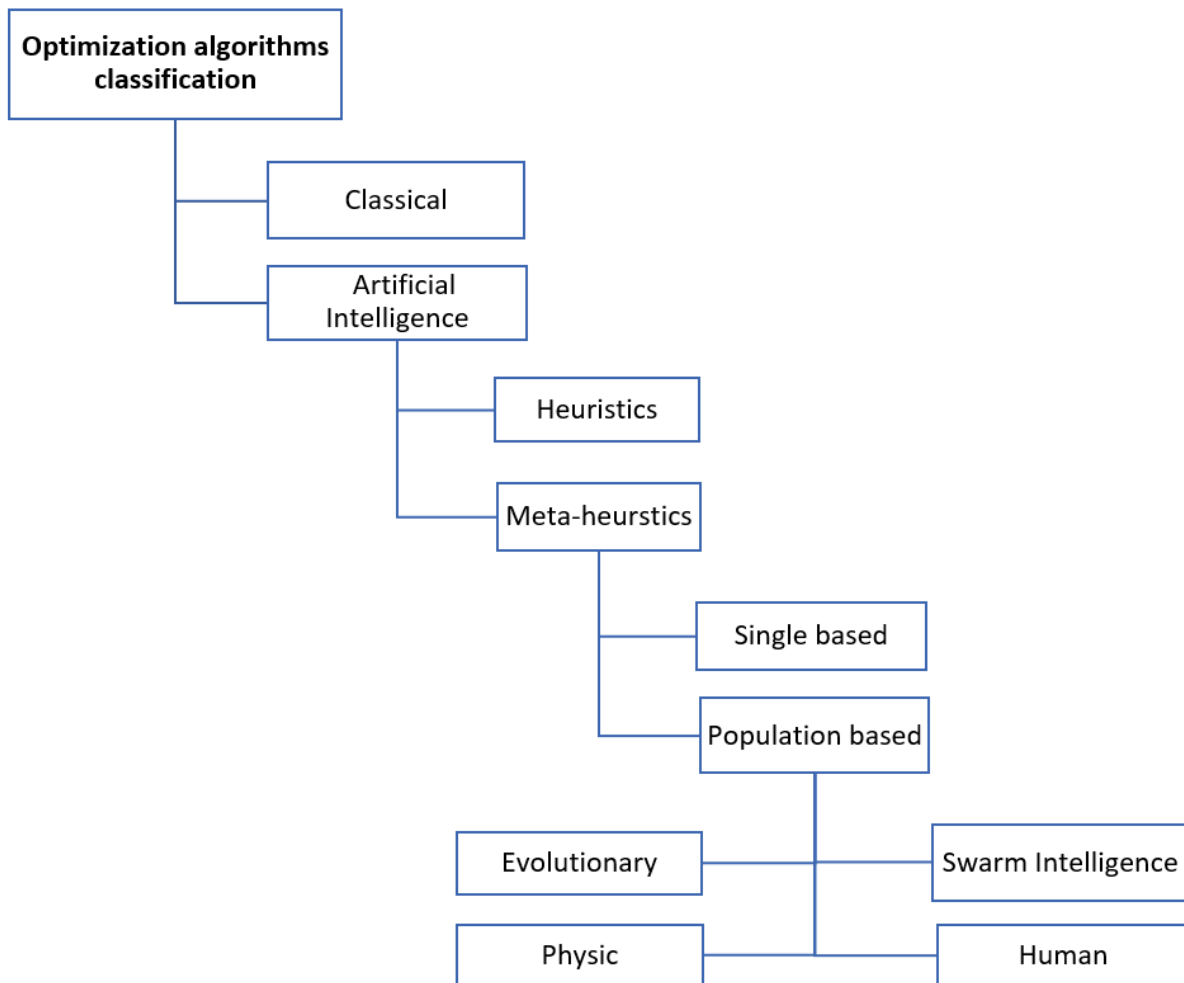


Figure 2.3: Classification of Optimization Algorithms

Categories of classical algorithms :

Search-Based Algorithms that explore all or a large portion of the solution space using exhaustive or blind search techniques. While simple and general, they are computationally expensive and often impractical for large-scale problems.

Tree-Based Algorithms that represent the problem as a decision tree and explore branches selectively, often using pruning strategies to reduce the search space.

Recursive/Deterministic Methods that solve problems by breaking them into overlapping subproblems and solving them recursively with deterministic strategies.

Mathematical Traditional optimization methods grounded in mathematical programming. These include linear, nonlinear, integer, and quadratic programming, suitable for problems that can be formulated with mathematical constraints and objective functions.

Constraint-Based Methods that focus on satisfying constraints rather than optimizing an explicit objective. Constraint Programming is commonly used in scheduling and combinatorial problems.

Convex Optimization A subclass of mathematical optimization where the objective and constraints form a convex set, enabling efficient identification of globally optimal solutions.

Geometric Programming A type of mathematical programming suitable for problems involving posynomial functions. Commonly applied in engineering design and resource allocation tasks.

Table 2.1: Classical Optimization Algorithms

Acronym	Category	Full Name	Reference
BF	Search-Based	Brute Force Search	Cormen et al. (2009)
BnB	Tree-Based	Branch and Bound	Land & Doig (1960)
BnC	Tree-Based	Branch and Cut	Padberg & Rinaldi (1991)
DP	Recursive/Deterministic	Dynamic Programming	Bellman (1957)
ILP	Mathematical	Integer Linear Programming	Wolsey (1998)
MILP	Mathematical	Mixed-Integer Linear Programming	Nemhauser & Wolsey (1988)
LP	Mathematical	Linear Programming	Dantzig (1947)
NLP	Mathematical	Nonlinear Programming	Bazaraa et al. (2006)
QP	Mathematical	Quadratic Programming	Gould et al. (1999)
CP	Constraint-Based	Constraint Programming	Tsang (1993)
SOCP	Convex Optimization	Second-Order Cone Programming	Alizadeh & Goldfarb (2003)
SDP	Convex Optimization	Semidefinite Programming	Vandenberghe & Boyd (1996)
DPG	Geometric Programming	Geometric Programming	Duffin et al. (1967)

2.5.2 Artificial Intelligence Algorithms

In addition to classical approaches, Artificial Intelligence (AI)-based or approximate algorithms have been widely adopted for solving optimization problems. These methods were primarily developed to overcome the limitations of exact algorithms, particularly their scalability issues. AI-based approaches offer advantages such as flexibility, cost-efficiency, and faster solution generation. However, their primary drawback is that they do not always guarantee an exact optimal solution. AI-based optimization methods are further divided into two main subcategories: heuristic algorithms and meta-heuristic algorithms.

2.5.2.1 Heuristic Algorithms

Heuristic algorithms are approximate techniques that utilize problem-specific knowledge or rules of thumb to find near-optimal solutions. Unlike general-purpose optimization methods, heuristics are typically tailored to the structure of a particular problem, which can limit their flexibility across diverse problem domains.

These algorithms are valued for their speed and simplicity, often producing good-quality solutions within reasonable computational time. However, they generally do not guarantee optimality and may perform poorly on large or highly complex problems. As such, their applicability is often best suited to small or medium-scale scenarios.

Common examples of heuristic algorithms include the **A-Star (A*)** algorithm and the **Greedy** algorithm, both widely used in pathfinding and search problems.

Table 2.2 summarizes several well-known heuristic algorithms used in optimization and search.

Table 2.2: Heuristic Algorithms

Acronym	Full Name	Reference
A*	A-Star Algorithm	Hart et al. (1968)
Greedy	Greedy Algorithm	Cormen et al. (2009)
Hill Climbing	Hill Climbing Algorithm	Russell & Norvig (2010)
BestFS	Best-First Search	Pearl (1984)
Beam Search	Beam Search	Lowerre (1976)

2.5.2.2 Meta-Heuristic Algorithms

Meta-heuristic algorithms are among the most widely used methods for solving optimization problems due to their efficiency, adaptability, and problem-independence. These algorithms balance exploration and exploitation, allowing them to find near-optimal solutions within a feasible time frame. However, similar to heuristics, they do not guarantee finding the exact optimal solution. Based on their search behavior, meta-heuristics can

be classified into two categories: **single-solution-based** and **population-based** algorithms.

1. Single-Solution-Based Algorithms

Single-solution-based meta-heuristics, also known as trajectory-based algorithms, generate and iteratively improve a single candidate solution throughout the optimization process [73]. These algorithms rely on neighborhood search mechanisms, where an initial solution is gradually refined through local modifications. They are particularly effective for problems where local search is computationally feasible and can lead to high-quality results.

Table 2.3 summarizes widely used single-solution-based meta-heuristics along with their references.

Table 2.3: Single-Solution-Based Meta-Heuristics

Acronym	Full Name	Reference
SA	Simulated Annealing	Kirkpatrick et al. (1983)
TS	Tabu Search	Glover (1986)
HC	Hill Climbing	Russell & Norvig (2010)
GLS	Guided Local Search	Voudouris & Tsang (1999)
ILS	Iterated Local Search	Lourenço et al. (2003)
RVND	Random Variable Neighborhood Descent	Mladenovi & Hansen (1997)
VND	Variable Neighborhood Descent	Hansen & Mladenovi (2001)
LAHC	Late Acceptance Hill Climbing	Burke & Bykov (2008)
RLS	Randomized Local Search	Hoos & Stützle (2004)

2. Population-Based Algorithms

Unlike single-solution-based methods, population-based meta-heuristics operate on a set of candidate solutions (a population) rather than a single solution. These algorithms simulate natural or social behaviors to explore and exploit the search space effectively. Population-based approaches can be further divided into four main categories as like summarized in table 2.4:

(a) Evolutionary-Based Algorithms

Evolutionary algorithms are inspired by natural evolution principles, such as Darwinian selection, crossover, and mutation. These methods iteratively evolve a population of solutions by applying genetic operations to improve fitness over successive generations.

(b) Swarm Intelligence-Based Algorithms

Table 2.4: Population-Based Meta-Heuristic Algorithms

Acronym	Full Name	Reference
Evolutionary-Based Algorithms		
GA	Genetic Algorithm	Holland (1975)
DE	Differential Evolution	Storn & Price (1997)
ES	Evolution Strategy	Rechenberg (1973)
BBO	Biogeography-Based Optimization	Simon (2008)
Swarm Intelligence-Based Algorithms		
PSO	Particle Swarm Optimization	Kennedy & Eberhart (1995)
ACO	Ant Colony Optimization	Dorigo & Gambardella (1997)
ABC	Artificial Bee Colony	Karaboga (2005)
GSO	Glowworm Swarm Optimization	Krishnanand & Ghose (2009)
GWO	Grey Wolf Optimization	Mirjalili et al. (2014)
FA	Firefly Algorithm	Yang (2008)
MPA	Marine Predator Algorithm	Faramarzi et al. (2020)
AO	Aquila Optimizer	Abualigah et al. (2021)
Physics-Based Algorithms		
AEFA	Artificial Electric Field Algorithm	Abdel-Basset et al. (2020)
GSA	Gravitational Search Algorithm	Rashedi et al. (2009)
MVO	Multi-Verse Optimizer	Mirjalili et al. (2016)
HGSO	Henry Gas Solubility Optimization	Hashim et al. (2019)
AOA	Arithmetic Optimization Algorithm	Abualigah et al. (2021)
Human-Based Algorithms		
TLBO	Teaching-Learning-Based Optimization	Rao et al. (2011)
HS	Harmony Search	Geem et al. (2001)
DTBO	Driving Training-Based Optimization	Ibrahim et al. (2021)
EMA	Exchange Market Algorithm	García-Borroto et al. (2014)
LCA	League Championship Algorithm	Rahimian et al. (2014)

Swarm Intelligence (SI) algorithms mimic the collective behavior of social organisms such as insects, birds, and fish. These methods utilize decentralized interactions among individuals to explore the search space efficiently.

(c) **Physics-Based Algorithms**

Physics-based meta-heuristics draw inspiration from natural physical phenomena and laws, such as gravitational forces, thermodynamics, and electromagnetic interactions. These methods simulate physical processes to optimize solutions.

(d) **Human-Based Algorithms**

Unlike the previously mentioned categories, human-based meta-heuristics are inspired by human behavior, decision-making processes, and learning mechanisms rather than natural phenomena. These algorithms model social and cognitive interactions to enhance optimization performance.

In conclusion, optimization algorithms provide a diverse range of methodologies for solving complex optimization problems. Classical approaches offer precise solutions but struggle with scalability, whereas AI-based techniques, particularly meta-heuristics, offer greater flexibility and efficiency. Understanding the different categories of optimization algorithms helps in selecting the most suitable method for a given problem, ensuring optimal performance in real-world applications.

2.6 Multi-Objective Optimization Problems (MOPs)

Optimization problems that require optimizing more than one objective simultaneously are referred to as Multi-Objective Optimization Problems (MOPs). These problems yield multiple optimal solutions rather than a single one [74].

Solving an MOP involves determining a decision variable vector $\mathbf{x} = \{x_1, x_2, \dots, x_n\}$ (decision space) that optimizes a vector of objective functions:

$$\mathbf{f}(\mathbf{x}) = \{f_1(x), f_2(x), \dots, f_n(x)\}$$

2.6.1 Objective function space

While satisfying a set of constraints, which may include equality constraints $h_i(x)$ or inequality constraints $g_i(x)$. The feasible solution space is bounded by the limits x_{min} and x_{max} , which define the search space for each decision variable [75].

The general mathematical formulation of an MOP is expressed in Eq. (2.6) [76]:

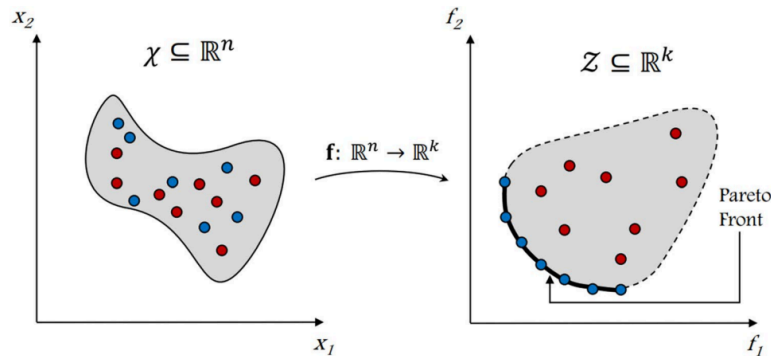


Figure 2.4: Regions of a design problem with two-variable and two objective functions [13]

$$\begin{aligned}
 \min \mathbf{f}(\mathbf{x}) &= \{f_1(\mathbf{x}), f_2(\mathbf{x}), \dots, f_n(\mathbf{x})\}, \\
 \text{subject to: } & h_i(\mathbf{x}) = 0, \quad i = 1, 2, \dots, p, \\
 & g_i(\mathbf{x}) \leq 0, \quad i = 1, 2, \dots, q, \\
 & x_{min} \leq \mathbf{x} \leq x_{max}.
 \end{aligned} \tag{2.6}$$

2.6.2 Pareto-Optimality in MOPs

Unlike single-objective optimization, where an absolute optimal solution exists, MOPs result in a set of optimal solutions known as **Pareto-optimal solutions**. According to Rao [77], a solution \mathbf{X} is Pareto-optimal if there is no other feasible solution \mathbf{Y} such that:

$$f_i(\mathbf{Y}) \leq f_i(\mathbf{X}), \quad \forall i = 1, 2, \dots, k,$$

with at least one strict inequality for some objective function j , meaning:

$$f_j(\mathbf{Y}) < f_j(\mathbf{X}).$$

This means that no feasible solution can improve one objective without deteriorating another, leading to a trade-off situation.

A commonly used approach to evaluate solutions in MOPs is the **Pareto Dominance Relationship**, which does not aim to find a single best solution but rather identifies a diverse set of non-dominated solutions forming the **Pareto Front (PF)** [66]. Each solution on the Pareto front represents an optimal trade-off, and the final selection depends on the decision-maker's preference.

Figures 2.4 and 2.4 illustrates the difference between the decision variable space and the objective function space, and and True Pareto front, highlighting non-dominated solutions (Pareto-optimal solutions) in blue.

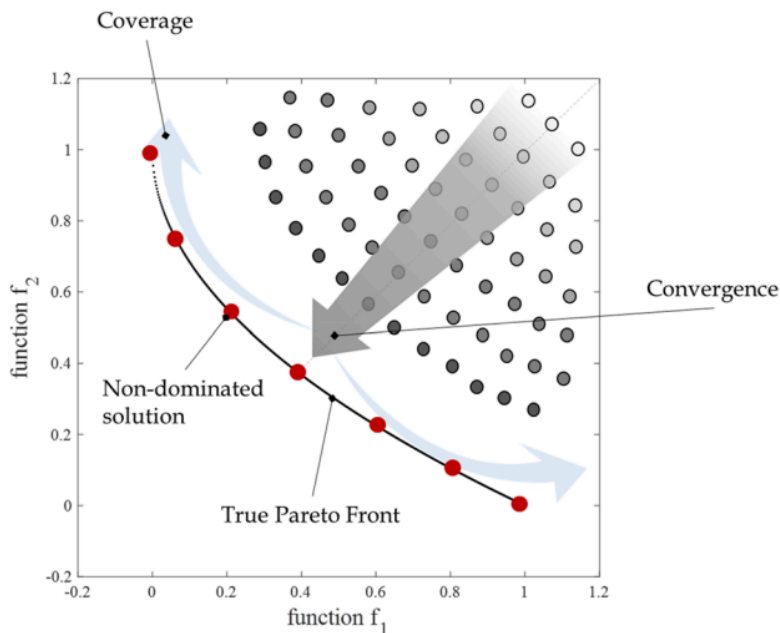


Figure 2.5: Non-dominated solutions and True Pareto front [13]

2.6.3 Characteristics of Pareto Fronts

The process of finding Pareto-optimal solutions is iterative, refining an initial approximation of the Pareto front over successive generations. Depending on the nature of the optimization problem, Pareto fronts can be **continuous or discontinuous (disconnected)**, **convex or concave** [78].

A multi-objective optimization problem is considered **convex** if both the feasible region and the objective functions are convex, leading to a convex Pareto front. If either the feasible region or one of the objectives is non-convex, the problem is considered **concave**, which may result in a Pareto front that is concave or even disconnected.

Not all regions of the objective function space are feasible; certain areas may contain no solutions due to inherent constraints, causing discontinuities in the Pareto front [66]. Figures 2.4,2.5 visually represents these discontinuities.

2.6.4 Essential Aspects of Multi-Objective Optimization

In **single-objective optimization**, the performance of meta-heuristic algorithms depends on their ability to balance **exploration** (avoiding local optima) and **exploitation** (refining known solutions) [79].

In **multi-objective optimization**, however, additional considerations come into play. A good multi-objective optimization algorithm must ensure:

1. **Precision (convergence)**: The solutions should be as close as possible to the true Pareto front.

2. **Diversity (coverage)**: The solutions should be well-distributed across the Pareto front.

This ensures that decision-makers have a broad range of trade-offs to choose from. Figures 2.4,2.5 illustrates these two essential properties in a Pareto front.

2.7 Key Approaches to Multi-Objective Problems

Several methodologies have been proposed to tackle Multi-Objective Problems (MOPs). These approaches are generally categorized based on when the decision maker (DM) provides their preferences during the optimization process as summarizing in the table 2.5. The four main categories include: **no preference methods**, **a priori methods**, **interactive methods**, and **a posteriori methods** [80].

2.7.1 No Preference Methods

No preference methods operate without requiring input from the DM. These techniques identify a single optimal solution that is typically positioned as close as possible to the ideal point.

2.7.1.1 Global Criterion Method

The **ideal point**, also known as the utopia solution, consists of the best achievable value for each objective function when optimized separately. This is mathematically represented in Eqs. (2.7) and (2.8) [66]:

$$f_i^0(x^{0i}) = \min f_i(x) \quad (2.7)$$

$$f^0 = [f_1^0, f_2^0, \dots, f_k^0]^T \quad (2.8)$$

Conversely, the **Nadir point** represents the worst values obtained for each objective function when optimized separately.

The optimal solution in this approach is given by:

$$L_p = \min \left(\sum_{i=1}^k |f_i(x) - f_i^0| \right)^{1/p} \quad (2.9)$$

where $f_i(x)$ represents the objective function values, and p determines the distance metric. Common choices include 1 (Manhattan), 2 (Euclidean), or ∞ (Chebyshev).

The main limitation of this method is its focus on a single solution, potentially ignoring other Pareto-optimal alternatives.

2.7.2 A Priori Preference Methods

A priori methods require the DM to specify preferences before the optimization begins. Limitations include:

- Potential misjudgment of objectives due to incomplete understanding [81].
- Requirement for multiple runs to capture the full Pareto front.
- Risk of missing non-obvious trade-off solutions [82].

2.7.2.1 Lexicographic Method

Objectives are prioritized. Optimization begins with the highest priority and continues sequentially [83].

2.7.2.2 Goal Programming

This method minimizes the deviation from pre-set targets [84]:

$$\min \sum_{i=1}^k |f_i(x) - T_i| \quad (2.10)$$

Additional methods: Min-Max Optimization [85], Multi-Attribute Utility Theory [86], ELECTRE [87], PROMETHEE [88].

2.7.3 Interactive Preference Methods

Interactive methods iteratively refine DM preferences [89, 90]:

1. Generate non-dominated solutions.
2. Get feedback from DM and adjust weights.
3. Repeat until satisfactory results are achieved [80].

Examples: PROTRADE, STEP, SMP, ISWT, GDF, SPOT, Tchebycheff Method, Reference Point Method [66].

2.7.4 A Posteriori Preference Methods

These methods generate a broad set of Pareto-optimal solutions for post-optimization selection. They are widely adopted due to their comprehensiveness [70, 91].

2.7.4.1 Weighting Method

Transforms the problem using weighted sums:

$$\min \sum_{i=1}^k w_i f_i(x) \tag{2.11}$$

Weights w_i must satisfy $\sum w_i = 1$. This method struggles with non-convex fronts.

2.7.4.2 ϵ -Constraint Method

Optimizes one objective while treating others as constraints [92]:

$$\begin{aligned} & \text{minimize} && f_l(x) \\ & \text{subject to} && f_j(x) \leq \epsilon_j, \quad j \neq l \end{aligned} \tag{2.12}$$

2.7.4.3 Normal Boundary Intersection (NBI)

Improves solution spread along the Pareto front [78]:

$$\max_{(x)} D \quad \text{s.t.} \quad \Phi w + D\eta = F(x) \tag{2.13}$$

2.7.4.4 TOPSIS

Technique for Order of Preference by Similarity to Ideal Solution (TOPSIS): Ranks solutions by proximity to ideal and distance from worst case [93]:

$$P_i = \frac{S_i^-}{S_i^+ + S_i^-} \tag{2.14}$$

where S_i^+ and S_i^- are Euclidean distances from the ideal and worst solutions.

Each preference method brings unique benefits. Choosing the right one depends on when decision input is available and the complexity of the objectives involved.

Table 2.5: Classification of MOO Approaches Based on Preference Timing

Category	Decision Timing	Representative Methods
No Preference	Before Optimization	Global Criterion Method
A Priori	Before Optimization	Lexicographic Method, Goal Programming, Min-Max Optimization, Utility Theory, ELECTRE, PROMETHEE
Interactive	During Optimization	Reference Point Method, Surrogate Worth Trade-Off, STEP Method, SMP, ISWT, GDF, Tchebycheff Method)
A Posteriori	After Optimization	Weighting Method, ϵ -Constraint Method, NBI, TOPSIS

2.8 Multi-Objective Optimization Algorithms

Multi-objective optimization (MOO) problems often require specialized algorithms capable of producing a diverse set of trade-off solutions. These algorithms are designed to find non-dominated (Pareto-optimal) solutions that balance conflicting objectives. Over the years, a wide range of meta-heuristic algorithms have been adapted or developed specifically for this purpose. These can be broadly classified into several categories: evolutionary algorithms, swarm-based algorithms, trajectory-based algorithms, immune-inspired methods, deterministic approaches, and nature-inspired algorithms.

2.8.1 Evolutionary Algorithms

Evolutionary Algorithms (EAs) are among the earliest and most widely used meta-heuristics for MOO. They simulate natural selection using operators such as selection, crossover, and mutation to evolve a population of candidate solutions. Notable examples include:

- **SPEA** – Strength Pareto Evolutionary Algorithm [?]
- **NSGA-II** – Non-dominated Sorting Genetic Algorithm II [94]
- **MOEA/D** – Multi-Objective Evolutionary Algorithm based on Decomposition [?]
- **PAES** – Pareto Archived Evolution Strategy [?]
- **VEGA** – Vector Evaluated Genetic Algorithm [95]

These algorithms are favored for their ability to maintain solution diversity and generate Pareto fronts in a single run.

2.8.2 Swarm-Based Algorithms

Swarm-based algorithms are inspired by the collective behavior of social organisms. They are decentralized and use population-based heuristics. Popular examples include:

- **MOPSO** – Multi-Objective Particle Swarm Optimization [96]
- **MOAQ** – Multi-Objective Ant-Q [97]
- **MOGWO** – Multi-Objective Grey Wolf Optimizer [?]
- **MOALO** – Multi-Objective Ant Lion Optimization [70]
- **MOSOA** – Multi-Objective Seagull Optimization Algorithm [98]

2.8.3 Trajectory-Based Algorithms

These algorithms explore the search space through a single candidate solution and iteratively refine it. Well-known trajectory-based methods for MOO include:

- **SAMO** – Simulated Annealing for Multi-Objective Optimization [99]
- **MOTS** – Multi-Objective Tabu Search [100]

2.8.4 Immune-Inspired Algorithms

Inspired by biological immune systems, these algorithms are known for their diversity preservation. An example is:

- **AIS** – Artificial Immune Systems [101]

2.8.5 Nature-Inspired Algorithms

These draw from natural phenomena beyond traditional biology, such as light propagation or plant behavior. Examples include:

- **MOSFO** – Multi-Objective Sunflower Optimization [102]
- **MO-SCA** – Multi-Objective Sine-Cosine Algorithm [103]
- **MOGOA** – Multi-Objective Grasshopper Optimization Algorithm [70]

2.8.6 Deterministic Approaches

These methods transform the multi-objective problem into a single-objective problem or use systematic decision-making rules. Key methods include:

- **NBI** – Normal Boundary Intersection [78]
- **E-Constraint** – ϵ -Constraint Method [92]
- **Weighting** – Weighting Method [93]

A comprehensive comparison of these algorithms is presented in Table 2.6, classifying them by their underlying inspiration and strategy.

Table 2.8 highlights the trade-offs between convergence, diversity, and computational complexity across various multi-objective optimization algorithms. Evolutionary algorithms such as NSGA-II and MOEA/D demonstrate strong convergence capabilities and balanced diversity, making them suitable for a wide range of applications. Swarm-based

methods like MOALO and MOPSO offer competitive performance with lower computational overhead, making them practical for time-sensitive problems. Deterministic methods like NBI are effective in convergence but often lack diversity, which can limit their exploratory capabilities. In contrast, simpler techniques such as the weighting method may be computationally efficient but are generally unsuitable for capturing complex Pareto fronts. These comparisons emphasize the need to align algorithm choice with problem-specific requirements, including dimensionality, objective interaction, and runtime constraints.

2.9 Conclusion

This chapter presented an extensive discussion on optimization problems, emphasizing their fundamental mathematical formulations, essential properties, and classification criteria. We analyzed various aspects that characterize optimization problems, including the nature of decision variables, the number of objectives, constraints, and computational complexity. Furthermore, we explored different solution strategies, contrasting classical optimization methods with modern AI-based techniques, while highlighting their respective strengths and weaknesses.

A clear understanding of these optimization methodologies is crucial for addressing real-world challenges, as selecting an appropriate approach significantly influences the quality of the solution and computational feasibility. The concepts and classifications outlined in this chapter provide a strong theoretical foundation for solving complex optimization problems effectively.

In the subsequent chapter, we will shift our focus to the LED placement problem in indoor VLC systems. We will examine its core objectives, associated constraints, and optimization difficulties. Additionally, we will review existing optimization methods applied in the literature, offering a critical perspective that will guide the development of our proposed solutions.

Table 2.6: Multi-Objective Optimization Algorithms

Acronym	Category	Full Name	Reference
Evolutionary Algorithms			
SPEA	Evolutionary	Strength Pareto Evolutionary Algorithm	Zitzler & Thiele (1999)
NSGA-II	Evolutionary	Non-dominated Sorting Genetic Algorithm II	Deb et al. (2002)
MOEA/D	Evolutionary	Multi-Objective Evolutionary Algorithm based on Decomposition	Zhang & Li (2007)
PAES	Evolutionary	Pareto Archived Evolution Strategy	Knowles & Corne (2000)
VEGA	Evolutionary	Vector Evaluated Genetic Algorithm	Schaffer (1985)
Swarm-Based Algorithms			
MOPSO	Swarm-Based	Multi-Objective Particle Swarm Optimization	Mostaghim & Teich (2003)
AWPSO	Swarm-Based	Adaptive Weighted Particle Swarm Optimization	Mahfouf et al. (2004)
MOAQ	Swarm-Based	Multi-Objective Ant-Q	Mariano et al. (1999)
MOALO	Swarm-Based	Multi-Objective Ant Lion Optimization	Mirjalili (2018)
MOGWO	Swarm-Based	Multi-Objective Grey Wolf Optimizer	Mirjalili et al. (2014)
MOSOA	Swarm-Based	Multi-Objective Seagull Optimization Algorithm	Dhiman (2021)
Trajectory-Based Algorithms			
SAMO	Trajectory-Based	Simulated Annealing for Multi-Objective Optimization	Serafini (1994)
MOTS	Trajectory-Based	Multi-Objective Tabu Search	Gandibleux & Freville (1997)

Table 2.7: Multi-Objective Optimization Algorithms

Acronym	Category	Full Name	Reference
Immune-Based Algorithms			
AIS	Immune-Based	Artificial Immune Systems	Coello Coello (2005)
Nature-Inspired Algorithms			
MOSFO	Nature-Inspired	Multi-Objective Sunflower Optimization	Pereira et al. (2022)
MO-SCA	Nature-Inspired	Multi-Objective Sine-Cosine Algorithm	Tawhid et al. (2019)
MOGOA	Nature-Inspired	Multi-Objective Grasshopper Optimization Algorithm	Mirjalili (2018)
Deterministic Methods			
NBI	Deterministic	Normal Boundary Intersection	Das & Dennis (1998)
E-Constraint	Deterministic	ϵ -Constraint Method	Haimes et al. (1971)
Weighting	Deterministic	Weighting Method	Hwang & Masud (1979)

Table 2.8: Comparison of Multi-Objective Optimization Algorithms

Algorithm	Category	Convergence	Diversity	Complexity
NSGA-II	Evolutionary	High	Good	Medium
MOEA/D	Evolutionary	High	Moderate	Medium
SPEA	Evolutionary	Moderate	Moderate	Medium
PAES	Evolutionary	Moderate	High	Low
MOPSO	Swarm-Based	Good	Good	Low
MOAQ	Swarm-Based	Good	Moderate	Medium
MOALO	Swarm-Based	High	High	Medium
SAMO	Trajectory-Based	Low	Low	Low
MOTS	Trajectory-Based	Moderate	Moderate	Medium
AIS	Immune-Based	Moderate	High	Medium
NBI	Deterministic	High	Low	High
Weighting	Deterministic	Low	Low	Low
E-Constraint	Deterministic	Moderate	Low	Medium

CHAPTER 3

AN IMPROVED APPROACH FOR SOLVING THE LEDS PLACEMENT PROBLEM IN INDOOR VLC SYSTEM

3.1 Introduction

Optimizing LED placement in indoor Visible Light Communication (VLC) systems is a crucial challenge that significantly influences network performance, particularly in terms of coverage and throughput. The efficiency of VLC networks relies on the strategic deployment of LEDs to ensure uniform illumination while maximizing data transmission rates. However, due to the NP-hard nature of this problem, finding an optimal solution within a reasonable computational time-frame remains a complex task. Meta-heuristic methods often struggle with scalability and convergence efficiency when applied to large-scale VLC optimization problems.

To tackle these challenges, this chapter explores the application of enhanced meta-heuristic algorithms, specifically the Enhanced Whale Optimization Algorithm (EWOA). This advanced optimization technique integrates chaotic maps [104,105] and Opposition-Based Learning (OBL) [106] to improve the exploration and exploitation capability, thereby enhancing search efficiency and accelerating convergence speed.

This chapter begins by detailing the LEDs Placement Problem in Indoor VLC Systems, and the advanced optimization techniques used in EWOA, emphasizing their modifications and improvements over standard meta-heuristic method. We then discuss their application to the LED placement problem, demonstrating how this method optimizes network coverage and throughput. Finally, we present simulation results, analyzing the impact of varying the number of LEDs and users, and provide a comparative evaluation against state-of-the-art optimization algorithms.

3.2 LEDs Placement Problem in Indoor VLC System

Visible Light Communication (VLC) is an emerging wireless technology that employs Light Emitting Diodes (LEDs) as both illumination sources and data transmitters. As an alternative to traditional Radio Frequency (RF) communication, VLC provides several advantages, including high-speed data transfer, enhanced security, and energy efficiency. These attributes make VLC particularly beneficial for indoor environments, such as residences, offices, and public facilities, where optimized system performance is essential. However, the strategic placement of LEDs significantly influences the overall efficiency and reliability of VLC systems.

The arrangement of LEDs directly impacts key performance metrics, including signal strength, coverage area, and data transmission rates. Factors such as room dimensions, obstacles, and user movement introduce additional challenges such as interference, shadowing, and uneven signal distribution. To achieve a balance between providing sufficient illumination and ensuring robust data transmission, precise LED placement is required.

An effective LED placement strategy aims to maximize uniform illumination, enhance signal coverage, and minimize interference and dead zones. Improper placement can lead to uneven illumination, signal degradation, and reduced communication efficiency. Therefore, optimizing LED positioning requires mathematical modeling and optimization techniques that account for variables such as ceiling height, room layout, and user mobility. Utilizing such methodologies allows engineers to improve VLC system performance, mitigating signal disruptions due to reflections, shadows, and interference.

The study of LED placement strategies is critical in the development of high-performance VLC systems. Researchers leverage advanced optimization models that consider spatial constraints, lighting requirements, and communication parameters to ensure an optimal trade-off between illumination and data transmission. As VLC technology progresses, further refinements in LED placement techniques will be necessary to achieve high-throughput, interference-free, and energy-efficient communication in diverse indoor settings.

3.2.1 System Model

We consider a standard indoor VLC system, represented as V , which operates within an empty conference room with dimensions $D \times W \times H$, as depicted in Figure 3.1. The room is equipped with multiple LEDs, serving as access points, and randomly distributed receiving users equipped with photo-detectors (PDs).

- L represents a set of N LEDs, defined as $L = \{L_1, L_2, \dots, L_N\}$, positioned on the ceiling at locations (x_i, y_i, z_i) , where $i \in (1, 2, 3, \dots, N)$.

- U denotes a set of M users, represented as $U = \{U_1, U_2, \dots, U_M\}$, where each user is equipped with a PD acting as a wireless receiver.

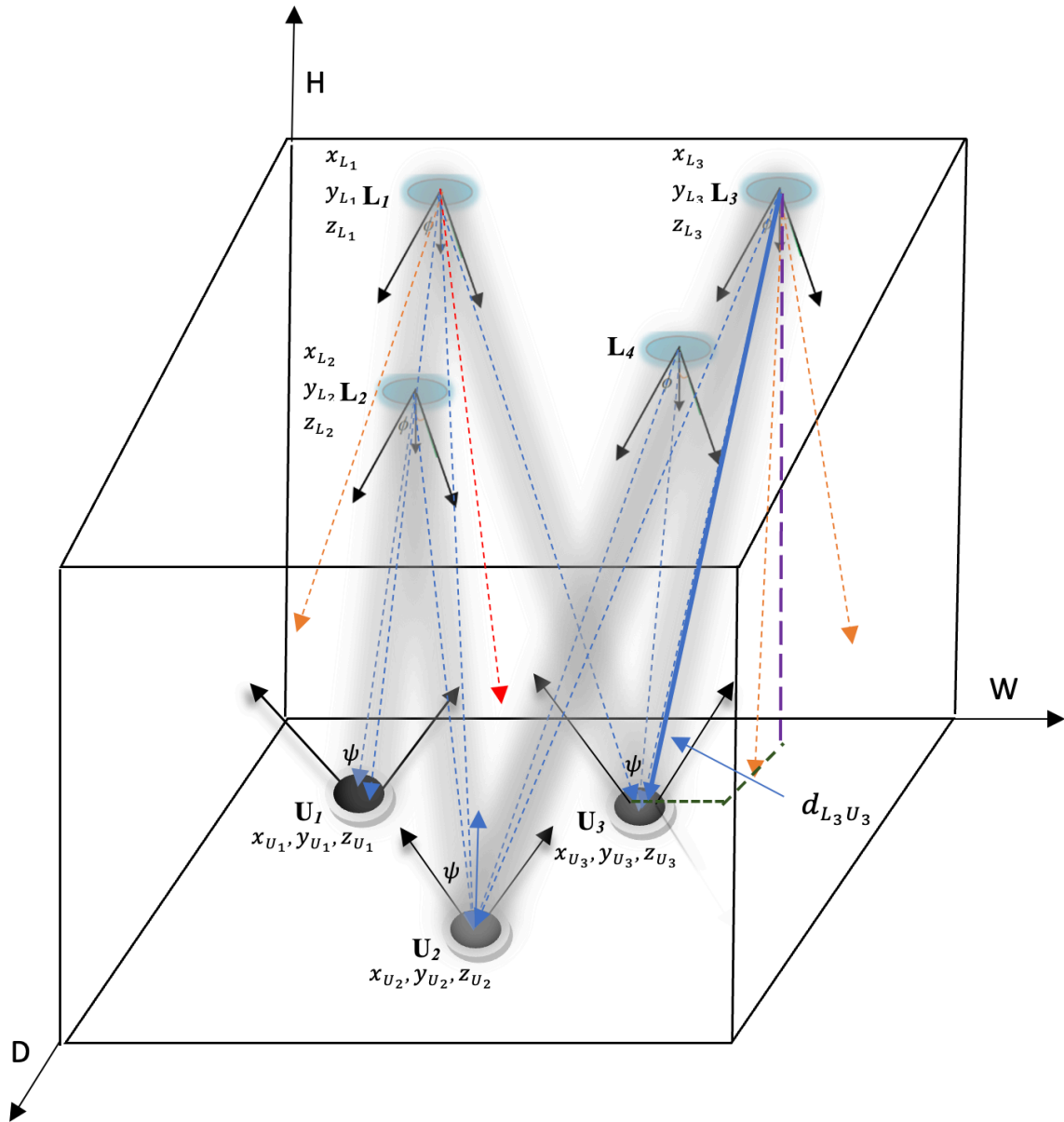


Figure 3.1: Indoor VLC Room Model

3.2.1.1 Channel Model

LEDs are modeled as Lambertian radiation sources, where the channel gain between the i^{th} LED and j^{th} user follows the Lambertian propagation model, given by Eq. 3.1 and depicted in Figure 3.2 [107]:

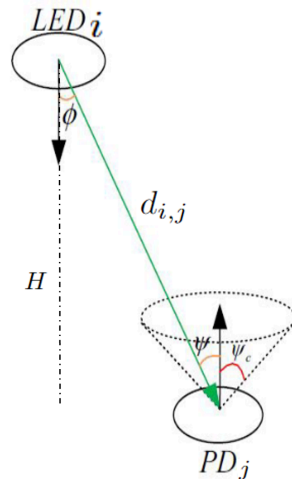


Figure 3.2: Channel model of visible light transmission

$$H(0)_{ij} = \begin{cases} \frac{(m+1)A}{2\pi d_{ij}^2} \cos^m(\phi_i) T_s(\psi_j) g(\psi_j) \cos(\psi_j), & \text{if } 0 \leq \psi_j \leq \psi_c \\ 0, & \text{if } \psi_j > \psi_c \end{cases} \quad (3.1)$$

where:

- m represents the Lambertian order, calculated as:

$$m = -\log 2 / \log (\cos (\phi_{1/2})) \quad (3.2)$$

where $\phi_{1/2}$ is the LED's half-power angle. - A is the photo-detector's active area. - d_{ij} is the distance between the i^{th} LED and the j^{th} user. - ϕ_i and ψ_j denote the radiation angle and incident angle, respectively. - $T_s(\psi_j)$ represents the gain of the optical filter. - $g(\psi_j)$ is the optical concentrator gain, calculated as:

$$g(\psi_j) = \begin{cases} \frac{n^2}{\sin^2(\psi_c)}, & 0 \leq \psi_j \leq \psi_c \\ 0, & \psi_j > \psi_c \end{cases} \quad (3.3)$$

where n is the refractive index of the optical concentrator. If P_{t_i} is the transmit power of the i^{th} LED, the received power at the j^{th} PD is given by:

$$P_{r_{ij}} = P_{t_i} \times H(0)_{ij} \quad (3.4)$$

The end-to-end signal-to-noise ratio (SNR) is defined in Eq. 3.5 [108]:

$$SNR_{ij} = \frac{(R \cdot P_{r_{ij}})^2}{\sigma_t^2} \quad (3.5)$$

where R is the photo-detector responsivity, and σ_t represents the total noise variance. Each user U_j is associated with a single LED L_i based on the highest received power.

3.2.2 Mathematical Model

To optimize VLC system performance, we consider two primary objectives:

1. Maximizing Coverage: Coverage is determined by the diffusion of transmitted power from LEDs, computed as:

$$Cov(V) = \sum_{j=1}^M \max_{i \in \{1, \dots, N\}} (Cov_{U_j}^{L_i}) \quad (3.6)$$

where $Cov_{U_j}^{L_i}$ represents the coverage of user U_j by LED L_i . A user is considered covered if its SNR exceeds a predefined threshold (P^{th}):

$$Cov_{U_j}^{L_i} = \begin{cases} 1, & \text{if } SNR_{ij} > P^{th} \\ 0, & \text{otherwise} \end{cases} \quad (3.7)$$

2. Maximizing Network Throughput: The total network throughput is given by:

$$Tr(V) = \sum_{j=1}^M \max_{i \in \{1, \dots, N\}} (Tr_{U_j}^{L_i}) \quad (3.8)$$

where the throughput for each user U_j , connected to LED L_i , is calculated using:

$$Tr_{U_j}^{L_i} = B \times \log_2(1 + SNR_{ij}) \quad (3.9)$$

where B denotes the system bandwidth.

3.2.2.1 The objective function Formulation

The optimization goal is to maximize both coverage and throughput while adhering to system constraints:

$$\text{Maximize } f = (\lambda) \left(\frac{Cov(V)}{M} \right) + (1 - \lambda) \left(\frac{Tr(V)}{M \times Tr^{th}} \right) \quad (3.10)$$

$$\begin{aligned} \text{Subject to : } & SNR_{ij} \geq P^{th} \\ & 0 \leq x_i \leq W, \quad 0 \leq y_i \leq D \end{aligned} \quad (3.11)$$

where λ is a weighting coefficient balancing coverage and throughput objectives.

3.3 PRELIMINARIES

3.3.1 Whale Optimizer Algorithm (WOA)

Inspired by the unique hunting strategy of humpback whales, Mirjalili et al. [109] introduced the Whale Optimizer Algorithm (WOA) in 2016. This meta-heuristic optimization

technique is based on the whales' natural ability to encircle prey, create spiral-shaped bubble nets, and effectively trap their targets.

Humpback whales utilize an intelligent hunting mechanism by surrounding their prey, using their flippers to generate a bubble net, and eventually restricting the preys movement. This behavior is modeled mathematically in WOA, incorporating three main phases: encircling prey, bubble-net attacking, and searching for prey. The following subsections detail the mathematical representation of these mechanisms.

3.3.1.1 Encircling Prey

When hunting, humpback whales continuously update their positions relative to the best-known solution in their search space. As the algorithm iterates, the whales adjust their positions toward the current optimal solution. The mathematical representation of this behavior is given by:

$$\vec{D} = \left| \vec{C} \cdot \vec{X}^*(t) - \vec{X}(t) \right| \quad (3.12)$$

$$\vec{X}(t+1) = \vec{X}^*(t) - \vec{A} \cdot \vec{D} \quad (3.13)$$

where t represents the current iteration, \vec{X}^* is the position vector of the best solution found so far, and \vec{X} is the position of a given whale. The absolute difference is represented by $||$. The coefficient vectors \vec{A} and \vec{C} regulate the movement towards the best solution and are defined as follows:

$$\vec{A} = 2 \cdot \vec{a} \cdot \vec{r} - \vec{a} \quad (3.14)$$

$$\vec{C} = 2 \cdot \vec{r} \quad (3.15)$$

where \vec{a} linearly decreases from 2 to 0 over iterations, controlling the transition between exploration and exploitation. The term \vec{r} is a randomly generated vector in the range $[0,1]$.

3.3.1.2 Bubble-Net Attacking Mechanism

The bubble-net attack is modeled using two strategies:

- **Shrinking Encircling Mechanism:**

This approach is achieved by gradually reducing the value of \vec{a} in Eq. 3.14, allowing the search agents to adjust their positions dynamically within a specific range around the best solution. When \vec{A} takes random values within $[-1,1]$, the search agents can move towards the best-known solution with varying intensities.

- **Spiral Updating Position:**

Humpback whales often follow a logarithmic spiral motion while moving towards their prey. This movement is expressed mathematically as:

$$\vec{X}(t+1) = \vec{D}' \cdot e^{bl} \cdot \cos(2\pi l) + \vec{X}^*(t) \quad (3.16)$$

where \vec{D}' is the distance between the whale and the best solution, b is a constant defining the shape of the logarithmic spiral, and l is a randomly generated number in $[-1,1]$.

To model the ****combined effect of these two behaviors****, a probability factor p is introduced to choose between shrinking encircling and spiral updating at each iteration:

$$\vec{X}(t+1) = \begin{cases} \vec{X}^*(t) - \vec{A} \cdot \vec{D} & \text{if } p \leq 0.5 \\ \vec{D}' \cdot e^{bl} \cdot \cos(2\pi l) + \vec{X}^*(t) & \text{if } p > 0.5 \end{cases} \quad (3.17)$$

where p is a random value between 0 and 1.

3.3.1.3 Search for Prey

During the ****exploration phase****, whales search for prey by randomly selecting a search agent and moving toward it. This behavior helps maintain diversity in the search space and avoids premature convergence. The mathematical representation of this phase is given by:

$$\vec{D} = |\vec{C} \cdot \overrightarrow{X_{\text{rand}}} - \vec{X}| \quad (3.18)$$

$$\vec{X}(t+1) = \overrightarrow{X_{\text{rand}}} - \vec{A} \cdot \vec{D} \quad (3.19)$$

where $\overrightarrow{X_{\text{rand}}}$ represents a randomly selected whale position from the current population.

3.3.1.4 Whale Optimizer Algorithm Pseudocode

The overall process of WOA is summarized in Algorithm 1 [109], which outlines the initialization, iterative optimization steps, and final output of the algorithm.

3.3.2 Chaotic Map

Chaos theory provides a deterministic framework for understanding the behavior of dynamic and nonlinear systems. This approach is characterized by key properties such as

Algorithm 1 The Pseudo-code of WOA Algorithm

```

0: Initialize: the whale's population  $X_i$  ( $i = 1, 2, \dots, n$ )
0: Calculate: Calculate the fitness of each search agent
0:  $X^*$  = the best search agent
0: while  $t <$  maximum number of iterations do
0:   for each search agent do
0:     Update  $a, A, C, l$ , and  $p$ 
0:     if  $p < 0.5$  then
0:       if  $|A| < 1$  then
0:         Update the position of the current search agent by Eq. (7)
0:       else if  $|A| \geq 1$  then
0:         Select a random search agent ( $X_{\text{rand}}$ )
0:         Update the position of the current search agent by Eq. (15)
0:       end if
0:     else if  $|A| \geq 0.5$  then
0:       Update the position of the current search agent by Eq. (11)
0:     end if
0:   end for
0:   Check if any search agent goes beyond the search space and amend it
0:   Calculate the fitness of each search agent
0:   Update  $X^*$  if there is a better solution
0:    $t = t + 1$ 
0: end while
0: return  $X^* = 0$ 

```

unpredictability, irregularity, boundedness, non-repetition, stochastic ergodicity, and aperiodicity. These features have led to the development of various mathematical functions known as chaotic maps, which are commonly used for generating randomized parameters in meta-heuristic algorithms. By incorporating chaotic maps into meta-heuristics, the convergence rate is accelerated, the exploration ability is enhanced, and the risk of getting stuck in local optima is minimized.

Several chaotic maps have been proposed in the literature, including the Tent map, Gauss map, Sine map, Logistic map, Circle map, Sinusoidal map, Piecewise map, Iterative map, and Chebyshev map [104, 105]. Among these, the Sine map is widely used due to its simplicity and strong ability to generate highly dynamic random sequences.

The mathematical representation of the Sine map is given as:

$$SM_{k+1} = \frac{ac}{4} \sin(\pi SM_k), 0 \leq SM_k \leq 1 \quad (3.20)$$

where:

- SM_k represents the chaotic value at the k^{th} iteration, constrained within the range $[0,1]$.
- ac is a control parameter influencing the chaotic behavior, with $0 < ac \leq 4$.

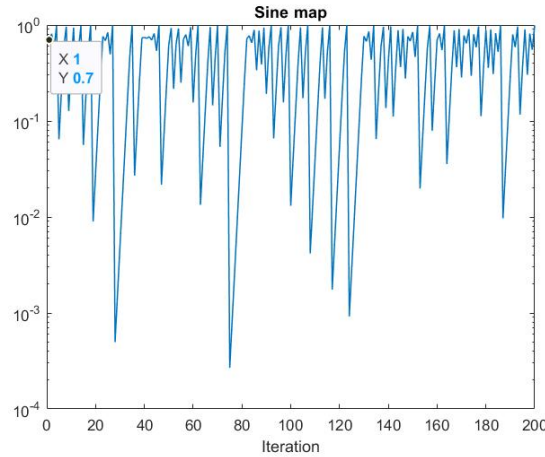


Figure 3.3: Chaotic value distributions over 200 iterations

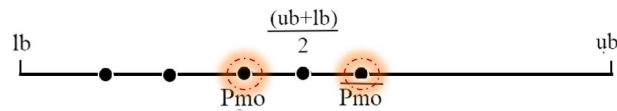


Figure 3.4: The point Pmo and its corresponding opposite in a one-dimensional search space.

For our experimental implementation, we set $ac = 4$ to induce fully chaotic behavior in the Sine map, ensuring maximum randomness and diversity in the generated values.

3.3.3 Opposition-Based Learning

Opposition-Based Learning (OBL) was first introduced by Tizhoosh in 2005 [106] and has since been widely adopted in the fields of machine learning and computational intelligence. This strategy has been effectively integrated with various meta-heuristic optimization algorithms to improve convergence rates and enhance exploration within the search space. The core idea of OBL is to simultaneously consider both a candidate solution and its opposite, thereby increasing the likelihood of reaching an optimal solution more efficiently.

The mathematical formulation of the opposite number for a given real number $Pmo \in [lb, ub]$ is expressed as:

$$Pmo^{\bar{}} = ub + lb - Pmo \quad (3.21)$$

In a one-dimensional search space, the opposite point is calculated similarly to the reflection of a point across the midpoint $(lb + ub)/2$, as illustrated in Figure 3.4.

The concept of OBL can be extended to a multidimensional search space, as defined by the following equation:

$$Pmo_i^{\bar{}} = ub_i + lb_i - Pmo_i, \quad i = 1, 2, \dots, d \quad (3.22)$$

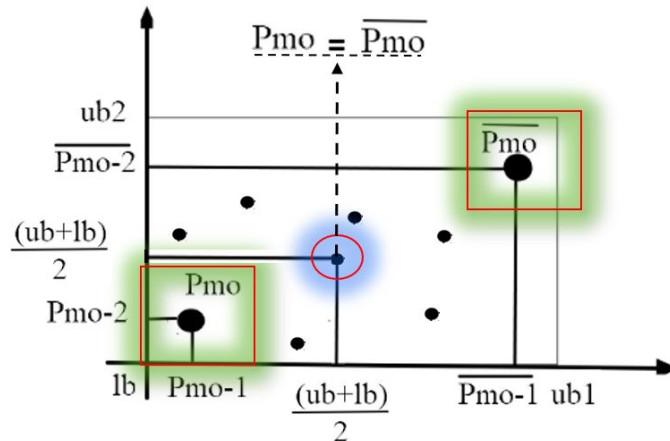


Figure 3.5: Illustration of the point P_{mo} and its opposite in a two-dimensional search space.

where $\bar{P}_{mo} \in R^d$ represents the opposite vector corresponding to the real vector $P_{mo} \in R^d$.

Figure 3.5 visualizes the concept of opposition in a two-dimensional search space, where both the original point and its opposite counterpart are considered to enhance the search process.

3.4 The Proposed EWOA for Solving the LEDs Placement Problem

One of the primary limitations of the standard WOA is its relatively slow convergence rate, as noted in [110]. To address this issue and enhance the algorithm's overall efficiency, we integrate two key strategies: Opposition-Based Learning (OBL) and Chaos Theory. These modifications significantly refine the exploration and exploitation phases, leading to improved global convergence speed.

First, OBL is employed to accelerate convergence and enhance the exploration of the search space. Second, chaotic maps are integrated into WOA to prevent stagnation in local optima and further improve convergence speed.

The pseudo-code of EWOA is provided in Algorithm 2, while Figure ?? presents its flowchart.

The EWOA follows the fundamental steps of the original WOA with a few key enhancements:

- **Opposition-Based Learning (OBL):** After generating an initial set of random solutions, we compute their opposite solutions using the OBL mechanism. The fitness values of both the original and opposite solutions are evaluated, and the best n solutions from this combined set $(\bar{X} \cup X)$ are retained for subsequent iterations.

- **Chaos-Based Parameter Adjustment:** The parameter p from Eq. (12) is dynamically adjusted using a Sine chaotic map throughout the optimization process. The updated equation is expressed as follows:

$$\vec{X}(t+1) = \begin{cases} \vec{X}^*(t) - \vec{A} \cdot \vec{D} & \text{if } p_i \leq 0.5 \\ \vec{D}' \cdot e^{bl} \cdot \cos(2\pi l) + \vec{X}^*(t) & \text{if } p_i \geq 0.5 \end{cases} \quad (3.23)$$

$$p_{i+1} = \frac{ac}{4} \sin(\pi p_i), \quad (3.24)$$

where p_i represents the chaotic map value of parameter p at iteration i , constrained within the range $[0,1]$. The control parameter ac is set to 4, with an initial value of $p_0 = 0.7$.

Algorithm 2 The pseudo-code of EWOA algorithm

```

0: Initialize: the whales population randomly  $X_i$  ( $i = 1, 2, \dots, n$ ).
0: Calculate: the Opposite  $\tilde{X}$  of the whale population.
0: Calculate: the fitness of each search agent  $X_i$  and Opposite  $\tilde{X}_i$ , and select the  $n$ 
   best from  $X_i \cup \tilde{X}_i$ .
0:  $X^* \leftarrow$  the best current from the  $n$  best.
0: Initialize: the value of the sine chaotic map.
0: while  $t <$  maximum number of iterations do
0:   Update: the chaotic value using Eq. (20).
0:   for each search agent do
0:     Update  $a$ ,  $A$ ,  $C$ , and  $I$ .
0:     Adjust the parameter  $p$  using the sine chaotic value (Eq. 20).
0:     if  $p < 0.5$  then
0:       if  $|A| < 1$  then
0:         Update the position of the current search agent using Eq. (7).
0:       else if  $|A| \geq 1$  then
0:         Select a random search agent ( $X_{\text{rand}}$ ).
0:         Update the position of the current search agent using Eq. (15).
0:       end if
0:     else
0:       Update the position of the current search agent using Eq. (11).
0:     end if
0:   end for
0:   Check if any search agent goes beyond the search space and amend it.
0:   Calculate the fitness of each search agent.
0:   Update  $X^*$  if there is a better solution.
0:    $t \leftarrow t + 1$ .
0: end while
0: Return  $X^*$ . =0

```

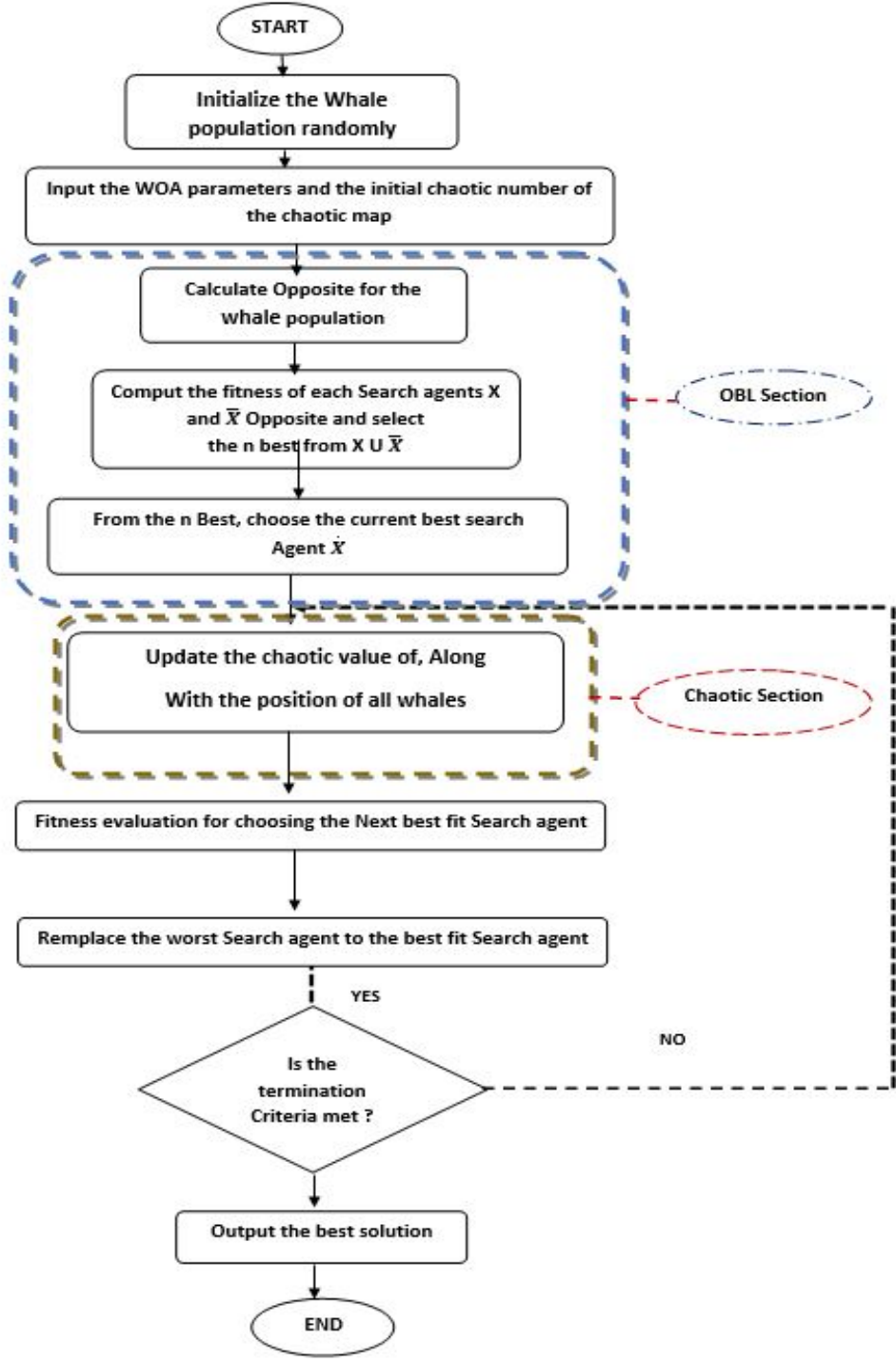


Figure 3.6: Flowchart of EWOA

Table 3.1: Coverage, mean throughput, and fitness under various values of number of LEDS and Users

number of LEDS	2	3	4	5	6	7	8	9	number of Users	5	10	15	20	25	30	35	40
Coverage (%)									Coverage (%)								
EWOA	58.8	76.22	88	95.44	98.2	100	100	100	EWOA	100	100	100	97.14	90.2	83.45	79.33	76.11
WOA	60.44	72.88	80.22	88.88	94.44	97.22	96.88	99.22	WOA	100	100	96.74	91.64	85.14	80.85	75.54	73.46
BA	51.11	60.77	69.11	79	80.55	84.44	87.33	85.22	BA	100	95.47	87.11	85.16	80	79.11	72.28	72
PSO	62.4	73.84	89.1	92.61	98	100	100	100	PSO	100	100	100	95	88.14	85.11	79.3	78.44
MRFO	58.7	63.45	73.1	85	95.8	97	100	100	MRFO	100	94.8	90	84	81.5	77.14	73.11	72
CHIO	59.22	75.66	87.11	94.55	97.33	100	100	100	CHIO	100	100	98.37	91.12	88.73	86.44	81.33	77.64
MPA	57.1	71.44	83.33	90	95.4	99	100	100	MPA	100	100	98.14	93.44	87.5	83.52	78.44	77.21
Mean throughput per user (Mbps)									Mean throughput per user (Mbps)								
EWOA	0.69	1.32	1.74	2.94	4.23	6.1	7.14	8.33	EWOA	18.3	12.44	10.84	7.71	4.44	3.33	2.63	2.1
WOA	0.65	1.30	1.59	1.94	2.48	2.48	4.26	4.87	WOA	13.35	9.73	7.70	5.21	3.50	2.09	1.84	2.62
BA	0.60	1.27	1.57	1.63	2.20	2.28	2.30	2.35	BA	6.50	5.26	4.27	3.31	2.64	1.68	1.48	1.41
PSO	0.71	1.34	1.59	2.15	2.84	3.23	4.87	5.1	PSO	17.4	13.11	10.2	7.31	4.14	3.11	2.87	2.24
MRFO	0.61	1.15	1.43	1.86	2.3	2.57	3.7	4.21	MRFO	7.4	6.81	6.1	3.62	2.91	2.14	1.81	1.44
CHIO	0.52	1.28	1.68	3.07	4.03	5.89	7.05	8.86	CHIO	16.41	12.88	9.08	6.09	4.42	3.19	2.83	2.56
MPA	0.62	1.21	1.89	2.63	3.8	4.2	4.33	4.83	MPA	14.3	9.45	9.03	8.32	5.74	3.51	2.92	1.84
Fitness									Fitness								
EWOA	0.36	0.42	0.45	0.51	0.57	0.58	0.60	0.64	EWOA	0.69	0.65	0.59	0.52	0.48	0.49	0.46	0.46
WOA	0.30	0.30	0.41	0.45	0.48	0.50	0.51	0.52	WOA	0.58	0.56	0.54	0.50	0.46	0.45	0.45	0.43
BA	0.26	0.31	0.35	0.40	0.41	0.43	0.44	0.44	BA	0.54	0.53	0.46	0.44	0.41	0.40	0.40	0.38
PSO	0.39	0.41	0.47	0.48	0.53	0.55	0.57	0.61	PSO	0.67	0.61	0.53	0.54	0.51	0.50	0.48	0.46
MRFO	0.27	0.33	0.37	0.44	0.46	0.47	0.49	0.51	MRFO	0.55	0.51	0.50	0.48	0.46	0.42	0.41	0.40
CHIO	0.31	0.39	0.46	0.49	0.52	0.53	0.54	0.55	CHIO	0.60	0.58	0.56	0.54	0.52	0.49	0.49	0.48
MPA	0.28	0.34	0.36	0.41	0.45	0.49	0.52	0.53	MPA	0.63	0.59	0.53	0.50	0.49	0.47	0.47	0.45

3.4.1 Simulation Results

This section evaluates the effectiveness of the Enhanced WOA (EWOA) algorithm in optimizing the placement of LEDs. We compare its performance with standard WOA, BA, PSO, MRFO, MPA, and CHIO algorithms.

All algorithms were implemented in MATLAB and tested on a Core i5-4310U processor (2.6 GHz) with 12GB RAM.

Figures 1 and 2 illustrate the typical room layout used for our simulations. The performance of EWOA was assessed based on two key metrics: mean throughput and coverage per user across 16 different test scenarios. These scenarios varied in terms of the number of LEDs (ranging from 2 to 9) and the number of users (ranging from 5 to 40). Each result reported in this chapter represents the average of 30 independent runs, with a total of 1000 iterations per run. The simulation parameters used for this study are detailed in Table 3.1.

3.4.2 Discussion and Analysis

To examine the impact of LED and user density on network performance, we conducted two sets of experiments:

1. Effect of Varying the Number of LEDs: In this experiment, the number of LEDs was increased from 2 to 9, while keeping the number of users fixed at 30. The corresponding results are presented in Table II and Figure 4. The findings reveal that as the number of LEDs increases, both throughput and coverage improve significantly. This effect becomes particularly pronounced when more than 7 LEDs are deployed, leading to nearly complete coverage of all users. Under these conditions, EWOA consistently outperforms the other algorithms in terms of both metrics.

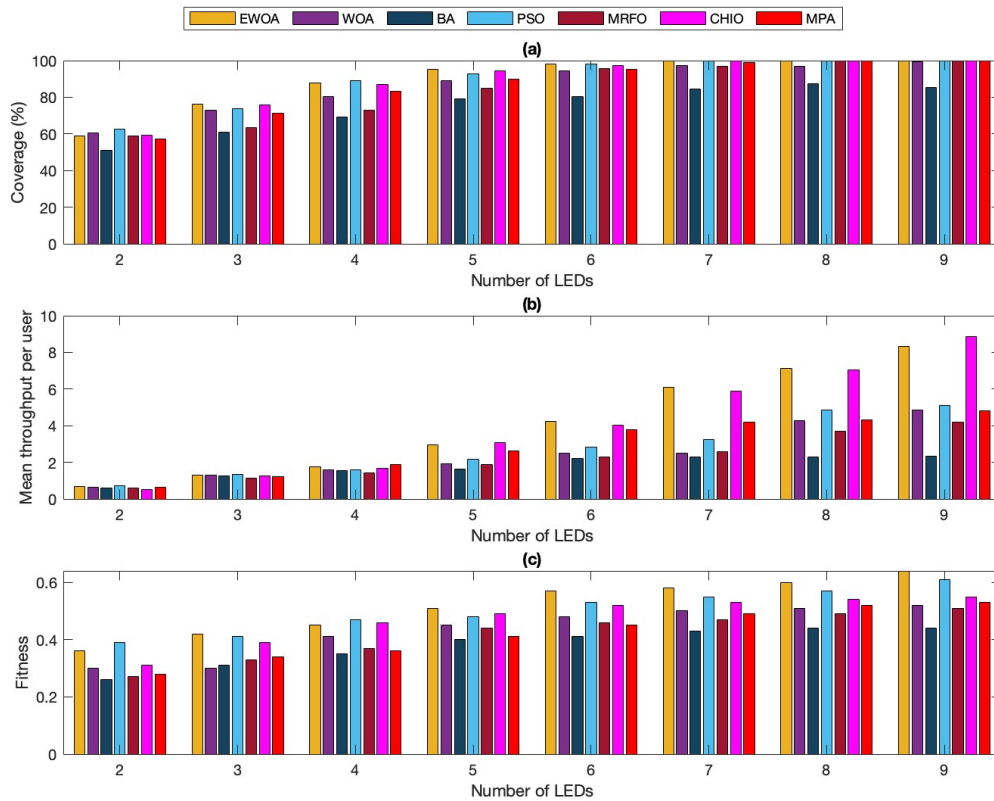


Figure 3.7: Coverage (a), Throughput (b) and Fitness (c) under various numbers of LEDs

2. Effect of Varying the Number of Users: In the second set of experiments, the number of users was varied from 5 to 40, while keeping the number of LEDs constant at 30. The results, shown in Table III and Figure 5, indicate that as the number of users increases, both coverage and throughput decline due to resource contention. However, despite this performance drop, EWOA still delivers superior results compared to other algorithms, maintaining better network coverage and throughput across most scenarios.

This analysis underscores the importance of optimizing the number of LEDs to achieve high system performance. Additionally, it highlights the need for robust optimization techniques such as EWOA to efficiently manage the challenges posed by increasing user density while maintaining effective coverage and high throughput.

3.5 Conclusion

One of the critical challenges in VLC systems is the strategic placement of LEDs in indoor environments. This aspect directly influences network coverage, data throughput, and overall signal quality. In this chapter, we introduced the LED placement problem as

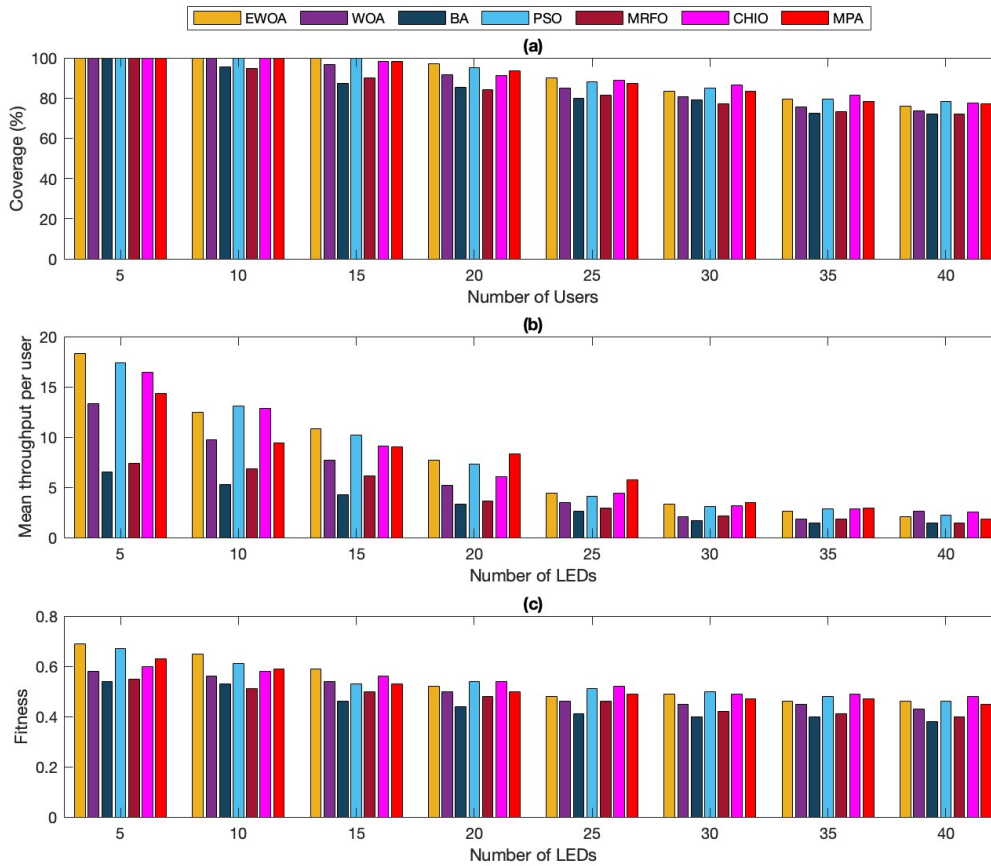


Figure 3.8: Coverage (a), Throughput (b) and Fitness (c) under various numbers of Users

a key factor affecting VLC performance.

Given the NP-hard nature of this problem, necessitating the use of advanced optimization techniques. We introduced and applied enhanced meta-heuristic algorithms to optimize the LED placement problem in VLC systems, addressing challenges related to coverage and throughput. We explored the Enhanced Whale Optimization Algorithm (EWOA), and integrate chaotic maps and Opposition-Based Learning (OBL) to improve search efficiency and convergence speed.

Our simulation results demonstrated that EWOA consistently outperformed traditional optimization methods, achieving better coverage and higher throughput across various scenarios. We analyze the impact of varying the number of LEDs and users, revealing that an optimal balance of these parameters is crucial to maximize the efficiency of the VLC network.

Overall, the findings presented in this chapter establish a strong foundation for future research on meta-heuristic optimization techniques in VLC systems. Future work will focus on hybrid meta-heuristic approaches, to further improve adaptability and efficiency in VLC environments.

CHAPTER 4

A HYBRID APPROACH FOR SOLVING THE LEDS PLACEMENT PROBLEM IN INDOOR VLC SYSTEM

4.1 Introduction

Visible Light Communication (VLC) systems have emerged as a promising technology for high-speed indoor wireless networks, leveraging LEDs as both illumination sources and data transmitters. However, optimizing the placement of LEDs is crucial to ensuring maximized network coverage, improved data throughput, and enhanced signal quality. Due to the non-line-of-sight (NLOS) limitations, multi-path fading, and user distribution variability, optimization techniques struggle to efficiently solve this nonlinear, multi-modal, and high-dimensional problem. As a result, meta-heuristic algorithms have gained increasing attention for their ability to provide effective and computationally efficient solutions.

This chapter explores hybrid meta-heuristic approach for solving the LED placement problem in indoor VLC systems, focusing on a powerful hybrid optimization techniques.

Our proposed meta-heuristic algorithm called "Hybrid Coronavirus Herd Immunity Optimizer (ICHIO-FA)" integrates the Coronavirus Herd Immunity Optimizer (CHIO) with the Firefly Algorithm (FA) to enhance exploration and exploitation capabilities. The CHIO framework ensures an efficient global search using chaotic maps for increased solution diversity, while Opposition-Based Learning (OBL) speeds up convergence. FA serves as a local search operator to fine-tune solutions, ensuring higher precision and better placement decisions.

This hybrid approach aim to maximize coverage, throughput, and improve system performance by striking a balance between global and local search mechanisms. Through comprehensive simulations under various LED configurations, user densities, and PD areas, we demonstrate the effectiveness of these hybrid techniques in outperforming state-of-the-art optimization algorithms such as CHIO, PSO, GA, MPA, WOA, MRFO, BA,

GWO, and SA.

This chapter provides a detailed analysis of our hybrid approach, discussing their implementation, optimization mechanisms, and performance in solving the LED placement problem. The results highlight the potential of hybrid meta-heuristics in enhancing VLC network design, paving the way for more efficient and adaptive LED deployment strategies in next-generation communication systems.

4.1.1 Coronavirus Herd Immunity Optimizer (CHIO)

The Coronavirus Herd Immunity Optimizer (CHIO), introduced by Al-Betar in 2021 [111], is a human-based optimization algorithm inspired by the concept of herd immunity and social distancing strategies observed in viral outbreaks. This algorithm has been successfully applied to various optimization problems due to its adaptability and efficiency.

CHIO simulates the natural progression of a population through different infection stages, including infection, susceptibility, immunity, and fatality. The optimization process is carried out through five key steps, which are explained below.

Step 1: Initialization of Parameters

In this step, the control parameters of CHIO are initialized. These include:

- The initial number of infected individuals (C_0),
- The basic reproduction rate (BR_r),
- The maximum age of infected cases (Max_{age}),
- Other essential parameters required for the search process.

Step 2: Population Initialization

The optimization process begins by randomly generating the herd immunity population X . This population is structured as a matrix of size $n_p \times d$, where:

- n_p represents the population size (total number of individuals),
- d denotes the number of decision variables (dimensions of the search space).

The population matrix is represented mathematically as:

$$\mathbf{X} = \begin{bmatrix} X_1^1 & X_1^2 & \cdots & X_1^d \\ X_2^1 & X_2^2 & \cdots & X_2^d \\ \vdots & \vdots & \cdots & \vdots \\ X_{n_p}^1 & X_{n_p}^2 & \cdots & X_{n_p}^d \end{bmatrix} \quad (4.1)$$

Each decision variable X_i^j is randomly initialized within its respective lower (lb_j) and upper (ub_j) bounds as follows:

$$X_i^j = lb_j + rand \times (ub_j - lb_j) \quad (4.2)$$

where $rand$ is a randomly generated number in the range $[0,1]$.

Step 3: Population Evolution

At this stage, the population undergoes an evolutionary process that simulates the spread of infection. Based on the basic reproduction rate (BR_r) and specific rules, the position of each individual X_i^j is updated using the following equation:

$$X_i^j(t+1) \leftarrow \begin{cases} C(X_i^j(t)) & r < \frac{1}{3} \times BR_r \\ N(X_i^j(t)) & r < \frac{2}{3} \times BR_r \\ R(X_i^j(t)) & r < BR_r \end{cases} \quad (4.3)$$

where:

- $C(X_i^j(t))$ represents infected cases,
- $N(X_i^j(t))$ represents susceptible cases,
- $R(X_i^j(t))$ represents immune cases.

Each case is updated using the following equations:

$$C(X_i^j(t)) = X_i^j(t) + r \times (X_i^j(t) - X_i^c(t)) \quad (4.4)$$

$$N(X_i^j(t)) = X_i^j(t) + r \times (X_i^j(t) - X_i^m(t)) \quad (4.5)$$

$$R(X_i^j(t)) = X_i^j(t) + r \times (X_i^j(t) - X_i^v(t)) \quad (4.6)$$

where:

- r is a randomly generated number in the range $[0,1]$.
- $X_i^c(t)$ is a randomly selected value from infected cases.
- $X_i^m(t)$ is a randomly chosen value from susceptible cases.
- $X_i^v(t)$ is a randomly chosen value from the best immune cases.

Step 4: Updating the Population

Each individual in the population undergoes an evaluation, and its updated position $X_i^j(t+1)$ is accepted into the population if its fitness value is better than its previous value $X_i^j(t)$.

If the condition $S_i = 1$ (indicating a stagnant solution), the age counter of the individual is incremented.

Step 5: Handling Fatality Cases

A case is considered dead if its infection level $S_i = 1$ remains unchanged for the number of iterations specified by the Max_{age} parameter. When this happens:

- The individual is removed from the population.
- The age counter Max_{age} is reset to zero.
- A new random individual X_i is introduced into the search space.

This mechanism prevents premature convergence and helps maintain diversity in the population, increasing the algorithms effectiveness.

4.1.1.1 CHIO Algorithm Pseudocode

Algorithm 3 provides the pseudo-code for CHIO, outlining the initialization, infection spread, immunity development, and fatality handling mechanisms.

4.1.2 Firefly Optimization Algorithm (FA)

The Firefly Algorithm (FA) is a population-based meta-heuristic optimization technique introduced by X.S. Yang in 2007 [112]. This algorithm falls under the category of Swarm Intelligence (SI) meta-heuristics, similar to other bio-inspired algorithms such as Particle Swarm Optimization (PSO), Ant Colony Optimization (ACO), and Artificial Bee Colony (ABC) optimization. FA is specifically inspired by the natural behavior of fireflies, particularly their bioluminescent communication patterns, which they use for mate attraction, prey detection, and synchronization of movements [113].

The social interaction of fireflies in FA follows three fundamental principles [114]:

1. Fireflies are unisex, meaning they are mutually attracted to one another regardless of gender.
2. The degree of attraction between fireflies is directly related to their brightness, which decreases as the distance between them increases. A firefly with lower brightness moves towards a brighter firefly. If there is no brighter firefly nearby, movement is random within the search space.
3. The brightness of a firefly is determined by the objective function value at its position.

Algorithm 3 The pseudo-code of the CHIO Algorithm

0: **Input:**

- CHIO Parameters: $d, n_p, lb, ub, C_0, BR_r, Max_{age}, Max_{itr}$.

0: **Output:**

- X_{best} : the best solution and its objective value

0: { — **Step 1: Initialize the CHIO parameters** — }

0: initialize the parameters (S_r , and Max_{age})

0: { — **Step 2: Generate herd immunity population** — }

0: Calculate the fitness of each search agent

0: Set $S_j = 0$ for $j = 1, 2, \dots, d$. Set $A_j = 0$ for $j = 1, 2, \dots, d$.

0: { — **Step 3: Herd immunity evolution** — }

0: **while** $t < Max_{itr}$ **do**

0: **for** $j = 1$ to d **do**

0: $is_Corona(\mathbf{X}^j(t+1)) = \text{false}$

0: **for** $i = 1$ to n_p **do**

0: Evolve $\mathbf{X}_i^j(t+1)$ based on Eqs. 4.3, 4.4, 4.5, and 4.6.

0: **end for**

0: { — **Step 4: Update Herd immunity population** — }

0: **if** $(f(\mathbf{X}^j(t+1)) \leq f(\mathbf{X}^j(t)))$ **then**

0: $\mathbf{X}^j(t) = \mathbf{X}^j(t+1)$

0: **else**

0: $A_j = A_j + 1$

0: **end if**

0: **if** $(f(\mathbf{X}^j(t+1)) < \frac{f(\mathbf{X})^j(t+1)}{\Delta f(\mathbf{x})} \wedge S_j = 0 \wedge is_Corona(\mathbf{X}^j(t+1)))$ **then**

0: $S_j = 1, A_j = 1;$

0: **end if**

0: **if** $(f(\mathbf{X}^j(t+1)) > \frac{f(\mathbf{X})^j(t+1)}{\Delta f(\mathbf{X})} \wedge S_j = 1)$ **then**

0: $S_j = 2, A_j = 0;$

0: **end if**

0: { — **Step 5: Fatality Condition** — }

0: **if** $((A_j \geq Max_{Age}) \wedge (S_j == 1))$ **then**

0: $\mathbf{x}_i^j = lb_i + (ub_i - lb_i)U(0, 1), \forall i = 1, 2, \dots, N, S_j = 0, A_j = 0;$

0: **end if**

0: **end for**

0: Rank the new positions found based on their fitness value and determine the best position X_{best} .

0: $t = t + 1$

0: **end while**

0: **return** the best position $X_{best} = 0$

4.1.2.1 Initialization

Initially, fireflies are randomly distributed across the search space according to:

$$X_i = X_{min} + rand.(X_{max} - X_{min}), \quad i = 1, \dots, N \quad (4.7)$$

where:

- X_i represents the position of the i^{th} firefly,
- X_{min} and X_{max} define the lower and upper boundaries of the search space,
- N is the total number of fireflies in the population,
- $rand$ is a random number generated within the range $[0,1]$.

4.1.2.2 Attractiveness and Movement Mechanism

Fireflies' brightness (I) diminishes with increasing distance (r) due to light absorption. The mathematical representation of brightness decay is given by:

$$I = I_0.e^{-\gamma r^2} \quad (4.8)$$

where:

- I_0 is the initial brightness intensity,
- γ is the light absorption coefficient,
- r represents the Euclidean distance between two fireflies.

The distance (r_{ij}) between two fireflies i and j is calculated using the Euclidean distance formula:

$$r_{ij} = \|X_j - X_i\| = \sqrt{(y_j - y_i)^2 + (x_j - x_i)^2} \quad (4.9)$$

Attractiveness (β) is modeled using the following exponential decay function:

$$\beta = \beta_0 e^{-\gamma r^2} \quad (4.10)$$

where:

- β_0 represents the attractiveness at $r = 0$,
- γ controls the rate at which attractiveness decreases over distance.

4.1.2.3 Position Update Mechanism

A firefly at position X_i moves toward a more attractive firefly at position X_j based on:

$$X_i = X_i + \beta_0 e^{-\gamma r_{ij}^2} (X_j - X_i) + \alpha \left(\text{rand} - \frac{1}{2} \right) \quad (4.11)$$

where:

- α is a randomization parameter in the range $[0, 1]$,
- The term $\alpha(\text{rand} - \frac{1}{2})$ introduces random movement to maintain diversity in the search space.

This movement rule ensures that less bright fireflies move towards brighter ones while maintaining randomness, preventing stagnation in local optima.

The Firefly Algorithm efficiently balances exploration and exploitation by simulating the social interaction of fireflies. It allows fireflies to move toward promising solutions based on attractiveness and randomness. The pseudo-code of FA is presented in Algorithm 2.

Algorithm 4 The pseudo-code of Firefly Algorithm

```

0: Initialize the FA parameters: Maximum number of iterations  $T$ , Population' size  $N$ ,
   Dimension  $Dim$ ,  $\alpha, \beta_0, \gamma_0$ .
0: Initialize the population of FA:  $X_i (i = 1, 2, \dots, N)$ 
0: Evaluate the positions  $X_i$  and determine the best fitness  $I_{best}$ .
0: while ( $t < T$ ) do
0:   for  $i = 1, 2, \dots, N$  do
0:     for  $j = 1, 2, \dots, N$  do
0:       if  $I_j > I_i$  then
0:         Calculate the distance between the fireflies  $i$  and  $j$  using Equation (4.9)
0:         Calculate the attractiveness using Equation (4.10)
0:         Move the firefly  $i$  toward the firefly  $j$  using Equation (4.11)
0:       end if
0:     end for
0:   end for
0:   Rank the new positions found based on their fitness value and determine the best
   position  $X_{best}$ 
0:    $t = t + 1$ 
0: end while
0: return The best position  $X_{best} = 0$ 

```

4.2 Hybrid Coronavirus Herd Immunity Optimizer (ICHIO-FA)

Optimizing the placement of Light Emitting Diodes (LEDs) in indoor Visible Light Communication (VLC) systems is a challenging problem that significantly affects network performance in terms of coverage and throughput. VLC systems utilize LEDs as transmitters and Photo-Detectors (PDs) as receivers, enabling both illumination and data communication. However, determining the optimal LED placement is classified as an NP-Hard problem, making it computationally difficult to obtain exact solutions efficiently. To overcome this challenge, meta-heuristic approaches provide an effective alternative, leveraging intelligent search mechanisms to explore large solution spaces.

This chapter presents a hybrid meta-heuristic algorithm, ICHIO-FA, designed to optimize LED placement in VLC systems. The proposed approach integrates the Improved Coronavirus Herd Immunity Optimizer (ICHIO) with the Firefly Algorithm (FA), leveraging chaotic maps and Opposition-Based Learning (OBL) to enhance convergence speed, improve exploration-exploitation balance, and prevent premature convergence to local optima [115] [105]. FA is employed as a local search mechanism to refine solutions obtained by ICHIO, ensuring more precise LED positioning.

The contributions of this chapter include:

- Development of ICHIO-FA, a hybrid optimization approach that enhances CHIO with FA, OBL, and chaotic maps for the LED placement problem in VLC environments.
- Comprehensive experimental evaluation, comparing ICHIO-FA with CHIO and nine state-of-the-art optimization techniques, including PSO, GA, MPA, WOA, MRFO, BA, GWO, and SA.
- Analysis of key performance factors, including the impact of varying LED numbers, user density, and PD area, on VLC system performance.

The remainder of this section is structured as follows: Section 4.2.1 details the proposed ICHIO-FA algorithm. Simulation results and performance comparisons are analyzed in Section 4.2.2. Finally, Section 4.3 presents the conclusion and future research directions.

The main notations used in this chapter and their descriptions are listed in Table 4.1,

4.2.1 The Proposed ICHIO-FA Algorithm for Solving the LEDs Placement Problem

This section presents the implementation of the proposed ICHIO-FA algorithm, which is based on a hybridization of ICHIO and FA algorithms to optimize LEDs placement.

Three key enhancements are introduced to improve the standard CHIO algorithm.

Firstly, instead of using randomly generated values within the range $[0, 1]$, the sine map is employed, allowing better control over solution updates and enhancing the diversity of solutions. Secondly, to accelerate convergence and ensure an efficient search space exploration, the Opposition-Based Learning (OBL) strategy is integrated. Lastly, Firefly Algorithm (FA) is incorporated as a local search operator to refine solutions obtained from ICHIO, specifically applied in the fourth stage of the Herd Immunity Evolution step during each iteration.

The ICHIO-FA implementation follows several key steps, including initialization, herd immunity population generation, OBL strategy application, herd immunity evolution, solution update, and finalizing the optimal LED positions.

- **Step 1: Initialization**

In this step, the parameters for CHIO, FA, and the VLC system environment (V) are initialized. Additionally, the control parameter r , which regulates solution evolution in CHIO, is set to an initial value of $r_0 = 0.7$.

- **Step 2: Generating Herd Immunity Population**

The initial population (solutions) X_0 is generated based on the scenarios described in Table 4.3.

- **Step 3: OBL Strategy Application**

At each iteration, the OBL strategy is applied to the solutions X_0 using Eq. 4.12 to generate opposite solutions \bar{X} . Both X_0 and \bar{X} are then evaluated using the fitness function f . Based on the fitness values, the top d solutions from $\bar{X} \cup X_0$ are selected for the evolution phase. This constitutes the first improvement in ICHIO-FA.

$$\bar{X}_j = ub_j + lb_j - X_j, \quad j = 1, 2, \dots, d \quad (4.12)$$

- **Step 4: Herd Immunity Evolution**

In this step, the chaotic variation of parameter r is computed using Eq. 4.13. Additionally, FA is applied as a local search operator during the fourth case of the evolution condition, refining the solutions obtained by ICHIO. This step introduces the second and third improvements to ICHIO-FA. The chaotic value of r at iteration i is determined as follows:

$$r_{i+1} = \frac{ac}{4} \sin(\pi r_i) \quad (4.13)$$

The FA-based local search operator updates the position of the fireflies using Eq. 4.14:

Algorithm 5 The pseudo-code of the proposed ICHIO-FA Algorithm for LED's placement problem

0: **Input:**

- Parameters of CHIO, FA, and VLC System

0: **Output:**

- X_{best} : the best solution and its objective value

0: {— **Step 1: Initialize the CHIO, FA, VLC System, and chaos parameters**—}

0: Initialize the parameters ($BR_r, C_0, Max_{age}, r_0, \phi, \psi, Pt, R, \sigma_t, N, M, P^{th}, B, \lambda, lb, ub, d, n_p$)

0: {— **Step 2: Generate herd immunity population**—}

0: Generate the initial population X_0

0: **while** ($t < Max_{itr}$) **do**

0: {—**Step 3: OBL Strategy Section**—}

0: Calculate the opposite positions \bar{X} for X_0 available in the initial population using Eq: 4.12

0: Calculate the fitness $f(X)$ through Eq: 5.13 of each X_0, \bar{X} and select then, the d best $X^j, j = 1, 2, \dots, d$ from $X_0 \cup \bar{X}$.

0: Set $S_j = 0$ for $j = 1, 2, \dots, d$, Set $A_j = 0$ for $j = 1, 2, \dots, d$;

0: {— **Step 4: Herd immunity evolution**—}

0: **for** $j = 1$ to d **do**

0: $is_Corona(\mathbf{X}^j(t+1)) = \text{false}$

0: **for** $i = 1$ to n_p **do**

0: Determine the chaos value of the parameter r based on Eq: 4.13

0: **if** ($r < \frac{1}{3} \times BR_r$) **then**

0: $X_i^j(t+1) = C(X_i^j(t)), is_Corona(\mathbf{X}^j(t+1)) = \text{true};$

0: **else if** ($r < \frac{2}{3} \times BR_r$) **then**

0: $X_i^j(t+1) = N(X_i^j(t))$

0: **else if** ($r < BR_r$) **then**

0: $X_i^j(t+1) = R(X_i^j(t))$

0: **else**

0: Evolve X_i^j using FA equation 4.14

0: **end if**

0: **end for**

0: {— **Step 5: Solution update**—}

0: {— **Step 6: Fatality cases**—}

0: **end for**

0: Determine the candidate that produced the maximum objective and save it in X_{best}

0: $t = t + 1$

0: **end while**

0: Output the best solution from $X_{best} = 0$

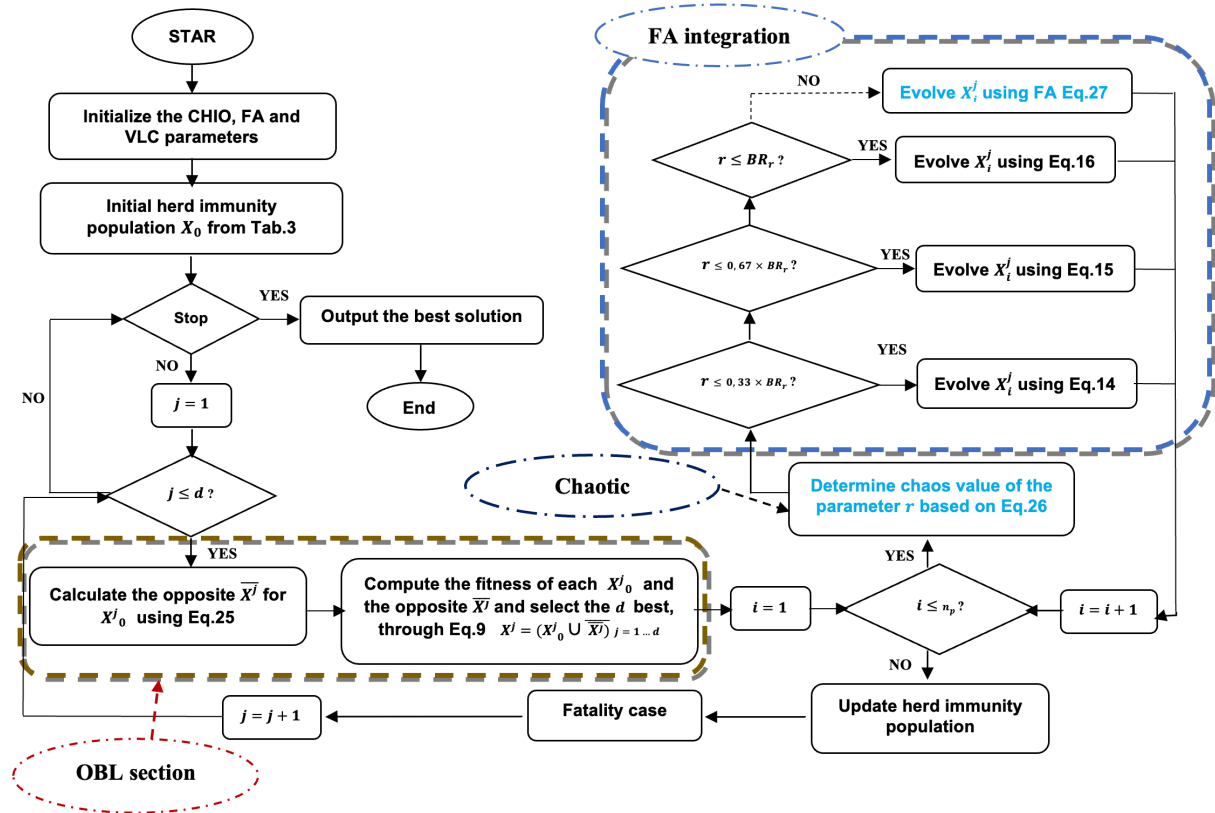


Figure 4.1: Flowchart of ICHO-FA

$$X_{i+1}^j = X_{i+1}^j + \beta_0 e^{-\gamma r_{ij}^2} (X_i^j - \hat{X}_{i+1}^j) + \alpha (\text{rand} - \frac{1}{2}) \quad (4.14)$$

where α is a randomization parameter, $\alpha \in [0, 1]$.

- **Step 5: Solution Update**

At this stage, ICHO-FA updates the solutions $X_{i..n_p}$ according to the three conditions outlined in Step 4 of the CHIO pseudo-code.

- **Step 6: Handling Fatality Cases**

This step applies the same rules as in CHIO to manage fatality cases in the solution population.

- **Output of Optimal LEDs Placement**

Steps 3 to 6 are repeated until the stopping condition is met. Once termination criteria are satisfied, the best-obtained solution is returned as the final LEDs placement. The optimal solution, determined by the objective function in Eq. 4.15, is then formatted into position coordinates:

$$X_{best} = \text{Maximize } f(X(t)) \quad (4.15)$$

$$X_{best} = \{L_1(x_1, y_1), L_2(x_2, y_2), \dots, L_N(x_N, y_N)\} \quad (4.16)$$

where N represents the number of LEDs, and (x, y) denote their respective coordinates.

Algorithm 5 presents the pseudo-code for the ICHIO-FA algorithm applied to the LEDs placement problem.

4.2.2 Simulation Results and Analysis

This section evaluates the performance of the proposed ICHIO-FA algorithm in optimizing LEDs placement. ICHIO-FA is compared against the original CHIO and nine well-established optimization algorithms, including FA, PSO, GA, MPA, WOA, MRFO, BA, GWO, and SA. All simulations were conducted on a Core i5 2.5 GHz CPU machine, with all algorithms implemented in MATLAB. The experimental setup assumes an empty conference room measuring $10m \times 10m \times 3m$, ensuring unobstructed line-of-sight (LOS) conditions. A typical representation of the room is shown in Figure 3.1. The complete set of simulation parameters is detailed in Tables 4.2, 4.5, and 4.3.

The performance of ICHIO-FA is assessed across multiple scenarios by varying key factors such as:

- The control parameter λ (ranging from 0 to 1),
- The number of LEDs (ranging from 1 to 10),
- The number of users (ranging from 5 to 40),
- The area of the photodetectors (PDs) (ranging from $0.6e^{-4}$ to $1.3e^{-4}$).

The evaluation considers three key performance metrics: coverage, mean throughput per user, and fitness value. Each simulation runs for 1000 iterations, and the reported results represent the average of 30 independent runs. The findings are summarized in Tables 4.4 and 4.6.

4.2.2.1 Impact of the Control Parameter λ

This section analyzes how varying the control parameter λ (between 0 and 1) affects coverage, mean throughput per user, and fitness metrics. The results are summarized in Table 4.4 and Figure 4.2.

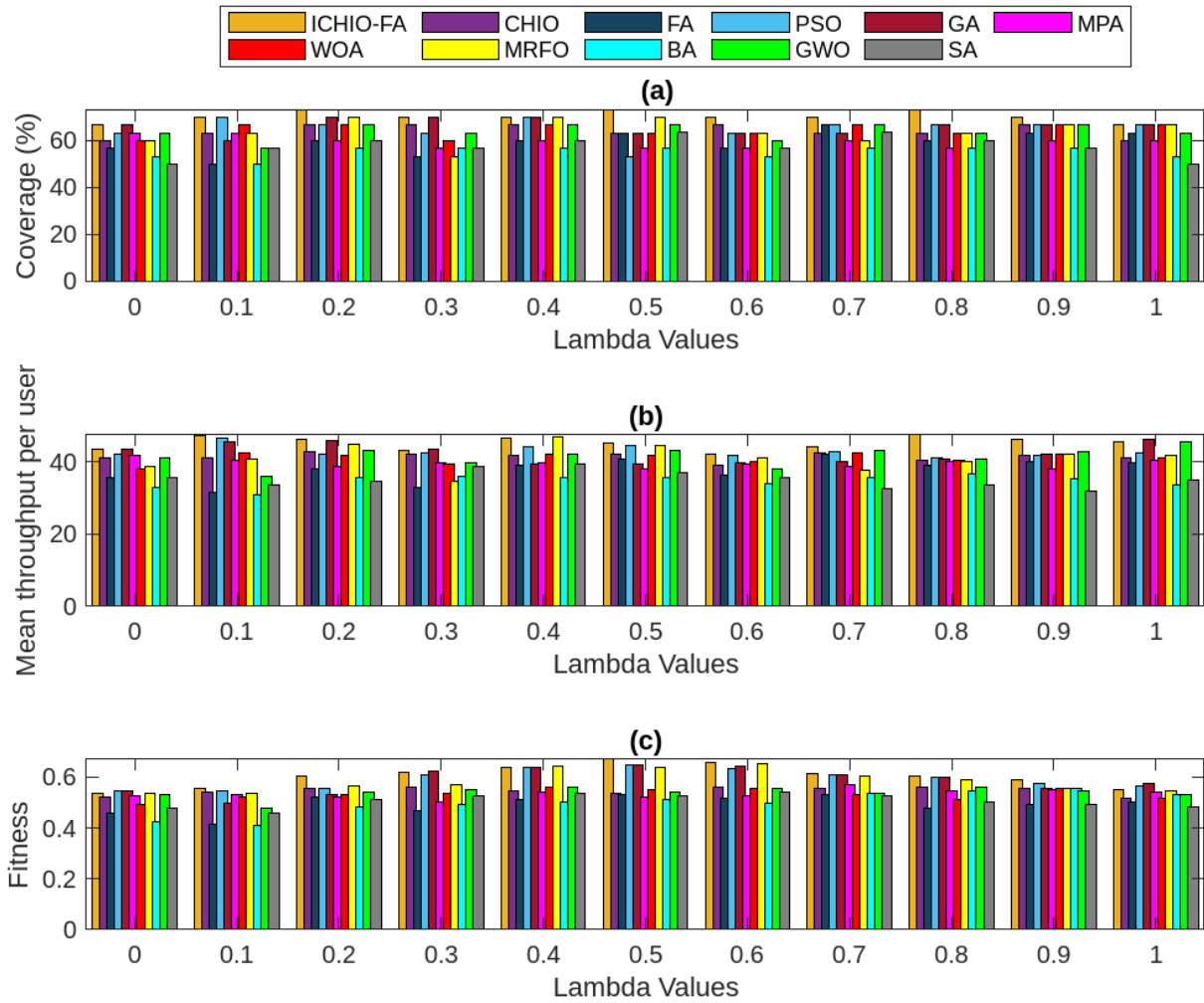


Figure 4.2: Coverage, Throughput and Fitness under various values of Lambda

Table 4.5: Simulation parameters of VLC System

Simulation Parameter	Value	Default Value
Number of users M	[5 40]	30
Number of LEDs N	[1 10]	5
Width W	10 m	
Length D	10 m	
Height H	3 m	
Population size n	30	
Number of runs R	30	
Number of iteration t_{max}	1000	
Area of a PD A	$[0.6e^{-4} \ 1.3e^{-4}]$	$1e^{-4}$

From Table 4.4 and Figures 4.2(a), 4.2(b), and 4.2(c), it is evident that changing λ produces consistent trends across most algorithms with minor variations. However, ICHIO-FA consistently outperforms the other algorithms in terms of coverage, mean throughput per user, and fitness. For instance, ICHIO-FA achieves a coverage range of [66.66% - 73.33%], compared to GWO, which attains only [60% - 66.66%]. Similarly, ICHIO-FA achieves a mean throughput range of [43.17 Mbps - 47.73 Mbps], surpassing GAs range of [39.35 Mbps - 46.49 Mbps]. Additionally, ICHIO-FA attains a fitness range of [0.536 - 0.671], whereas FA achieves a narrower range of [0.414 - 0.530]. Based on these observations, a value of $\lambda = 0.5$ is selected for subsequent experiments to maintain a balanced emphasis on both coverage and throughput.

4.2.2.2 Impact of Varying the Number of LEDs

This section examines how changing the number of LEDs (from 1 to 10) affects the system's performance while keeping the number of users fixed at 30. The results are presented in Table 4.6 and Figure 4.3.

Figure 4.3(a) illustrates the impact of increasing the number of LEDs on coverage. As expected, increasing the number of LEDs enhances coverage, eventually reaching full coverage when deploying more than 9 LEDs with the ICHIO-FA algorithm. This is because additional LEDs provide more light sources, increasing the likelihood that users receive adequate illumination. Among the compared algorithms, ICHIO-FA consistently achieves full coverage at 8 LEDs, while CHIO and GA require at least 10 LEDs to reach the same level.

Figure 4.3(b) depicts the effect of LED count on mean throughput per user. The results show that throughput improves as more LEDs are deployed, enhancing the signal-to-noise ratio (SNR). Notably, when increasing the LED count from 9 to 10, ICHIO-FA boosts throughput from 63.73 Mbps to 65.09 Mbps, while PSO improves from 62.04 Mbps to 64.84 Mbps.

Figure 4.3(c) displays the fitness scores for all tested algorithms. Fitness improves

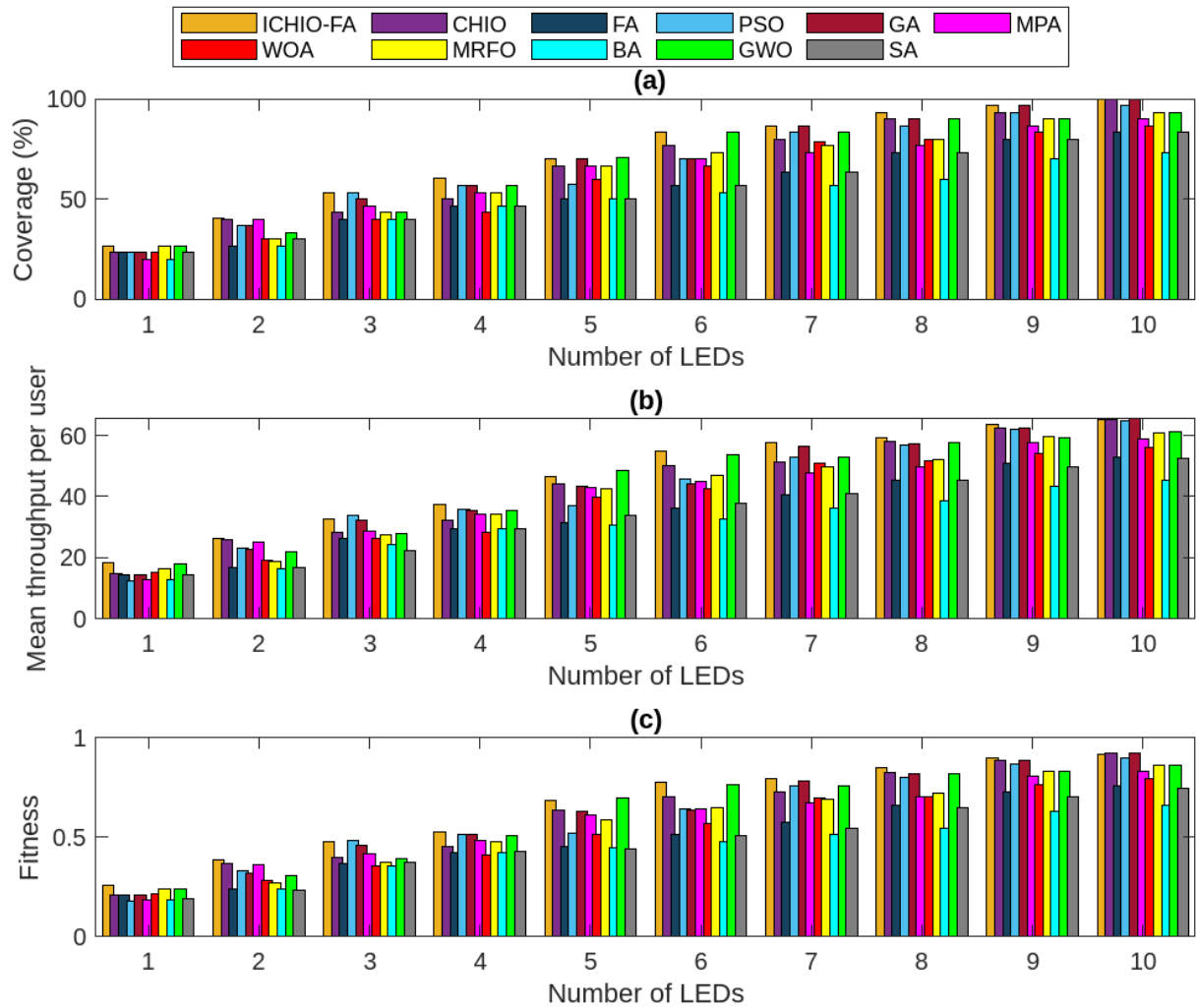


Figure 4.3: Coverage (a), Throughput (b) and Fitness (c) under various numbers of LEDs

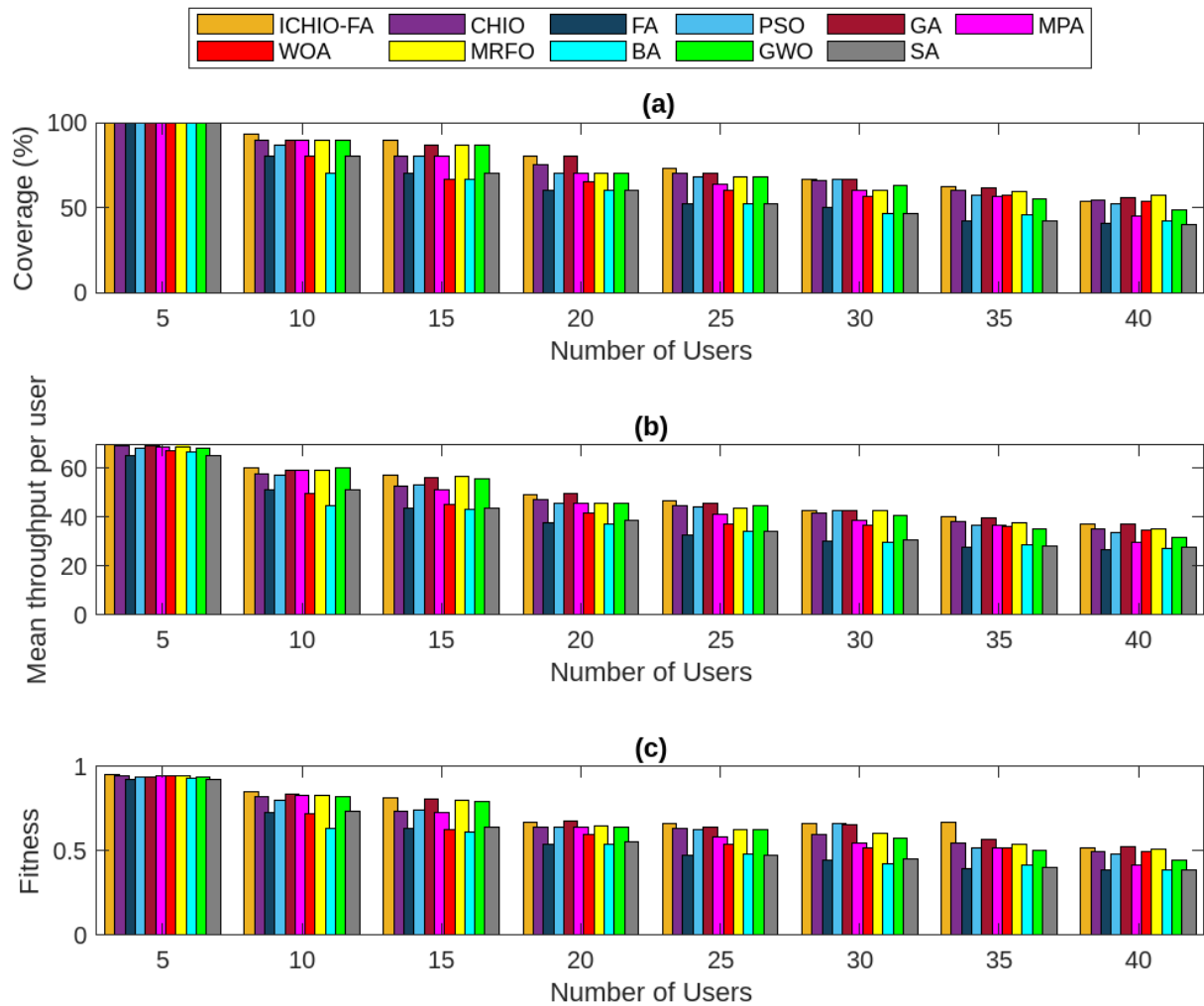


Figure 4.4: Coverage (a), Throughput (b) and Fitness (c) under various number of Users

with the number of LEDs, with ICHIO-FA outperforming competitors in seven out of ten cases. Even when it does not achieve the best result, its performance remains close to the leading algorithm. For instance, when the LED count is set to 3, 5, and 10, PSO, GWO, and GA score slightly higher (0.485, 0.697, and 0.922, respectively) compared to ICHIO-FA (0.476, 0.682, and 0.917, respectively).

4.2.2.3 Impact of Varying the Number of Users

This section examines the effect of increasing the number of users (from 5 to 40) while keeping the LED count fixed at 5. The results are presented in Table 4.6 and Figure 4.4.

Figure 4.4(a) illustrates that coverage declines as more users are introduced. This is expected since additional users may fall outside the illumination range of the deployed LEDs. Nonetheless, ICHIO-FA outperforms all other algorithms in seven out of eight cases (when the number of users varies between 10 and 35).

Figure 4.4(b) examines mean throughput per user. As more users share the network,

throughput per user declines due to increased competition for resources. However, ICHIO-FA consistently achieves higher throughput than other algorithms. Specifically, when the number of users is set to 5, 10, 15, 25, and 35, ICHIO-FA outperforms the alternatives. In cases where it is not the best, it remains close to the highest-performing algorithm. For example, at 20, 30, and 40 users, GA achieves 49.52 Mbps, PSO 42.64 Mbps, and GA again 37.19 Mbps, whereas ICHIO-FA records 49.04 Mbps, 42.59 Mbps, and 36.86 Mbps, respectively.

Figure 4.4(c) shows the fitness trend as the number of users increases. The fitness value declines with additional users, but ICHIO-FA maintains superior performance in five out of eight cases. Even in the remaining cases, its results remain competitive. For example, at 20, 30, and 40 users, GA scores 0.673, PSO 0.661, and GA again 0.526, while ICHIO-FA achieves 0.668, 0.659, and 0.515, respectively.

4.2.2.4 Impact of Varying the Area of Photo detectors (PDs)

In the final scenario, we examine how varying the PD area (from $0.6e^{-4}$ to $1.3e^{-4}$) influences system performance. The LED and user counts remain fixed at 5 and 30, respectively. The results are presented in Table 4.4 and Figure 4.5.

Figure 4.5(a) demonstrates that as the PD area increases, coverage improves, eventually reaching near-total coverage. This occurs because larger PDs capture more light, enhancing the chance of illumination. ICHIO-FA outperforms all other algorithms across most PD area values.

Figure 4.5(b) reveals that mean throughput per user follows a similar trend, improving as PD size increases due to enhanced light capture and SNR. ICHIO-FA consistently delivers better performance across most scenarios.

Figure 4.5(c) presents fitness values. Again, ICHIO-FA excels in most cases, ranking highest in six out of eight scenarios. Even when it does not achieve the best score, its performance remains close to the leading algorithm.

Conclusion: Across all tested scenarios, ICHIO-FA consistently outperforms alternative algorithms in terms of coverage, mean throughput per user, and fitness metrics, demonstrating its effectiveness in optimizing LEDs placement.

4.2.3 Statistical Analysis

To conduct a rigorous comparison among the ten optimization algorithms and verify the effectiveness of the proposed ICHIO-FA approach, we employ the Friedman test to analyze the distribution of results across all cases. The outcomes of this statistical evaluation are provided in Tables 4.8 to 4.19.

The results indicate that the ICHIO-FA algorithm consistently delivers superior performance, achieving the highest minimum, maximum, and mean fitness values across all

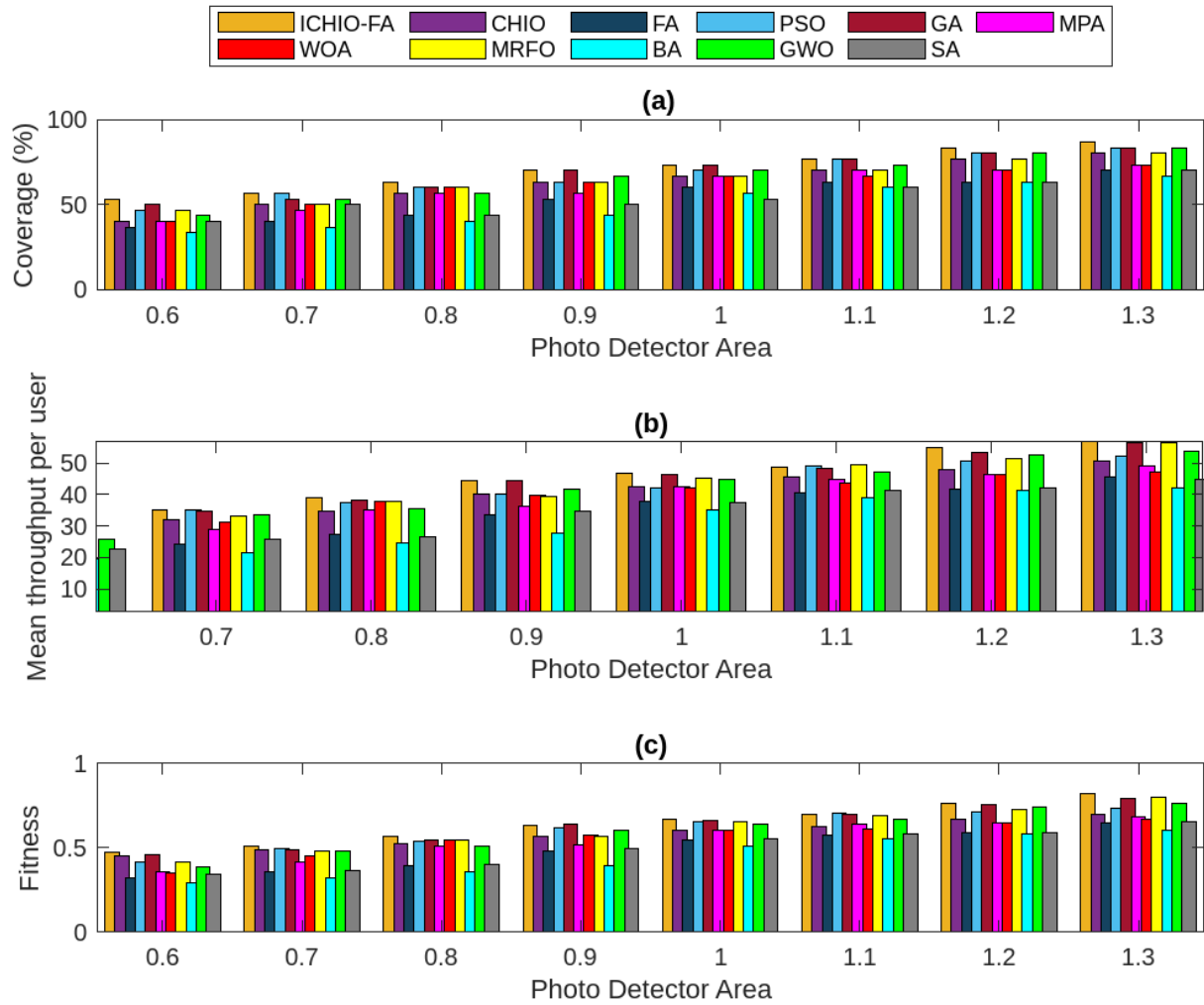


Figure 4.5: Coverage (a), Throughput (b) and Fitness (c) under various values of Photo-Detector Area

scenarios. Among the alternative meta-heuristics, the performance of ICHIO-FA remains closely aligned with that of PSO and GA, demonstrating its reliability. Examining the mean ranking for coverage, mean throughput per user, and fitness, ICHIO-FA maintains the highest ranking compared to its competitors. Additionally, the statistical significance level is below 5%, suggesting that the medians of all tested algorithms are not equal, which leads to the rejection of the null hypothesis (H_0).

To further analyze significant differences among the algorithms, we conducted Post-hoc multiple comparison tests using the Least Significant Difference (LSD) test. The results are summarized in Tables 4.20 to 4.31. These findings confirm a statistically significant difference between ICHIO-FA and the competing algorithms (CHIO, FA, PSO, GA, MPA, WOA, MRFO, BA, GWO, and SA) based on the confidence intervals and the corresponding p-values.

Tables 4.20, 4.21, and 4.22 summarize the Post-hoc test results for coverage, mean throughput, and fitness across different values of the control parameter λ . The analysis reveals statistically significant differences between the algorithms, as indicated by p-values consistently below 5%. Furthermore, the confidence intervals remain strictly positive, reinforcing the statistical significance and leading to the rejection of the null hypothesis (H_0).

Conversely, Tables 4.23 to 4.31 summarize the Post-hoc analysis results for varying the number of LEDs, users, and the photo-detector (PD) area. The findings show that the significance values across all algorithms exceed 0.5, indicating the absence of a statistically significant difference in these cases. As a result, the null hypothesis (H_0) is accepted, suggesting that the performance differences among the tested algorithms in these specific scenarios are not statistically significant.

The statistical analysis confirms the superiority of ICHIO-FA over its competitors in most test cases. The Friedman test demonstrates that ICHIO-FA achieves the highest performance rankings across coverage, throughput, and fitness metrics. Furthermore, the Post-hoc LSD test validates that the improvements provided by ICHIO-FA are statistically significant, particularly in the lambda parameter variation tests. However, in scenarios involving variations in the number of LEDs, users, or PD area, the performance differences among the algorithms are statistically insignificant, suggesting similar behavior in these cases.

4.2.4 Convergence Analysis

In this section, the convergence behavior of the proposed ICHIO-FA algorithm is analyzed in comparison with other meta-heuristic algorithms, including CHIO, FA, PSO, GA, MPA, WOA, MRFO, BAT, GWO, and SA. The evaluation is based on two key aspects: convergence efficiency (fitness value) and convergence speed. The convergence assessment is

performed using two scenarios described in Table 4.7, with each result obtained as the average of 30 independent runs.

Figures 4.6 and 4.7 illustrate the convergence behavior of all considered algorithms concerning both convergence efficiency and time. The results consistently indicate that ICHIO-FA surpasses other meta-heuristics across nearly all test scenarios. The ICHIO-FA algorithm exhibits two key convergence characteristics:

- **Rapid Initial Convergence:** As shown in Figure 4.6, ICHIO-FA demonstrates an exceptionally fast convergence speed, with the fitness value increasing from 0.51 to 0.549 within the first 100 iterations. In contrast, CHIO progresses from 0.485 to 0.505, while GA only improves from 0.518 to 0.526 within the same range.
- **Ability to Escape Local Optima:** The ICHIO-FA algorithm effectively avoids premature convergence by escaping local optima at multiple stages throughout the optimization process. Figure 4.6 highlights three such stagnation phases:
 - The first between iterations 100 and 300
 - The second between iterations 301 and 390

Similarly, in Figure 4.7, stagnation is observed:

- Between iterations 105 and 207
- Between iterations 208 and 300
- Between iterations 301 and 380

Additionally, the number of iterations required for convergence remains independent of the number of LEDs or the size of the room, demonstrating the stability and scalability of the ICHIO-FA algorithm. While ICHIO-FA may require additional iterations to reach the global optimum, it consistently achieves higher fitness values than competing algorithms in most cases.

The improved performance of ICHIO-FA is attributed to the following enhancements:

- **Opposition-Based Learning (OBL):**
 - Enhances population diversity.
 - Accelerates convergence by directing the search process toward promising regions.
- **Sine Map-Based Chaos Integration:**
 - Provides better control over parameter updates.
 - Ensures a more diverse set of solutions, preventing premature convergence.

[b]0.45

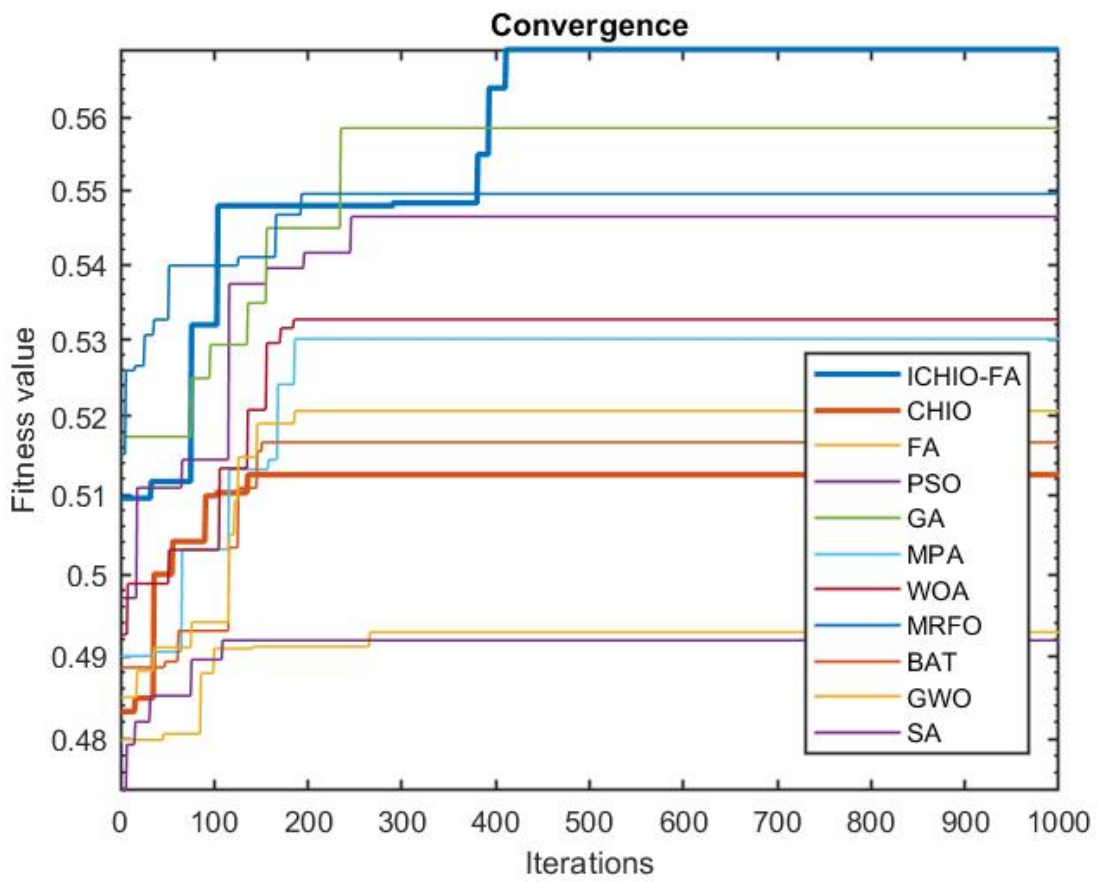
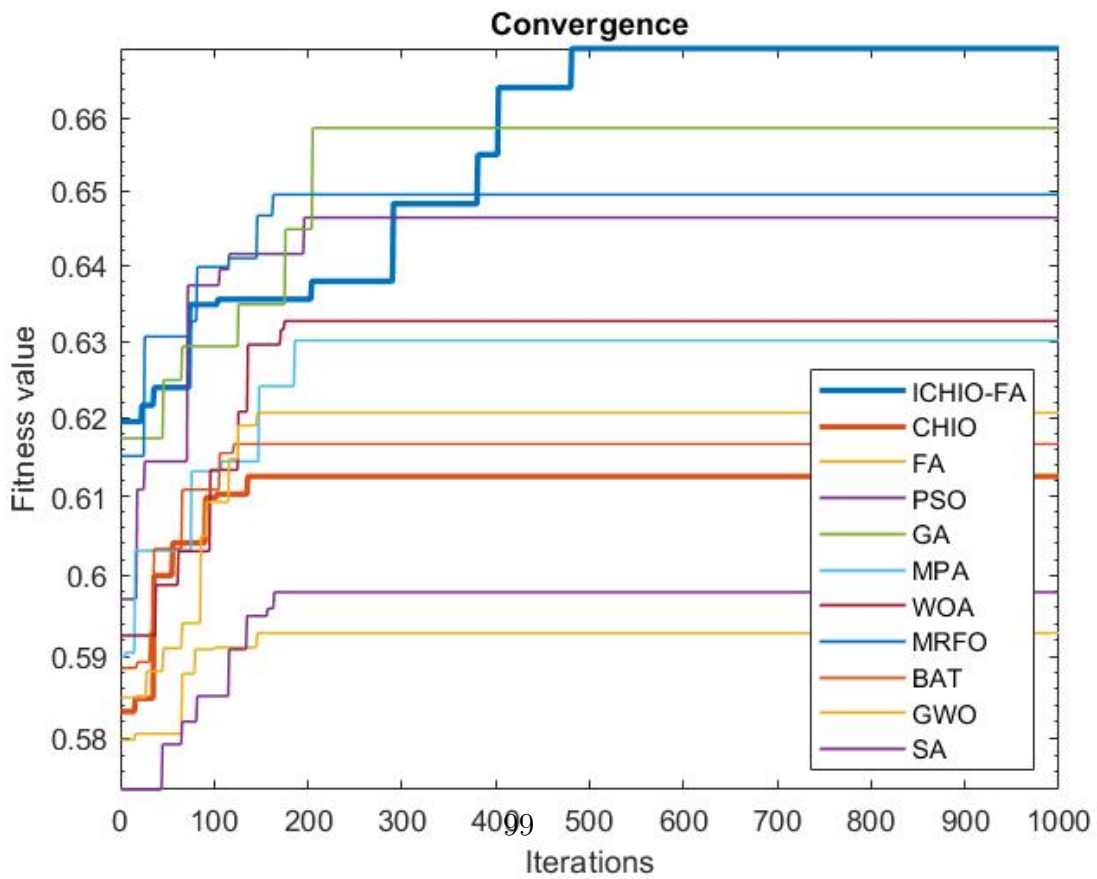


Figure 4.6: Scenario 1
[b]0.45



- Firefly Algorithm (FA) as a Local Search Operator:
 - Enhances the ability to escape local optima by refining promising solutions.
 - Improves the overall robustness of the algorithm.
 - Increases the likelihood of identifying the global optimal solution.

The convergence analysis confirms that ICHIO-FA outperforms traditional meta-heuristics in terms of convergence speed, efficiency, and robustness. The algorithms hybrid approach, integrating OBL, chaotic sine maps, and FA, allows for effective exploration and exploitation of the search space, leading to higher-quality solutions in complex optimization problems.

4.3 Conclusion

This chapter presented a hybrid human-based and swarm intelligence approaches for solving the LED placement problem in indoor VLC systems. We introduced an enhanced hybrid algorithm (ICHIO-FA), which combine powerful meta-heuristic techniques to optimize network coverage, throughput, and overall fitness.

IMPA-FA integrates the Coronavirus Herd Immunity Optimizer Algorithm (CHIO) with the Firefly Algorithm (FA), leveraging chaotic maps to increase solution diversity, Opposition-Based Learning (OBL) to accelerate convergence, and FA to refine local search and to prevent stagnation in local optima.

Comprehensive simulations were conducted in an indoor environment with varying LED configurations, user densities, and photo-detector (PD) areas. The results consistently demonstrated that ICHIO-FA outperformed state-of-the-art algorithms, including CHIO, PSO, GA, MPA, WOA, MRFO, BA, GWO, and SA, in terms of network performance metrics. Statistical and convergence analyses further validated the efficiency and robustness of our proposed methods, confirming their superior ability to balance exploration and exploitation while maintaining high-quality solutions.

These findings underscore the potential of hybrid meta-heuristic approach in tackling complex VLC system optimization challenges. The next research direction includes extending these methods for multi-objective optimization. The insights from this study contribute significantly to the field of intelligent optimization in VLC networks, paving the way for more adaptive and efficient LED placement strategies in next-generation communication systems.

Table 4.1: The main notations used in this paper

Parameter	Description	Parameter	Description
LOS	Line-of-sight	VLC	Visible Light Communication
PD	Photo-detector	LEDs	Light Emitting Diodes
V	VLC system	D	Length of V
W	Width of V	H	Height of V
U	Users	L	LEDs
M	Number of Users	N	Number of LEDs
d	Dimensions	$H(0)$	Channel current gain
m	Lambertian order	A	Area of a PD
ϕ	Radiation angle	ψ	Incident angle
$\phi_{1/2}$	Half power angle	$T_s(\psi)$	Gain of the optical filter
$B(r)$	Attractiveness of a firefly at r distance	n	Refractive index of the optical concentrator
P_t	Transmit power	P_r	Receiving power
SNR	Signal-to-Noise Ratio	R	Responsivity
σ_t^2	Total noise variance	$Cov(V)$	Coverage of the system V
$Tr(V)$	Throughput of the system V	B	Bandwidth
X_0	Initial solution (Population)	$C()$	Infected case
BR_r	Basic reproduc- tion rate	up	Upper bound
n_p	Population size	Max_{age}	Maximum age of infected cases
$N()$	Susceptible case	$R()$	Immune case
Max_{itr}	Max iteration	$FADs$	Fish aggregat- ing devices
$I(r)$	Light intensity at r distance	I_s	Light source
$g(\psi)$	Gain of optical concentrator	Tr^{th}	Threshold value of Throughput
SM_{k+1}	Chaotic Sine map value at the k -th itera- tion	$P\bar{m}o$	Opposite vec- tor of the real vector P
lb	Lower bound	P^{th}	Threshold value of SNR

Table 4.2: Parameter values of the algorithms considered in our simulations

Algorithm	Parameter	Value
<i>ICHIO-FA</i>	<i>FADs</i>	0.2
	Fixed number P	0.5
	Control parameter β	1.5
	Chaotic parameter ac	4
	Chaotic initial value r_0	0.7
	Chaotic initial value R_0	0.7
	Light absorption coefficient γ	1
	Initial attraction coefficient β_0	2
	Control parameter α	rand
<i>CHIO</i>	Nbr of primary infected cases C_0	1
	Basic reproduction rate BR_r	0.05
	Max infected cases age Max_{age}	100
<i>FA</i>	Light absorption coefficient γ	1
	Initial light intensity coefficient I_0	2
	Initial attraction coefficient β_0	2
	Control parameter α	rand
<i>MPA</i>	<i>FADs</i>	0.2
	Fixed number P	0.5
	Control parameter β	1.5
<i>PSO</i>	Inertia maximum weight ω_{Max}	0.9
	Inertia minimum weight ω_{Min}	0.4
	Acceleration parameter C_1	2
	Acceleration parameter C_2	2
<i>GA</i>	Crossover probability p_c	0.8
	Mutation probability p_m	0.2
	Elitism probability	0.2
<i>MRFO</i>	Somersault factor S	2
	Control parameter a_{min}	0
<i>WOA</i>	Control parameter a_{max}	2
	Minimum frequency f_{Min}	0
<i>BA</i>	Maximum frequency f_{Min}	2
	Initial loudness A_0	1
	Initial pulse emission rate r_0	1
	Loudness constant α	0.5
	Emission rate constant γ	0.5
<i>GWO</i>	Control parameter a_{min}	0
	Control parameter a_{max}	2
<i>SA</i>	Initial Temp T_0	0.025
	Reduction Rater α	0.99

CHAPTER 4. A HYBRID APPROACH FOR SOLVING THE LEDS PLACEMENT PROBLEM IN INDOOR VLC SYSTEM

Table 4.3: Scenarios settings

Scenario for LED	Scenario for Users	LED _{1..n}	Coordinates
SC1 : User ₁ +LED ₁	SC9 : User _{1..5} +LED _{1..5}	LED ₁	x ₁ = 18 84 97 82 85 84 41 93 14 33 55 78 81 5 72 2 37 98 4 99 72 14 85 14 93 78 67 50 90 75 ; y ₁ = 88 2 98 55 21 34 86 17 84 30 97 14 84 17 0 16 26 37 8 90 36 20 60 82 39 0 14 35 3 58;
SC2 : User ₁ +LED _{1,2}	SC10 : User _{1..10} +LED _{1..5}	LED ₂	x ₂ = 84 48 86 91 10 0 21 87 66 9 98 28 73 30 15 16 21 10 51 55 18 9 33 44 28 92 41 10 22 31; y ₂ = 66 100 15 62 24 67 55 68 44 11 89 58 84 15 85 30 93 9 97 14 28 59 54 18 57 69 51 41 72 79 ;
SC3 : User ₁ +LED _{1,2,3}	SC11 : User _{1..15} +LED _{1..5}	LED ₃	x ₃ = 25 5 66 79 21 58 58 52 24 13 91 51 32 41 35 95 57 34 43 100 76 30 27 88 74 4 90 1 22 7; y ₃ = 12 44 38 97 66 5 85 9 51 23 96 80 53 48 91 32 56 42 53 14 36 69 46 65 40 9 14 30 32 47;
SC4 : User ₁ +LED _{1..4}	SC12 : User _{1..20} +LED _{1..5}	LED ₄	x ₄ = 53 43 16 86 18 13 62 80 60 69 36 43 15 75 18 42 15 28 45 27 78 73 17 26 73 33 80 5 35 78; y ₄ = 29 56 84 23 14 26 88 87 96 96 22 52 21 10 10 42 38 9 93 3 85 90 13 17 89 83 39 43 27 69;
SC5 : User ₁ +LED _{1..5}	SC13 : User _{1..25} +LED _{1..5}	LED ₅	x ₅ = 50 14 61 9 13 50 57 92 56 56 9 70 92 63 32 61 51 90 81 79 19 68 41 67 16 73 8 22 57 72; y ₅ = 95 40 1 92 17 94 18 0 85 61 3 8 34 83 49 69 100 35 99 1 10 37 71 46 78 60 95 40 87 44;
SC6 : User ₁ +LED _{1..6}	SC14 : User _{1..30} +LED _{1..5}	LED ₆	x ₆ = 24 20 5 50 17 84 86 71 31 60 78 69 11 81 10 61 51 61 11 2 34 77 47 67 6 46 39 83 53 33; y ₆ = 88 15 83 91 8 64 27 51 59 24 70 59 71 25 3 37 83 19 63 77 14 41 51 50 5 52 29 80 38 40;
SC7 : User ₁ +LED _{1..7}	SC15 : User _{1..35} +LED _{1..5}	LED ₇	x ₇ = 10 97 71 72 83 33 76 48 79 90 81 64 99 98 34 100 72 73 47 34 97 71 43 28 55 51 99 14 85 86; y ₇ = 74 3 20 39 80 98 54 19 21 96 14 8 39 70 62 67 47 51 36 80 74 35 11 32 54 92 41 38 85 14;
SC8 : User ₁ +LED _{1..8}	SC16 : User _{1..40} +LED _{1..5}	LED ₈	x ₈ = 80 16 5 18 34 87 33 50 50 38 25 35 96 14 36 31 59 5 48 58 75 69 68 93 99 37 13 65 1 4; y ₈ = 33 6 58 54 92 87 12 62 74 35 44 81 37 14 75 9 65 20 87 22 75 50 89 2 80 20 72 88 51 97;
User _{1..40}	x y = 67 56; 23 27; 22 24; 28 16; 37 48; 26 30; 27 46; 76 87; 18 28; 42 52; 30 98; 22 16; 49 71; 97 86; 21 15; 30 81; 93 35; 49 37; 76 27; 15 31; 25 84; 90 4; 68 52; 48 78; 78 64; 60 22; 4 58; 76 10; 4 73; 76 56; 76 75; 39 66; 17 71; 3 27; 4 9; 40 41; 1 55; 6 44; 14 62; 34 65;		

Table 4.4: Coverage, mean throughput, and fitness under various values of the parameter λ and the Area of the Photo-Detector

lambda _s	0	0.1	0.2	0.3	0.4	0.5	0.6	0.7	0.8	0.9	1	Area a of a PD, e ⁻¹	0.6	0.7	0.8	0.9	1	1.1	1.2	1.3
Coverage (%)												Coverage (%)								
*ICHIOFA	66.66	70	73.33	70	70	73.33	70	70	73.33	70	66.66	*ICHIOFA	53.33	56.66	63.33	70	73.33	76.66	83.33	86.66
CHIO	60	63.33	66.66	66.66	63.33	66.66	63.33	63.33	63.33	66.66	60	CHIO	40	50	56.66	63.33	66.66	70	76.66	80
FA	56.66	50	60	53.33	60	63.33	56.66	66.66	60	63.33	63.33	FA	36.66	40	43.33	53.33	60	63.33	63.33	70
PSO	63.33	70	66.66	63.33	70	53.33	63.33	66.66	66.66	66.66	66.66	PSO	46.66	56.66	60	63.33	70	76.66	80	83.33
GA	66.66	60	70	70	70	63.33	63.33	63.33	66.66	66.66	66.66	GA	50	53.33	60	70	73.33	76.66	80	83.33
MPA	63.33	63.33	60	56.66	60	56.66	56.66	60	56.66	60	60	MPA	40	46.66	56.66	56.66	66.66	70	70	73.33
WOA	60	66.66	66.66	60	66.66	63.33	63.33	66.66	63.33	66.66	66.66	WOA	40	50	60	63.33	66.66	66.66	70	73.33
MRFO	60	63.33	70	53.33	70	70	63.33	60	63.33	66.66	66.66	MRFO	46.66	50	60	63.33	66.66	70	76.66	80
BA	53.33	50	56.66	56.66	56.66	56.66	53.33	56.66	56.66	56.66	53.33	BA	33.33	36.66	40	43.33	56.66	60	63.33	66.66
GWO	63.33	56.66	66.66	63.33	66.66	66.66	60	66.66	63.33	66.66	63.33	GWO	43.33	53.33	56.66	66.66	70	73.33	80	83.33
SA	50	56.66	60	56.66	60	63.66	56.66	63.66	60	56.66	50	SA	40	50	43.33	50	53.33	60	63.33	70
Mean throughput per user (Mbps)												Mean throughput per user (Mbps)								
*ICHIOFA	43.53	47.21	46.22	43.17	46.82	45.42	42.34	44.21	47.73	46.26	45.62	*ICHIOFA	32.85	35.05	38.88	44.29	46.65	48.75	54.72	59.26
CHIO	41.13	41.04	42.85	42.29	41.98	42.33	39.02	42.42	40.47	41.96	41.25	CHIO	28.82	32.05	34.88	40.29	42.65	45.75	47.96	50.53
FA	35.62	31.44	38.11	32.85	39.11	40.80	36.36	42.29	39.06	40.31	39.67	FA	21.99	24.40	27.34	33.51	37.72	40.48	41.86	45.73
PSO	42.15	46.73	42.31	42.53	44.40	44.57	41.80	43.07	41.08	41.91	42.68	PSO	28.67	34.94	37.33	40.25	42.22	49.11	50.79	52.10
GA	43.75	45.68	46.12	43.55	39.48	39.35	39.67	40.31	40.76	42.38	46.49	GA	30.40	34.66	38.19	44.52	46.51	48.31	53.41	56.53
MPA	41.88	40.55	38.92	39.75	39.79	38.21	39.57	38.86	39.99	38.23	40.49	MPA	24.16	28.74	35.12	36.11	42.49	44.83	46.45	49.00
WOA	38.16	42.73	41.77	39.48	42.31	42.02	40.04	42.66	40.62	42.33	41.09	WOA	23.68	31.37	37.89	39.92	42.23	43.63	46.45	47.14
MRFO	38.72	40.96	44.99	34.69	47.05	44.68	41.02	37.62	40.23	42.19	41.91	MRFO	27.83	33.11	37.95	39.20	45.25	49.40	51.29	56.40
BA	32.83	30.90	35.74	36.02	35.64	35.77	34.08	35.70	36.59	35.44	33.52	BA	19.66	21.61	24.64	27.70	34.96	39.14	41.49	42.18
GWO	41.16	36.18	43.31	39.95	42.18	43.33	38.22	43.38	40.99	42.89	45.66	GWO	25.89	33.51	35.66	41.70	44.70	47.09	52.59	53.52
SA	35.73	33.62	34.84	38.62	39.52	37.23	35.63	32.52	33.62	31.84	34.95	SA	22.59	25.64	26.42	34.73	37.24	41.38	42.26	44.84
Fitness												Fitness								
*ICHIOFA	0.536	0.554	0.604	0.618	0.640	0.671	0.656	0.613	0.602	0.589	0.552	*ICHIOFA	0.471	0.509	0.567	0.635	0.670	0.697	0.763	0.818
CHIO	0.523	0.539	0.554	0.561	0.548	0.534	0.561	0.557	0.561	0.554	0.516	CHIO	0.451	0.489	0.527	0.565	0.607	0.627	0.671	0.701
FA	0.458	0.414	0.523	0.467	0.512	0.529	0.517	0.530	0.480	0.491	0.503	FA	0.324	0.357	0.392	0.482	0.542	0.577	0.586	0.644
PSO	0.547	0.548	0.555	0.609	0.639	0.648	0.633	0.607	0.601	0.573	0.566	PSO	0.417	0.492	0.540	0.615	0.655	0.706	0.710	0.735
GA	0.546	0.496	0.532	0.623	0.638	0.650	0.644	0.609	0.598	0.554	0.573	GA	0.462	0.488	0.546	0.642	0.662	0.700	0.757	0.794
MPA	0.526	0.533	0.520	0.501	0.539	0.522	0.528	0.570	0.548	0.549	0.540	MPA	0.355	0.418	0.509	0.515	0.606	0.638	0.649	0.682
WOA	0.491	0.521	0.531	0.535	0.562	0.549	0.556	0.531	0.511	0.554	0.516	WOA	0.352	0.452	0.544	0.573	0.605	0.614	0.649	0.670
MRFO	0.538	0.538	0.563	0.572	0.644	0.637	0.651	0.605	0.590	0.554	0.546	MRFO	0.412	0.483	0.544	0.569	0.657	0.691	0.730	0.796
BA	0.422	0.408	0.481	0.494	0.502	0.513	0.495	0.534	0.547	0.555	0.533	BA	0.293	0.322	0.358	0.395	0.508	0.552	0.583	0.604
GWO	0.530	0.476	0.539	0.550	0.562	0.542	0.556	0.534	0.562	0.545	0.533	GWO	0.383	0.482	0.512	0.601	0.637	0.669	0.738	0.761
SA	0.478	0.456	0.512	0.526	0.537	0.526	0.541	0.524	0.504	0.4934	0.484	SA	0.345	0.362	0.398	0.498	0.555	0.584	0.592	0.651

CHAPTER 4. A HYBRID APPROACH FOR SOLVING THE LEDS PLACEMENT PROBLEM IN INDOOR VLC SYSTEM

Table 4.6: Coverage, mean throughput, and fitness under various values of number of LEDS and Users

number of LEDS	1	2	3	4	5	6	7	8	9	10	Number of users	5	10	15	20	25	30	35	40
Coverage (%)											Coverage (%)								
*ICHIOFA	26.66	40.66	53.33	60.33	70	83.33	86.66	93.33	100	100	*ICHIOFA	100	93.33	90	80	73	66.66	62.33	54.28
CHIO	23.33	40	43.33	50	66.66	76.66	80	90	93.33	100	CHIO	100	90	80	75	70	65.71	60	52
FA	23.33	26.66	40	46.66	50	56.66	63.33	73.33	80	83.33	FA	100	80	70	60	52	50	42.5	40.85
PSO	23.33	36.66	53.33	56.66	57.33	70	83.33	86.66	93.33	96.66	PSO	100	86.66	80	70	68	66.66	57.14	52.5
GA	23.33	36.66	50	56.66	70	70	86.66	90	96.6	100	GA	100	90	86.66	80	70	66.66	61.71	55.66
MPA	20	40	46.66	53.33	66.66	70	73.33	76.66	86.66	90	MPA	100	90	80	70	64	60	56.66	45
WOA	23.33	30	40	43.33	60	66.66	78.33	80	83.33	86.66	WOA	100	80	66.66	65	60	56.66	57.14	54
MRFO	26.66	30	43.33	53.33	66.66	73.33	76.66	80	90	93.33	MRFO	100	90	86.66	70	68	60	59.45	57.5
BA	20	26.66	40	46.66	50	53.33	56.66	60	70	73.33	BA	100	70	66.66	60	52	46.66	45.71	42.5
GWO	26.66	33.33	43.33	56.66	70.66	83.33	83.33	90	90	93.33	GWO	100	90	86.66	70	68	63.33	55	48.88
SA	23.33	30	40	46.66	50	56.66	63.33	73.33	80	83.33	SA	100	80	70	60	52	46.66	42.5	40
Mean throughput per user (Mbps)											Mean throughput per user (Mbps)								
*ICHIOFA	18.12	26.32	32.73	37.45	46.64	54.74	57.47	59.36	63.73	65.09	*ICHIOFA	69.64	60.20	57.24	49.04	46.63	42.59	40.13	36.86
CHIO	14.71	25.72	28.35	32.09	44.15	50.07	51.36	57.96	62.38	65.12	CHIO	69.33	57.75	52.49	47.17	44.52	41.41	38.18	34.97
FA	14.38	16.81	26.08	29.40	31.32	36.25	40.55	45.32	50.86	52.79	FA	65.12	51.02	43.61	37.54	32.72	30.23	27.64	26.45
PSO	12.48	22.99	33.99	35.83	36.86	45.58	52.90	56.67	62.04	64.84	PSO	68.11	57.01	52.87	45.43	44.15	42.64	36.50	33.79
GA	14.36	22.51	32.40	35.60	43.42	44.10	56.36	57.31	62.59	65.65	GA	69.34	59.34	56.10	49.52	45.41	42.45	39.44	37.19
MPA	12.79	25.08	28.83	34.17	42.92	45.07	47.67	49.88	57.58	58.77	MPA	68.71	59.17	51.19	45.49	41.18	38.51	36.70	29.56
WOA	15.13	19.10	26.36	28.11	39.82	42.57	50.97	51.73	54.12	56.20	WOA	66.95	49.59	45.02	41.74	37.25	36.54	35.98	34.60
MRFO	16.14	18.78	27.35	34.32	42.41	46.80	49.63	51.93	59.53	60.96	MRFO	69.35	59.01	56.73	45.67	43.79	42.56	37.74	35.09
BA	12.78	16.49	24.28	29.38	30.68	32.50	36.02	38.41	43.21	45.53	BA	66.49	44.57	42.90	37.01	33.98	29.81	28.53	27.30
GWO	17.76	21.94	27.77	35.25	48.71	53.69	52.92	57.53	59.41	61.20	GWO	68.11	60.04	55.44	45.38	44.33	40.61	34.89	31.54
SA	14.33	16.83	22.43	29.62	33.62	37.73	40.84	45.25	49.62	52.38	SA	65.33	51.13	43.73	38.35	33.93	30.43	28.03	27.42
Fitness											Fitness								
*ICHIOFA	0.256	0.389	0.476	0.528	0.682	0.774	0.796	0.849	0.896	0.917	*ICHIOFA	0.950	0.847	0.811	0.668	0.659	0.659	0.672	0.515
CHIO	0.211	0.365	0.399	0.456	0.634	0.705	0.730	0.823	0.885	0.919	CHIO	0.946	0.821	0.737	0.641	0.632	0.595	0.545	0.496
FA	0.209	0.241	0.367	0.422	0.451	0.516	0.577	0.658	0.727	0.756	FA	0.919	0.728	0.630	0.541	0.470	0.444	0.390	0.384
PSO	0.180	0.331	0.485	0.514	0.520	0.643	0.757	0.798	0.866	0.900	PSO	0.938	0.800	0.740	0.642	0.624	0.661	0.520	0.480
GA	0.209	0.321	0.458	0.512	0.629	0.633	0.781	0.819	0.886	0.922	GA	0.939	0.833	0.804	0.673	0.641	0.653	0.569	0.526
MPA	0.182	0.361	0.418	0.486	0.609	0.640	0.673	0.704	0.804	0.828	MPA	0.942	0.831	0.729	0.642	0.580	0.547	0.519	0.415
WOA	0.214	0.282	0.356	0.410	0.512	0.567	0.698	0.703	0.765	0.795	WOA	0.945	0.719	0.623	0.593	0.539	0.518	0.517	0.492
MRFO	0.237	0.272	0.374	0.478	0.588	0.648	0.690	0.724	0.833	0.859	MRFO	0.946	0.829	0.798	0.644	0.622	0.607	0.540	0.511
BA	0.182	0.239	0.356	0.422	0.447	0.475	0.515	0.547	0.628	0.659	BA	0.928	0.636	0.609	0.538	0.478	0.425	0.412	0.388
GWO	0.242	0.307	0.395	0.510	0.697	0.762	0.757	0.820	0.832	0.860	GWO	0.938	0.824	0.790	0.642	0.625	0.578	0.499	0.447
SA	0.193	0.234	0.375	0.426	0.443	0.507	0.543	0.647	0.703	0.744	SA	0.922	0.734	0.642	0.552	0.472	0.448	0.403	0.388

Table 4.7: Convergence analyses scenarios

Scenario 1		Scenario 2	
Room size	5 m x 5 m x 3,5 m	Room size	10 m x 10 m x 4 m
Number of Users	10	Number of Users	20
Number of LEDS	3	Number of LEDS	5

Table 4.8: The Friedman test of the Coverage under parameter various of number of LEDS

	Results	ICHIO-FA	CHIO	FA	PSO	GA	MPA	WOA	MRFO	BA	GWO	SA
Descriptive statistics	N	10	10	10	10	10	10	10	10	10	10	10
	Mean	71,0960	66,3310	54,3300	65,72960	67,9970	62,3300	59,1640	63,3300	49,6640	67,0630	54,6640
	SD	25,18568	25,93702	20,96805	24,570858	26,06784	22,05677	23,45440	23,88289	17,17400	25,22374	20,49970
	Minimum	26,66	23,33	23,33	23,330	23,33	20,00	23,33	26,66	20,00	26,66	23,33
	Maximum	100,00	100,00	83,33	96,660	100,00	90,00	86,66	93,33	73,33	93,33	83,33
Mean rank	Mean rank	10,45	7,65	2,70	7,50	8,60	5,65	4,15	6,50	1,55	8,30	2,95
Test Statistics	N	10										
	Chi-square	76,922710										
	Df	10										
Asymp. sig.	< 0.001											

Table 4.9: The Friedman test of the Mean Throughput under parameter various of number of LEDS

	Results	ICHIO-FA	CHIO	FA	PSO	GA	MPA	WOA	MRFO	BA	GWO	SA
Descriptive statistics	N	10	10	10	10	10	10	10	10	10	10	10
	Mean	46,1650	43,1910	34,3760	42,4180	43,4300	40,2760	38,4110	40,7850	30,9280	43,6180	34,2650
	SD	16,59702	17,13374	13,26452	17,09391	17,27813	14,80627	15,21653	16,03317	10,71295	16,41718	13,34699
	Minimum	18,12	14,71	14,38	12,48	14,36	12,79	15,13	16,14	12,78	17,76	14,33
	Maximum	65,09	65,12	52,79	64,84	65,65	58,77	56,20	60,96	45,53	61,20	52,38
Mean rank	Mean rank	10,60	8,30	2,90	7,20	8,20	5,70	4,60	6,30	1,30	8,20	2,70
Test Statistics	N	10										
	Chi-square	74,818182										
	Df	10										
Asymp. sig.	< 0.001											

CHAPTER 4. A HYBRID APPROACH FOR SOLVING THE LEDS
PLACEMENT PROBLEM IN INDOOR VLC SYSTEM

Table 4.10: The Friedman test of the Fitness value under parameter various of number of LEDs

	Results	ICHIO-FA	CHIO	FA	PSO	GA	MPA	WOA	MRFO	BA	GWO	SA
Descriptive statistics	<i>N</i>	10	10	10	10	10	10	10	10	10	10	10
	Mean	0,65630	0,61270	0,49240	0,59940	0,61700	0,57050	0,53020	0,57030	0,44700	0,61820	0,48150
	SD	0,230276	0,242181	0,190197	0,236229	0,241263	0,205667	0,208522	0,222058	0,154743	0,233560	0,185647
	Minimum	,0256	0,211	0,209	0,180	0,209	0,182	0,214	0,237	0,182	0,242	0,193
	Maximum	0,917	0,919	0,756	0,900	0,922	0,828	0,795	0,859	0,659	0,860	0,744
Mean rank	Mean rank	10,60	8,30	3,20	7,35	8,25	5,85	4,15	6,10	1,55	8,15	2,50
Test Statistics	<i>N</i>	10										
	Chi-square	74,082005										
	<i>Df</i>	10										
	Asymp. sig.	< 0.001										

Table 4.11: The Friedman test of the Coverage under parameter various of number of users

	Results	ICHIO-FA	CHIO	FA	PSO	GA	MPA	WOA	MRFO	BA	GWO	SA
Descriptive statistics	<i>N</i>	8	8	8	8	8	8	8	8	8	8	8
	Mean	77,4150	74,3738	61,9188	72,6200	76,3362	70,7075	67,4325	73,9512	60,4413	72,7337	61,3950
	SD	16,21029	15,29465	20,38038	15,62702	15,31520	18,26375	15,50463	16,14315	18,88010	17,87781	20,81427
	Minimum	54,00	54,28	40,85	52,50	55,66	45,00	54,00	57,50	42,50	48,88	40,00
	Maximum	100	100	100,00	100	100	100	100,00	100	100	100	100
Mean rank	Mean rank	9,75	8,06	2,88	6,63	9,13	5,75	4,56	7,63	2,50	6,56	2,56
Test Statistics	<i>N</i>	8										
	Chi-square	58,560760										
	<i>Df</i>	10										
	Asymp. sig.	< 0.001										

Table 4.12: The Friedman test of the Mean Throughput under parameter various of number of users

	Results	ICHIO-FA	CHIO	FA	PSO	GA	MPA	WOA	MRFO	BA	GWO	SA
Descriptive statistics	<i>N</i>	8	8	8	8	8	8	8	8	8	8	8
	Mean	50,2913	48,2275	39,2913	47,5625	49,8488	46,3138	43,4588	48,7425	38,8238	47,5425	39,7938
	SD	11,20441	11,28981	13,37558	11,28912	11,03377	12,82686	10,79451	11,79302	12,88307	12,65364	13,15701
	Minimum	36,86	34,97	26,45	33,79	37,19	29,56	34,60	35,09	27,30	31,54	27,42
	Maximum	69,64	69,33	65,12	68,11	69,34	68,71	66,95	69,35	66,49	68,11	65,33
Mean rank	Mean rank	10,63	7,75	1,63	6,69	9,63	6,00	4,25	8,38	1,88	6,44	2,75
Test Statistics	<i>N</i>	8										
	Chi-square	68,169414										
	<i>Df</i>	10										
	Asymp. sig.	< 0.001										

Table 4.13: The Friedman test of The Fitness Value under parameter various of number of users

	Results	ICHIO-FA	CHIO	FA	PSO	GA	MPA	WOA	MRFO	BA	GWO	SA
Descriptive statistics	<i>N</i>	8	8	8	8	8	8	8	8	8	8	8
	Mean	0,72263	0,67663	0,56325	0,67562	0,70475	0,65063	0,61825	0,68713	0,55175	0,66788	0,57013
	SD	0,137181	0,149726	0,186591	0,148782	0,141068	0,174119	0,151232	0,153355	0,177272	0,169093	0,185860
	Minimum	0,515	0,496	0,384	0,480	0,526	0,415	0,492	0,511	0,388	0,447	0,388
	Maximum	0,950	0,946	0,919	0,938	0,939	0,942	0,945	0,946	0,928	0,938	0,922
Mean rank	Mean rank	10,63	7,44	1,75	6,81	9,63	6,00	4,50	8,31	1,94	6,19	2,81
Test Statistics	<i>N</i>	8										
	Chi-square	65,436395										
	<i>Df</i>	10										
	Asymp. sig.	< 0.001										

Table 4.14: The Friedman test of the Coverage under various of Lambda

	Results	ICHIO-FA	CHIO	FA	PSO	GA	MPA	WOA	MRFO	BA	GWO	SA
Descriptive statistics	<i>N</i>	11	11	11	11	11	11	11	11	11	11	11
	Mean	70,3009	64,2382	59,3909	65,1473	66,0573	59,3909	64,5409	64,2400	55,1464	63,9345	57,6327
	SD	2,33628	2,61820	4,90246	4,56174	3,27251	2,50438	2,69410	5,18376	2,28955	3,27112	4,58006
	Minimum	66,66	60,00	50,00	53,33	60,00	56,66	60,00	53,33	50,00	56,66	50,00
	Maximum	73,33	66,66	66,66	70,00	70,00	63,33	66,66	70,00	56,66	66,66	63,66
Mean rank	Mean rank	10,55	6,45	3,82	7,73	8,05	3,73	7,00	6,86	1,73	6,68	3,41
Test Statistics	<i>N</i>	11										
	Chi-square	69,876										
	<i>Df</i>	10										
	Asymp. sig.	< 0.001										

CHAPTER 4. A HYBRID APPROACH FOR SOLVING THE LEDS PLACEMENT PROBLEM IN INDOOR VLC SYSTEM

Table 4.15: The Friedman test of the Mean Throughput under parameter various of Lambda

	Results	ICHIO-FA	CHIO	FA	PSO	GA	MPA	WOA	MRFO	BA	GWO	SA
	<i>N</i>	11	11	11	11	11	11	11	11	11	11	11
Descriptive statistics	Mean	45.3209	41.5218	37.7836	43.0209	42.5036	39.6582	41.2009	41.2782	34.7482	41.5682	35.2836
	SD	1.77096	1.09731	3.37834	1.61785	2.76933	1.09025	1.47895	3.52834	1.72222	2.67670	2.41920
	Minimum	42.34	39.02	31.44	41.08	39.35	38.21	38.16	34.69	30.90	36.18	31.84
	Maximum	47.73	42.85	42.29	46.73	46.49	41.88	42.73	47.05	36.59	45.66	39.52
Mean rank	Mean rank	10.55	6.45	3.09	8.55	8.00	4.73	6.55	6.73	1.55	7.64	2.18
	<i>N</i>	11										
Test Statistics	Chi-square	79.355										
	<i>Df</i>	10										
	Asymp. sig.	< 0.001										

Table 4.16: The Friedman test of Fitness value under parameter various of Lambda

	Results	ICHIO-FA	CHIO	FA	PSO	GA	MPA	WOA	MRFO	BA	GWO	SA
	<i>N</i>	11	11	11	11	11	11	11	11	11	11	11
Descriptive statistics	Mean	0.060318	0.54618	0.49309	0.59327	0.58755	0.53418	0.53245	0.58527	0.49855	0.53900	0.50740
	SD	0.043377	0.015968	0.035940	0.037377	0.050979	0.018187	0.021810	0.043033	0.047538	0.023715	0.026935
	Minimum	0.536	0.516	0.414	0.547	0.496	0.501	0.491	0.538	0.408	0.476	0.456
	Maximum	0.671	0.561	0.530	0.648	0.650	0.570	0.562	0.651	0.555	0.562	0.541
Mean rank	Mean rank	10.36	6.18	2.09	9.45	8.68	4.64	5.00	8.59	2.82	5.64	2.55
	<i>N</i>	11										
Test Statistics	Chi-square	85.775										
	<i>Df</i>	10										
	Asymp. sig.	< 0.001										

Table 4.17: The Friedman test of the Coverage under parameter various of Area of the Photo-Detector A

	Results	ICHIO-FA	CHIO	FA	PSO	GA	MPA	WOA	MRFO	BA	GWO	SA
	<i>N</i>	8	8	8	8	8	8	8	8	8	8	8
Descriptive statistics	Mean	70.4125	62.9138	53.7475	67.0800	68.3313	59.9962	61.2475	64.1638	49.9962	65.8300	53.7488
	SD	12.00988	13.50257	12.40139	2.65494	12.47136	12.08489	11.11652	11.78535	13.09271	13.77345	10.14778
	Minimum	53.33	40.00	36.66	46.66	50.00	40.00	40.00	46.66	33.33	43.33	40.00
	Maximum	86.66	80.00	70.00	83.33	83.33	73.33	73.33	80.00	66.66	83.33	70.00
Mean rank	Mean rank	10.69	5.75	2.50	8.81	9.50	4.63	5.44	6.69	1.31	8.00	2.69
	<i>N</i>	8										
Test Statistics	Chi-square	71.973										
	<i>Df</i>	10										
	Asymp. sig.	< 0.001										

Table 4.18: The Friedman test of the Mean Throughput per under parameter various of Area of the Photo-Detector A

	Results	ICHIO-FA	CHIO	FA	PSO	GA	MPA	WOA	MRFO	BA	GWO	SA
	<i>N</i>	8	8	8	8	8	8	8	8	8	8	8
Descriptive statistics	Mean	45.0563	40.3662	34.1288	41.9263	44.0663	38.3625	39.0388	42.5538	31.4225	41.8325	34.3875
	SD	9.25179	7.81709	8.75104	8.30004	9.07597	8.84243	8.00551	9.71447	9.13121	9.63424	8.51520
	Minimum	32.85	28.82	21.99	28.67	30.40	24.16	23.68	27.83	19.66	25.89	22.59
	Maximum	59.26	50.53	45.73	52.10	56.53	49.00	47.14	56.40	42.18	53.52	44.84
Mean rank	Mean rank	10.63	6.50	2.38	7.50	9.75	4.81	5.06	8.13	1.00	7.63	2.63
	<i>N</i>	8										
Test Statistics	Chi-square	70.534395										
	<i>Df</i>	10										
	Asymp. sig.	< 0.001										

Table 4.19: The Friedman test of the Fitness value under parameter various of Area of the Photo-Detector A

	Results	ICHIO-FA	CHIO	FA	PSO	GA	MPA	WOA	MRFO	BA	GWO	SA
	<i>N</i>	8	8	8	8	8	8	8	8	8	8	8
Descriptive statistics	Mean	0.64125	0.57975	0.48800	0.60875	0.63138	0.54650	0.55738	0.61025	0.45188	0.59788	0.49813
	SD	0.120727	0.087681	0.118374	0.115234	0.122195	0.117329	0.107078	0.130458	0.124020	0.130831	0.116371
	Minimum	0.471	0.451	0.324	0.417	0.462	0.355	0.352	0.412	0.293	0.383	0.345
	Maximum	0.818	0.701	0.644	0.735	0.794	0.682	0.670	0.796	0.604	0.761	0.651
Mean rank	Mean rank	10.63	6.50	2.00	8.38	9.75	4.69	5.13	7.94	1.00	7.00	3.00
	<i>N</i>	8										
Test Statistics	Chi-square	71.780432										
	<i>Df</i>	10										
	Asymp. sig.	< 0.001										

CHAPTER 4. A HYBRID APPROACH FOR SOLVING THE LEDS
PLACEMENT PROBLEM IN INDOOR VLC SYSTEM

Multiple Comparison						
Dependent variable: Coverage						
Algorithm (I)	Algorithm (J)	Mean difference (I-J)	SE	Sig	95 % confidence interval	
				Lower bound		Upper bound
<i>ICHIO-FA</i>	<i>CHIO</i>	6,0627	1,54912	<0,001	2,9927	9,1327
	<i>FA</i>	10,9100	1,54912	<0,001	7,8400	13,9800
	<i>PSO</i>	5,1536	1,54912	0,001	2,0836	8,2236
	<i>GA</i>	4,2436	1,54912	0,007	1,1736	7,3136
	<i>MPA</i>	10,9100	1,54912	<0,001	7,8400	13,9800
	<i>WOA</i>	5,7600	1,54912	<0,001	2,6900	8,8300
	<i>MRFO</i>	6,0609	1,54912	<0,001	2,9909	9,1309
	<i>BA</i>	15,1545	1,54912	<0,001	12,0845	18,2245
	<i>GWO</i>	6,3664	1,54912	<0,001	3,2964	9,4364
	<i>SA</i>	12,6682	1,54912	<0,001	9,5982	15,7382

Table 4.20: The Post-Hoc test of the Coverage for each algorithm under various values of Lambda

Multiple Comparison						
Dependent variable: Mean Throughput						
Algorithm (I)	Algorithm (J)	Mean difference (I-J)	SE	Sig	95 % confidence interval	
				Lower bound		Upper bound
<i>ICHIO-FA</i>	<i>CHIO</i>	3,79909	0,977842	<0,001	1,86124	5,73694
	<i>FA</i>	7,53727	0,977842	<0,001	5,59942	9,47513
	<i>PSO</i>	2,30000	0,977842	0,020	0,36215	4,23785
	<i>GA</i>	2,81727	0,977842	0,005	0,87942	4,75513
	<i>MPA</i>	5,66273	0,977842	<0,001	3,72487	7,60058
	<i>WOA</i>	4,12000	0,977842	<0,001	2,18215	6,05785
	<i>MRFO</i>	4,04273	0,977842	<0,001	2,10487	5,98058
	<i>BA</i>	10,57273	0,977842	<0,001	8,63487	12,51058
	<i>GWO</i>	3,75273	0,977842	<0,001	1,81487	5,69058
	<i>SA</i>	10,03727	0,977842	<0,001	8,09942	11,97513

Table 4.21: The Post-Hoc test of the Throughput for each algorithm under various values of Lambda

Multiple Comparison						
Dependent variable: Fitness Value						
Algorithm (I)	Algorithm (J)	Mean difference (I-J)	SE	Sig	95 % confidence interval	
				Lower bound		Upper bound
<i>ICHIO-FA</i>	<i>CHIO</i>	0,05700	0,015010	<0,001	0,02725	0,08675
	<i>FA</i>	0,11009	0,015010	<0,001	0,08035	0,13984
	<i>PSO</i>	0,00991	0,015010	0,511	-0,01984	0,03965
	<i>GA</i>	0,01564	0,015010	0,300	-0,01411	0,04538
	<i>MPA</i>	0,06900	0,015010	<0,001	0,03925	0,09875
	<i>WOA</i>	0,07073	0,015010	<0,001	0,04098	0,10047
	<i>MRFO</i>	0,01791	0,015010	0,235	-0,01184	0,04765
	<i>BA</i>	0,10464	0,015010	<0,001	0,07489	0,13438
	<i>GWO</i>	0,06418	0,015010	<0,001	0,03444	0,09393
	<i>SA</i>	0,09578	0,015010	<0,001	0,06604	0,12553

Table 4.22: The Post-Hoc test of the Fitness for each algorithm under various values of Lambda

CHAPTER 4. A HYBRID APPROACH FOR SOLVING THE LEDS
PLACEMENT PROBLEM IN INDOOR VLC SYSTEM

Multiple Comparison							
Dependent variable: Coverage							
Algorithm (I)	Algorithm (J)	Mean difference (I-J)	SE	Sig	95 % confidence interval		
						Lower bound	Upper bound
<i>ICHIO-FA</i>	<i>CHIO</i>	4,7650	10,43455	0,649	-15,9394	25,4694	
	<i>FA</i>	16,7660	10,43455	0,111	-3,9384	37,4704	
	<i>PSO</i>	5,3664	10,43455	0,608	-15,3380	26,0708	
	<i>GA</i>	3,0990	10,43455	0,767	-17,6054	23,8034	
	<i>MPA</i>	8,7660	10,43455	0,403	-11,9384	29,4704	
	<i>WOA</i>	11,9320	10,43455	0,256	-8,7724	32,6364	
	<i>MRFO</i>	7,7660	10,43455	0,458	-12,9384	28,4704	
	<i>BA</i>	21,4320	10,43455	0,043	0,7276	42,1364	
	<i>GWO</i>	4,0330	10,43455	0,700	-16,6714	24,7374	
	<i>SA</i>	16,4320	10,43455	0,119	-4,2724	37,1364	

Table 4.23: The Post-Hoc test of the Coverage for each algorithm under various numbers of LEDs

Multiple Comparison							
Dependent variable: Mean Throughput							
Algorithm (I)	Algorithm (J)	Mean difference (I-J)	SE	Sig	95 % confidence interval		
						Lower bound	Upper bound
<i>ICHIO-FA</i>	<i>CHIO</i>	2,9740	6,88341	0,667	-10,6842	16,6322	
	<i>FA</i>	11,7890	6,88341	0,090	-1,8692	25,4472	
	<i>PSO</i>	3,7470	6,88341	0,587	-9,9112	17,4052	
	<i>GA</i>	2,7350	6,88341	0,692	-10,9232	16,3932	
	<i>MPA</i>	5,8890	6,88341	0,394	-7,7692	19,5472	
	<i>WOA</i>	7,7540	6,88341	0,263	-5,9042	21,4122	
	<i>MRFO</i>	5,3800	6,88341	0,436	-8,2782	19,0382	
	<i>BA</i>	15,2370	6,88341	0,029	1,5788	28,8952	
	<i>GWO</i>	2,5470	6,88341	0,712	-11,1112	16,2052	
	<i>SA</i>	11,9000	6,88341	0,087	-1,7582	25,5582	

Table 4.24: The Post-Hoc test of the Throughput for each algorithm under various numbers of LEDs

Multiple Comparison							
Dependent variable: Fitness Value							
Algorithm (I)	Algorithm (J)	Mean difference (I-J)	SE	Sig	95 % confidence interval		
						Lower bound	Upper bound
<i>ICHIO-FA</i>	<i>CHIO</i>	0,04360	0,096287	0,652	-0,14745	0,23465	
	<i>FA</i>	0,16390	0,096287	0,092	-0,02715	0,35495	
	<i>PSO</i>	0,05690	0,096287	0,556	-0,13415	0,24795	
	<i>GA</i>	0,03930	0,096287	0,684	-0,15175	0,23035	
	<i>MPA</i>	0,08580	0,096287	0,375	-0,10525	0,27685	
	<i>WOA</i>	0,12610	0,096287	0,193	-0,06495	0,31715	
	<i>MRFO</i>	0,08600	0,096287	0,374	-0,10505	0,27705	
	<i>BA</i>	0,20930	0,096287	0,032	0,01825	0,40035	
	<i>GWO</i>	0,03810	0,096287	0,693	-0,15295	0,22915	
	<i>SA</i>	0,17480	0,096287	0,072	-0,01625	0,36585	

Table 4.25: The Post-Hoc test of the Fitness value for each algorithm under various numbers of LEDs

CHAPTER 4. A HYBRID APPROACH FOR SOLVING THE LEDS
PLACEMENT PROBLEM IN INDOOR VLC SYSTEM

Multiple Comparison						
Dependent variable: Coverage						
Algorithm (I)	Algorithm (J)	Mean difference (I-J)	SE	Sig	95 % confidence interval	
					Lower bound	Upper bound
<i>ICHIO-FA</i>	<i>CHIO</i>	3,0412	8,70565	0,728	-14,2939	20,3764
	<i>FA</i>	15,4962	8,70565	0,079	-1,8389	32,8314
	<i>PSO</i>	4,7950	8,70565	0,583	-12,5402	22,1302
	<i>GA</i>	1,0787	8,70565	0,902	-16,2564	18,4139
	<i>MPA</i>	6,7075	8,70565	0,443	-10,6277	24,0427
	<i>WOA</i>	9,9825	8,70565	0,255	-7,3527	27,3177
	<i>MRFO</i>	3,4638	8,70565	0,692	-13,8714	20,7989
	<i>BA</i>	16,9737	8,70565	0,055	-0,3614	34,3089
	<i>GWO</i>	4,6813	8,70565	0,592	-12,6539	22,0164
	<i>SA</i>	16,0200	8,70565	0,070	-1,3152	33,3552

Table 4.26: The Post-Hoc test of the Coverage for each algorithm under various number of Users

Multiple Comparison						
Dependent variable: Mean Throughput						
Algorithm (I)	Algorithm (J)	Mean difference (I-J)	SE	Sig	95 % confidence interval	
					Lower bound	Upper bound
<i>ICHIO-FA</i>	<i>CHIO</i>	2,0638	6,03100	0,733	-9,9455	14,0730
	<i>FA</i>	11,0000	6,03100	0,072	-1,0093	23,0093
	<i>PSO</i>	2,7288	6,03100	0,652	-9,2805	14,7380
	<i>GA</i>	0,4425	6,03100	0,942	-11,5668	12,4518
	<i>MPA</i>	3,9775	6,03100	0,512	-8,0318	15,9868
	<i>WOA</i>	6,8325	6,03100	0,261	-5,1768	18,8418
	<i>MRFO</i>	1,5487	6,03100	0,798	-10,4605	13,5580
	<i>BA</i>	11,4675	6,03100	0,061	-,5418	23,4768
	<i>GWO</i>	2,7488	6,03100	0,650	-9,2605	14,7580
	<i>SA</i>	10,4975	6,03100	0,086	-1,5118	22,5068

Table 4.27: The Post-Hoc test of the Throughput for each algorithm under various number of Users

Multiple Comparison						
Dependent variable: Fitness value						
Algorithm (I)	Algorithm (J)	Mean difference (I-J)	SE	Sig	95 % confidence interval	
					Lower bound	Upper bound
<i>ICHIO-FA</i>	<i>CHIO</i>	0,04600	0,081094	0,572	-0,11548	0,20748
	<i>FA</i>	0,15937	0,081094	0,053	-0,00210	0,32085
	<i>PSO</i>	0,04700	0,081094	0,564	-0,11448	0,20848
	<i>GA</i>	0,01787	0,081094	0,826	-0,14360	0,17935
	<i>MPA</i>	0,07200	0,081094	0,377	-0,08948	0,23348
	<i>WOA</i>	0,10437	0,081094	0,202	-0,05710	0,26585
	<i>MRFO</i>	0,03550	0,081094	0,663	-0,12598	0,19698
	<i>BA</i>	0,17087	0,081094	0,038	0,00940	0,33235
	<i>GWO</i>	0,05475	0,081094	0,502	-0,10673	0,21623
	<i>SA</i>	0,15250	0,081094	0,064	-0,00898	0,31398

Table 4.28: The Post-Hoc test of the Fitness value for each algorithm under various number of Users

CHAPTER 4. A HYBRID APPROACH FOR SOLVING THE LEDS
PLACEMENT PROBLEM IN INDOOR VLC SYSTEM

Multiple Comparison							
Dependent variable: Coverage							
Algorithm (I)	Algorithm (J)	Mean difference (I-J)	SE	Sig	95 % confidence interval		
						Lower bound	Upper bound
<i>ICHIO-FA</i>	<i>CHIO</i>	7,4987	6,15824	0,227	-4,7639	19,7614	
	<i>FA</i>	16,6650	6,15824	0,008	4,4024	28,9276	
	<i>PSO</i>	3,3325	6,15824	0,590	-8,9301	15,5951	
	<i>GA</i>	2,0812	6,15824	0,736	-10,1814	14,3439	
	<i>MPA</i>	10,4162	6,15824	0,095	-1,8464	22,6789	
	<i>WOA</i>	9,1650	6,15824	0,141	-3,0976	21,4276	
	<i>MRFO</i>	6,2488	6,15824	0,313	-6,0139	18,5114	
	<i>BA</i>	20,4162	6,15824	0,001	8,1536	32,6789	
	<i>GWO</i>	4,58250	6,15824	0,459	-7,6801	16,8451	
	<i>SA</i>	16,6637	6,15824	0,008	4,4011	28,9264	

Table 4.29: The Post-Hoc test of the Coverage for each algorithm under various of photo-detector Area

Multiple Comparison							
Dependent variable: Mean Throughput							
Algorithm (I)	Algorithm (J)	Mean difference (I-J)	SE	Sig	95 % confidence interval		
						Lower bound	Upper bound
<i>ICHIO-FA</i>	<i>CHIO</i>	4,6900	4,42077	0,292	-4,1129	13,4929	
	<i>FA</i>	10,9275	4,42077	0,016	2,1246	19,7304	
	<i>PSO</i>	3,1300	4,42077	0,481	-5,6729	11,9329	
	<i>GA</i>	,9900	4,42077	0,823	-7,8129	9,7929	
	<i>MPA</i>	6,6938	4,42077	0,134	-2,1091	15,4966	
	<i>WOA</i>	6,0175	4,42077	0,177	-2,7854	14,8204	
	<i>MRFO</i>	2,5025	4,42077	0,573	-6,3004	11,3054	
	<i>BA</i>	13,6338	4,42077	0,003	4,8309	22,4366	
	<i>GWO</i>	3,2238	4,42077	0,468	-5,5791	12,0266	
	<i>SA</i>	10,6687	4,42077	0,018	1,8659	19,4716	

Table 4.30: The Post-Hoc test of the Throughput for each algorithm under various of photo-detector Area

Multiple Comparison							
Dependent variable: Fitness value							
Algorithm (I)	Algorithm (J)	Mean difference (I-J)	SE	Sig	95 % confidence interval		
						Lower bound	Upper bound
<i>ICHIO-FA</i>	<i>CHIO</i>	0,0615	0,05893	0,300	-0,0558	,1788	
	<i>FA</i>	0,1532	0,05893	0,011	0,0359	0,2706	
	<i>PSO</i>	0,0325	0,05893	0,583	-0,0848	0,1498	
	<i>GA</i>	0,0099	0,05893	0,867	-0,1075	0,1272	
	<i>MPA</i>	0,0948	0,05893	0,112	-0,0226	0,2121	
	<i>WOA</i>	0,0839	0,05893	0,159	-0,0335	0,2012	
	<i>MRFO</i>	0,0310	0,05893	0,600	-0,0863	0,1483	
	<i>BA</i>	0,1894	0,05893	0,002	,00720	,03067	
	<i>GWO</i>	0,0434	0,05893	0,464	-0,0740	0,1607	
	<i>SA</i>	0,1431	0,05893	0,017	0,0258	0,2605	

Table 4.31: The Post-Hoc test of the Fitness value for each algorithm under various of photo-detector Area

CHAPTER 5

A MULTI-OBJECTIVE APPROACH FOR SOLVING THE LEDS PLACEMENT PROBLEM IN INDOOR VLC SYSTEM

5.1 Introduction

Visible Light Communication (VLC) is a promising wireless technology that utilizes Light Emitting Diodes (LEDs) for high-speed data transmission while simultaneously providing illumination. The dual-functionality of VLC introduces multi-objective optimization (MOO) challenges, as system designers must balance trade-offs between communication performance, illumination constraints, security, and energy efficiency.

Recent advancements in metaheuristic and evolutionary algorithms have enabled multi-objective optimization to efficiently solve complex VLC system design problems. We explore recent applications of multi-objective optimization algorithms in VLC, highlighting key methodologies and their impact on system performance.

VLC systems require optimization across multiple objectives, including: Maximizing Data Rate and Coverage to ensuring high throughput while maintaining broad signal coverage. Energy Efficiency to reducing power consumption while maintaining illumination quality. Minimizing Blockage and Interference to addressing line-of-sight (LOS) obstructions and interference from multiple light sources. Security and Robustness to Preventing eavesdropping while maintaining reliable communication. Deployment Optimization to finding the best LED placement and power allocation.

In this context Ajith et al. [116] (2022) proposed a Multi-Objective Natural Aggregation Algorithm (MONAA) for optimizing user allocation in VLC. Their approach simultaneously maximized data rate while minimizing blockage probability, outperforming NSGA-II, MOEA/D, and MOPSO in both constrained and unconstrained function optimization.

Fan et al. [117] (2016) developed a p-optimality-based Clonal Selection Algorithm

(CLONALG) for optimizing VLC illumination uniformity and energy consumption. Their method outperformed traditional Pareto-optimality methods by efficiently balancing trade-offs between power usage and illumination quality.

Do et al. [118](2014) applied Non-Dominated Sorting Genetic Algorithm-II (NSGA-II) to optimize LED placement for maximizing signal-to-noise ratio (SNR) and received power while minimizing energy consumption. Their findings demonstrated that optimal LED positioning could enhance link quality without increasing power consumption.

Liua et al. [119](2024) explored multi-objective optimization for UAV-assisted VLC networks. Their MOEA/D-based approach optimized UAV location and power to improve energy efficiency, minimize eavesdropping, and ensure uniform power distribution across receiving surfaces.

Solis et al. [120](2023) applied Multi-Objective Particle Swarm Optimization (MOPSO) to optimize MIMO VLC systems in underground mining. Their work balanced error rate minimization and throughput maximization, demonstrating that MOPSO improved link robustness and spectral efficiency

Amanor et al. [121](2017) utilized NSGA-II with the TOPSIS decision-making method to optimize signal-to-noise ratio (SNR) and power consumption in LED-based inter-satellite VLC links. Their approach yielded over 3 dB improvement in SNR while maintaining optimal power settings.

Multi-objective optimization has become an essential tool for enhancing VLC system performance by balancing conflicting objectives such as coverage, throughput, energy efficiency, and security. Various algorithms, including NSGA-II, MOPSO, MOEA, and hybrid approaches, have been successfully applied to solve LED placement, and others VLC challenges.

In indoor Visible Light Communication (VLC) systems, one of the primary challenges is the optimal placement of multiple LEDs to efficiently accommodate varying numbers of users. This problem belongs to the class of NP-Hard problems, making it computationally infeasible to determine exact solutions within a reasonable time frame. Consequently, employing approximation techniques, particularly single-objective or multi-objective meta-heuristics, serves as an effective strategy for addressing this complexity.

In this chapter, we introduce a multi-objective version of the PUMA optimizer algorithm, incorporating non-dominated sorting, and crowding distance mechanisms. These enhancements ensure a well-distributed set of optimized solutions along the Pareto front.

The proposed Multi-Objective PUMA Optimizer (MOPO) is evaluated through multiple iterations, considering key performance metrics such as throughput and user coverage. Simulation results validate the efficiency and accuracy of MOPO, demonstrating its superiority in identifying an optimal Pareto front when benchmarked against existing algorithms, including the NSGA-II and the Multi-Objective Whale Optimization Algorithm (MOWOA).

The main contributions of this chapter are given below:

- Formulating the multi-objective LEDs placement problem in an indoor environment, aiming to optimize the throughput and coverage metrics.
- Proposing a multi-objective version of PUMA optimizer algorithm based of the non-dominated sorting, ranking-based selection, and crowding distance. for solving multi-objective LEDs placement problem in indoor VLC systems.
- Implementing the proposed MOPO algorithm, NSGA-II, and MOWOA algorithms for solving multi-objective LEDs placement problem in indoor VLC systems.
- Evaluating the performance of the proposed IMOPO algorithm in comparison with NSGA-II and MOWOA algorithms by investigating the effect of varying the number iterations.

The remainder of this chapter is structured as follows: Section ?? describes the Puma Optimizer algorithm. Section ?? presents the proposed Multi-Objective Puma Optimizer (MOPO) algorithm for LED placement optimization. Section 4.2.1 formulates the multi-objective LED placement problem in VLC. Section 4.2.2 provides a detailed performance evaluation, including simulation results, Pareto front analysis, and comparisons with NSGA-II and MOWOA. Finally, Section 4.3 concludes the chapter with key findings and future research directions.

The main notations used in this paper and their descriptions are listed in Table

5.2 Puma Optimizer (PO)

The Puma Optimizer (PO) is inspired by the adaptive hunting strategies of pumas, which dynamically balance exploration and exploitation based on their environment. This adaptive behavior makes PO well-suited for high-dimensional optimization problems. The algorithm follows a structured process that mimics real-world predation phases to improve search efficiency.

5.2.1 Mathematical Model

The PO algorithm operates in two primary phases:

5.2.1.1 Phase Selection Mechanism

Pumas rely on past experiences to make strategic decisions about hunting locations. The optimizer emulates this by distinguishing between exploitation (searching previously successful regions) and exploration (searching new areas). In the initial iterations, both

phases are applied simultaneously, after which a scoring mechanism determines the dominant phase for subsequent iterations.

The phase selection is computed using:

$$Score_{Explore} = (PF_1 \cdot f_{Explore}^1) + (PF_2 \cdot f_{Explore}^2) \quad (5.1)$$

$$Score_{Exploit} = (PF_1 \cdot f_{Exploit}^1) + (PF_2 \cdot f_{Exploit}^2) \quad (5.2)$$

where higher scores determine the selected phase. This approach ensures a smooth transition from initial random searches to targeted refinements.

5.2.1.2 Exploration Phase

In this phase, pumas randomly search for food or utilize information from other pumas successful hunts. Mathematically, this is modeled as:

$$X_{new} = X_{a,G} + G \cdot (X_{a,G} - X_{b,G}) \quad (5.3)$$

where $X_{a,G}$ and $X_{b,G}$ represent candidate solutions, and G is a random scaling factor ensuring diverse exploration.

5.2.1.3 Exploitation Phase

Pumas employ ambush hunting and high-speed pursuit strategies to capture prey. These behaviors are modeled mathematically to enhance solution refinement:

$$X_{new} = \frac{\left(\frac{mean(Sol_{total})}{N_{pop}}\right) \cdot X_i - (-1)^\theta \cdot X_i}{1 + (\alpha \cdot rand_3)} \quad (5.4)$$

This function accelerates convergence while maintaining diversity in the search process.

5.2.2 Algorithm Workflow

The PO algorithm follows a structured workflow:

1. Initialization: A population of pumas is randomly generated.
2. Early Exploration: Both exploration and exploitation occur simultaneously for the first three iterations.
3. Phase Transition: A scoring mechanism determines whether the algorithm should continue exploring or focus on refining existing solutions.
4. Dynamic Optimization: The search agents adaptively switch between hunting strategies based on past success rates.

5. Termination: The process continues until the stopping criteria are met, producing an optimal Pareto front.

By leveraging adaptive learning, experience-based phase selection, and diverse search strategies, the PO algorithm achieves efficient optimization performance in complex, multi-objective problems.

5.2.3 Computational Complexity Analysis

Despite the challenges associated with implementing the PO algorithm, it generally maintains a low computational complexity, which varies depending on the phase being executed. The overall computational cost of PO can be categorized into three primary operations: initialization, fitness evaluation, and solution generation.

- Initialization Phase: Given a population size of N , the computational complexity of initializing the population is $\mathcal{O}(N)$.
- Exploitation Phase: This phase involves generating new solutions, identifying the best location, and updating the position of each Puma. The computational complexity for these operations is $\mathcal{O}(N \times (T + TD))$.
- Exploration Phase: This phase is responsible for generating new candidate solutions and applying alternation mechanisms. The computational complexity for these operations is $\mathcal{O}((2T + 1) \times N \times D)$. Additionally, sorting operations used during exploration can contribute to an additional complexity of $\mathcal{O}(N^2)$ in the worst-case scenario.

Considering all these factors, the overall computational complexity of PO is given by:

$$\mathcal{O}((2T + 1)N^2 \times N \times D)$$

where:

- T represents the maximum number of iterations,
- D is the problem dimension,
- N is the total population size.

This complexity analysis highlights the computational efficiency of PO, making it a viable approach for solving large-scale optimization problems while balancing exploration and exploitation.

5.3 Mathematical Definition of Multi-Objective Optimization Problems

The definition of multi-objective optimization problems is mathematically described as:

$$\min | \max \mathbf{f}(\mathbf{x}) = (f_1(\mathbf{x}), f_2(\mathbf{x}), \dots, f_m(\mathbf{x})), \quad (5.5)$$

where $\mathbf{x} = (x_1, x_2, \dots, x_d)$ denotes the d -dimensional decision vector of a solution in the decision space Ω , and $\mathbf{f}(\mathbf{x})$ denotes the objective vector containing m conflicting functions to be minimized or maximized.

5.3.1 Pareto Dominance

Definition 1: For any two solutions \mathbf{x} and \mathbf{y} , \mathbf{x} is said to dominate \mathbf{y} :

In minimization problems: $\mathbf{f}(\mathbf{x}) < \mathbf{f}(\mathbf{y})$, if and only if $f_i(\mathbf{x}) \leq f_i(\mathbf{y})$ for all $i = 1, 2, \dots, m$ and $f_j(\mathbf{x}) < f_j(\mathbf{y})$ for at least one $j = 1, 2, \dots, m$.

In maximization problems: $\mathbf{f}(\mathbf{x}) > \mathbf{f}(\mathbf{y})$, if and only if $f_i(\mathbf{x}) \geq f_i(\mathbf{y})$ for all $i = 1, 2, \dots, m$ and $f_j(\mathbf{x}) > f_j(\mathbf{y})$ for at least one $j = 1, 2, \dots, m$.

5.3.2 Pareto Optimality and Crowding Distance Mechanism

Definition 2: A solution \mathbf{x} is said to be Pareto optimal if and only if there does not exist any solution \mathbf{y} in the decision space Ω dominating \mathbf{x} . All Pareto optimal solutions are non-dominated with each other.

Definition 3: The Pareto optimal set is defined as:

$$PS = \{\mathbf{x} \in \Omega \mid \nexists \mathbf{y} \in \Omega \rightarrow \mathbf{f}(\mathbf{y}) < \mathbf{f}(\mathbf{x})\}. \quad (5.6)$$

Definition 4: The Pareto front is defined as:

$$PF = \{\mathbf{f}(\mathbf{x}) \mid \mathbf{x} \in PS\}. \quad (5.7)$$

Definition 5: The crowding distance (CD) is defined as:

$$CD_j^i = \frac{f_l(X_{i+1}) - f_l(X_{i-1})}{f_l^{max} - f_l^{min}} \quad (5.8)$$

where f_l^{min} and f_l^{max} are the minimum and maximum values of the l^{th} fitness function. A higher CD ensures diversity in solutions.

5.4 Multi-objective LED's placement problem

The LED placement problem belongs to the family of NP-hard problems, making it computationally challenging to find an optimal solution within a reasonable time-frame. As a result, meta-heuristic algorithms offer a practical and efficient alternative for addressing this problem. In this research, we adopt a similar approach by leveraging a meta-heuristic optimization algorithm to tackle the LED placement challenge. Specifically, we propose a novel multi-objective bio-inspired optimization algorithm, called Multi-Objective Puma Optimizer (MOPO) algorithm, which has been successfully applied to various optimization problems.

The primary objective of our LED placement optimization is to simultaneously optimize two objectives: maximizing total coverage and throughput in a VLC system, while ensuring compliance with predefined constraints. The problem can be formally defined as follows:

$$Cov(V) = \sum_{j=1}^M \max_{i \in \{1, \dots, N\}} (Cov_{U_j}^{L_i}) \quad (5.9)$$

$$f_1 = \frac{Cov(V)}{M} \quad (5.10)$$

$$Tr(V) = \sum_{j=1}^M \max_{i \in \{1, \dots, N\}} (Tr_{U_j}^{L_i}) \quad (5.11)$$

$$f_2 = \frac{Tr(V)}{M \times Tr_{max}} \quad (5.12)$$

$$\text{Maximize } f = (f_1, f_2) \quad (5.13)$$

$$\text{S.t. } \begin{cases} SNR_{ij} \geq P^{th} \\ 0 \leq x_i \leq W & i \in \{1, \dots, N\}, j \in \{1, \dots, M\} \\ 0 \leq y_i \leq D \end{cases} \quad (5.14)$$

5.5 Multi-Objective Puma Optimizer (MOPO) for solving LEDs Placement in indoor VLC System

Optimizing the placement of LEDs in Visible Light Communication (VLC) systems presents a multi-objective challenge, requiring a balance between maximizing coverage and enhancing throughput. To address this challenge, we propose a Multi-Objective version of the Puma optimizer algorithm (MOPO), inspired by NSGA-II, which integrates non-

dominated sorting, ranking-based selection, and crowding distance to ensure a diverse set of optimized solutions.

The MOPO algorithm employs a ranking-based population sorting mechanism, where non-dominated solutions are assigned Rank 1, while subsequent ranks are allocated to dominated solutions in a hierarchical manner. To maintain diversity in the Pareto front, the algorithm utilizes crowding distance, which measures the relative proximity of each solution to its immediate neighbors (i.e., the preceding and succeeding solutions). Solutions located in less crowded regions are favored, fostering exploration of diverse areas in the solution space and preventing premature convergence.

To enhance search efficiency, MOPO incorporates a dynamic archive mechanism that continuously updates and stores optimal solutions throughout the evolutionary process. A leader selection process is employed to choose the most promising solutions from this archive, ensuring a strategic balance between exploration (searching new regions) and exploitation (refining known solutions). This mechanism allows MOPO to systematically refine the Pareto-optimal front, making it well-suited for complex multi-objective optimization problems such as LED placement in VLC systems.

By leveraging these strategies, MOPO provides decision-makers with a comprehensive perspective on trade-offs between conflicting objectives, rather than converging toward a single optimal solution. This diversity is crucial in real-world applications, enabling system designers to select optimal configurations based on specific constraints and requirements.

5.5.1 Implementation procedure of MOPO algorithm

Optimizing the placement of LEDs in Visible Light Communication (VLC) systems presents a multi-objective challenge, requiring a balance between maximizing coverage and enhancing throughput. To address this challenge, we propose the Multi-Objective LED Placement Optimization (MOPO) algorithm, inspired by NSGA-II, which integrates non-dominated sorting, ranking-based selection, and crowding distance to ensure a diverse set of optimized solutions.

The MOPO algorithm employs a ranking-based population sorting mechanism, where non-dominated solutions are assigned Rank 1, while subsequent ranks are allocated to dominated solutions in a hierarchical manner. To maintain diversity in the Pareto front, the algorithm utilizes crowding distance, which measures the relative proximity of each solution to its immediate neighbors (i.e., the preceding and succeeding solutions). Solutions located in less crowded regions are favored, fostering exploration of diverse areas in the solution space and preventing premature convergence.

To enhance search efficiency, MOPO incorporates a dynamic archive mechanism that continuously updates and stores optimal solutions throughout the evolutionary process.

A leader selection process is employed to choose the most promising solutions from this archive, ensuring a strategic balance between exploration (searching new regions) and exploitation (refining known solutions). This mechanism allows MOPO to systematically refine the Pareto-optimal front, making it well-suited for complex multi-objective optimization problems such as LED placement in VLC systems.

By leveraging these strategies, MOPO provides decision-makers with a comprehensive perspective on trade-offs between conflicting objectives, rather than converging toward a single optimal solution. This diversity is crucial in real-world applications, enabling system designers to select optimal configurations based on specific constraints and requirements.

The leader selection process in MOPO is determined based on crowding distance, where the selection probability (P) of each solution is directly proportional to its crowding distance, giving higher preference to solutions with greater crowding distances, treating them as extreme cases within the population.

The selection of the p -th PUMA in MOPO is governed by the crowding distance evaluation, ensuring a balanced trade-off between solution quality and diversity.

In MOPO, offspring solutions (of size P_{size}) are merged with the parent population, forming a mixed population of size $2P_{\text{size}}$. The algorithm then calculates the **ranks** and **crowding distances** for all individuals in this mixed population. A new population of size P_{size} is subsequently selected based on these ranking and diversity metrics.

The new population is constructed by prioritizing solutions with superior ranks. In cases where multiple solutions share the same rank, those with higher crowding distances are preferred, ensuring a well-distributed Pareto front. This approach is aligned with the **NSGA-II framework**, which emphasizes both **elitism** and **solution diversity** to enhance convergence towards optimal trade-offs.

The flowchart and the pseudo-code of the proposed **MOPO** algorithm are depicted in Figure and Algorithm. The following is the stepwise transformation of the PO algorithm into the MOPO framework, integrating Pareto sorting and crowding distance mechanisms:

1. **Initialization:** Define the multi-objective problem space and initialize the population P_{size} with potential solutions.
2. **Pareto Sorting:** Assess the populations positions via the Pareto sorting mechanism. Identify non-dominated solutions and store them in the Pareto Archive, ensuring the best solutions are preserved.
3. **Crowding Distance Calculation:** Compute the crowding distance for each individual within the Pareto Archive to maintain solution diversity.
4. **Evaluation and update:** Calculate the position solutions by PO algorithm operations to explore new areas of the solution space $P_{\text{size}^{\text{new}}}$.

5. **Update:** Combine P_{size} solutions with P_{size}^{new} and forming an updated mixed population by PO algorithm.
6. **Re-calculation Pareto and Crowding Distance:** Recalculate ranks and crowding distances for the mixed population $2P_{size}$.
7. **Ranking-based selection:** Select the next population P_{size} of solutions based on rank and diversity preservation and remove the necessary according to archive size with the lowest crowding distance value.
8. **Convergence Check:** If the maximum number of iterations Max_{iter} is not reached, return to Step 2. Otherwise, output the final Pareto-optimal front.

This structured approach enables MOPO to effectively balance exploration and exploitation, ensuring robust multi-objective optimization capabilities.

Algorithm 6 Pseudo-code of MOPO

```

0: % PO setting
0: Inputs: The population size  $N$  and the maximum number of iterations and parameter settings
0: Outputs: Return the best Pareto-optimal Front.
0: % initialization
0: Create a random population and calculate Pumas fitness and sort it.
0: Determine the non-dominated solution of the initial population and save them in Pareto archive.
0: Calculate crowding distance for each Pareto archive member.
0: Select a position vector based on crowding distance values.
0: for  $iter = 1 : Max_{iter}$  do
0:   Calculate and update the position position vector using PO algorithm.
0:   Calculate Pumas fitness values of all the updated position.
0:   Determine the new non-dominated solutions in the population and save them in Pareto archive and eliminate any dominated solution in the Pareto archive.
0:   Calculate the crowding distance value for each Pareto archive member and remove the necessary according to archive size with the lowest crowding distance value.
0:   Perform non-dominated sorting according to crowding distance and select the global best Pumas position based on the ranking.
0: end for=0

```

5.5.2 Simulation results and performance evaluation

In this section, we evaluate and analyze the performance of our proposed MOPO algorithm in solving the LED placement problem. To assess its effectiveness, we conduct a comparative analysis against four other state-of-the-art multi-objective optimization algorithms.

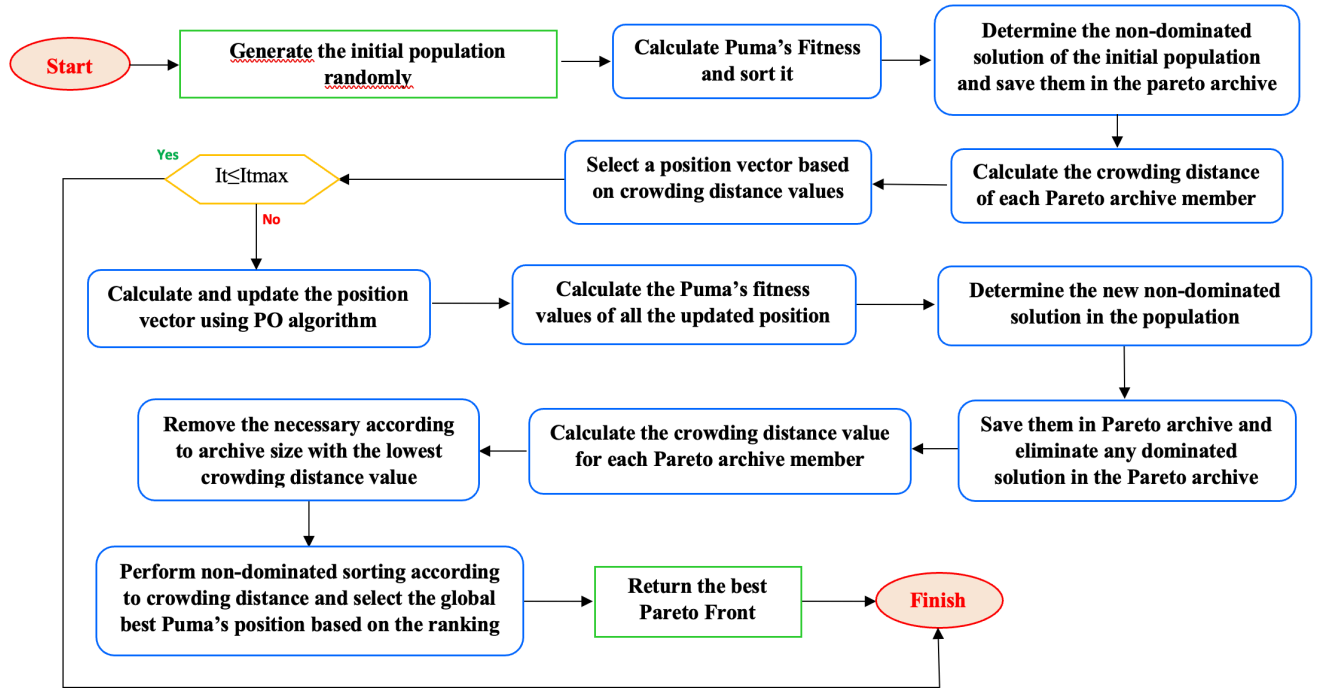


Figure 5.1: Flowchart of MOPO

All simulations are executed on a Mac OS M1 machine, with MATLAB used to implement and run all algorithms. The evaluation is conducted within an empty conference room of dimensions $10m \times 10m \times 3m$, ensuring an unobstructed line-of-sight (LOS) communication environment. A schematic representation of this room is shown in Figure 3.1.

To validate the efficiency of the MOPO algorithm, we explore multiple scenarios by varying the number of Iteration (ranging from **100 to 1000**).

The results are examined through **Pareto-optimal front** analysis, which provides insights into the trade-offs between **mean coverage** (the first function f_1) and **mean throughput per user** (the second function f_2). By analyzing these trade-offs, we assess the MOPO algorithms capability in achieving an optimal balance between these objectives.

The experimental results demonstrate the effectiveness of the proposed MOPO in solving the LED placement problem in indoor VLC systems, where the objectives are to maximize mean coverage and throughput simultaneously. As shown in Figures 5.2 and 5.3, the Pareto fronts obtained by MOPO were compared against NSGA-II, MOWOA, and the True Pareto Front (PF) at different iterations.

During the initial stages (100600 iterations), MOPO rapidly improved its solution quality, progressively converging toward the True PF while maintaining a balanced trade-off between coverage and throughput. In contrast, NSGA-II exhibited slower convergence, while MOWOA struggled to maintain solution diversity and often failed to optimize both

objectives simultaneously. As iterations increased, MOPO ensured that LEDs were positioned optimally to enhance both user coverage and data transmission rates, leading to a more efficient signal distribution and improved network performance.

By 700 iterations, MOPO had already aligned closely with the True PF, demonstrating its ability to optimize LED placement for both maximum coverage and high throughput. At 1000 iterations, MOPO achieved an almost optimal Pareto front, surpassing NSGA-II in convergence speed, solution diversity, and trade-off accuracy. The superior performance of MOPO in balancing both objectives allows for greater flexibility in network design, enabling configurations that maximize the number of covered users while maintaining optimal data transmission rates.

Meanwhile, MOWOA exhibited poor convergence and struggled to provide well-distributed solutions along the Pareto front, highlighting its inefficiency in addressing the complex trade-offs between coverage and throughput. These results confirm that MOPO outperforms NSGA-II and MOWOA in achieving a well-balanced, high-quality Pareto front, making it a powerful optimization framework for LED placement in VLC systems.

5.6 Conclusion

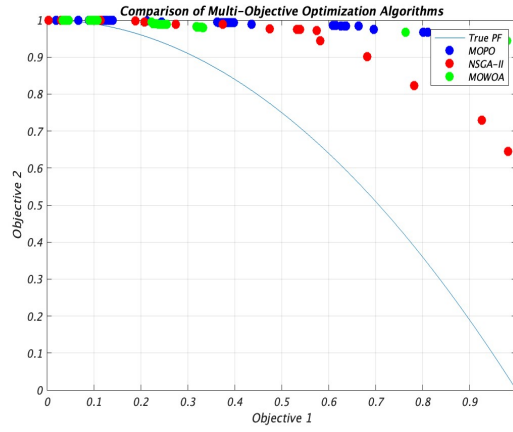
In this chapter, we introduced MOPO, a multi-objective optimization algorithm based on the PUMA Optimizer, designed to enhance LED placement efficiency in indoor VLC systems. The proposed MOPO algorithm integrates non-dominated sorting, ranking-based selection, and crowding distance mechanisms to maintain solution diversity and improve optimization convergence.

Comprehensive simulations were conducted to assess MOPOs effectiveness in balancing network coverage and throughput. The results demonstrated that MOPO outperformed NSGA-II and MOWOA, achieving superior Pareto-optimal solutions with better convergence speed and diversity preservation. Key findings include:

MOPO consistently produced well-distributed Pareto fronts, ensuring a diverse set of trade-off solutions. MOPO exhibited faster convergence rates, reaching high-quality solutions in fewer iterations compared to NSGA-II and MOWOA. MOPO maintained a better balance between throughput and coverage, making it a robust solution for real-world VLC deployment scenarios.

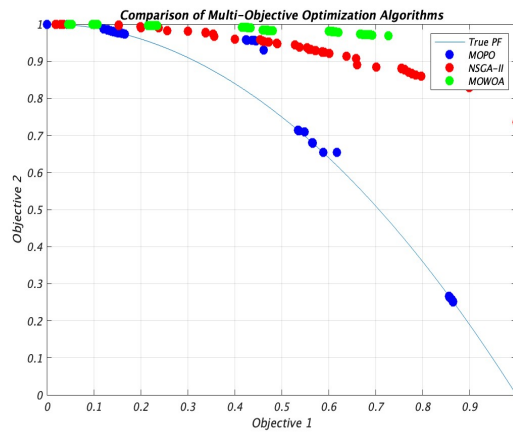
Future research directions include extending MOPO to optimize additional VLC parameters, such as power allocation, interference mitigation, and security constraints. Investigating hybrid optimization approaches, integrating MOPO with machine learning or reinforcement learning for adaptive LED placement. Applying MOPO to broader wireless communication challenges, including UAV-assisted VLC, smart city lighting networks, and visible light positioning systems. The findings in this chapter highlight the significance of multi-objective optimization in VLC systems, demonstrating that MOPO offers

a scalable and efficient solution for next-generation communication networks.



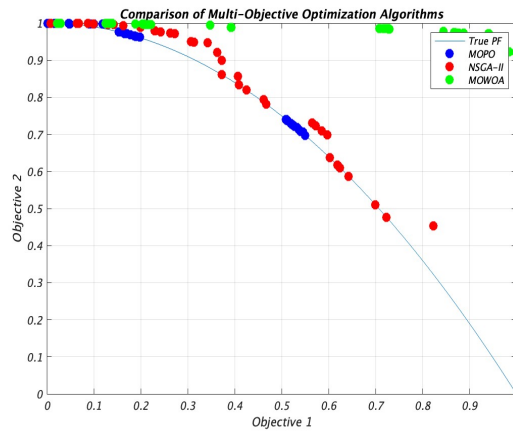
[b]0.45

Figure 5.2: 100 iterations



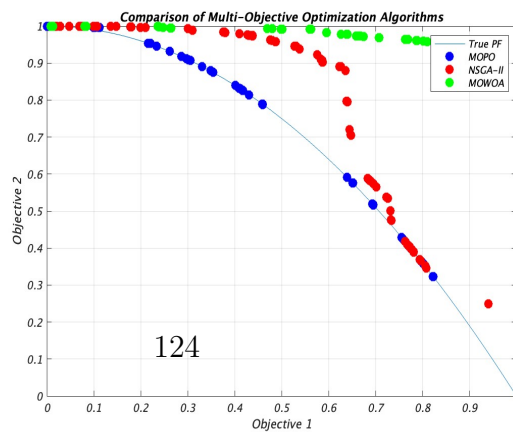
[b]0.45

Figure 5.3: 200 iterations



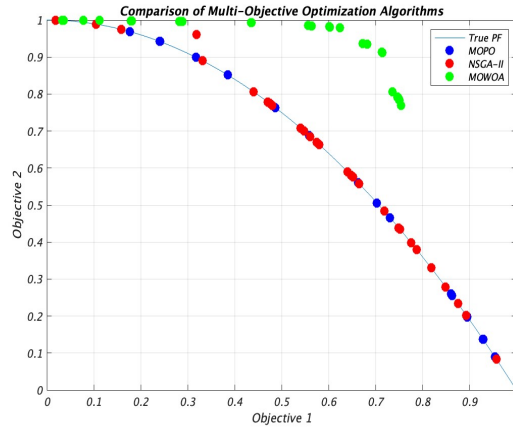
[b]0.45

Figure 5.4: 300 iterations



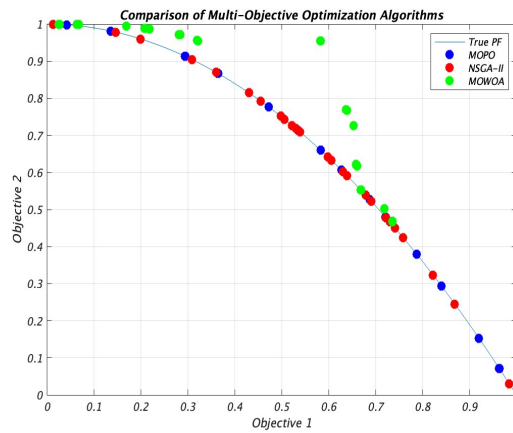
124

[b]0.45



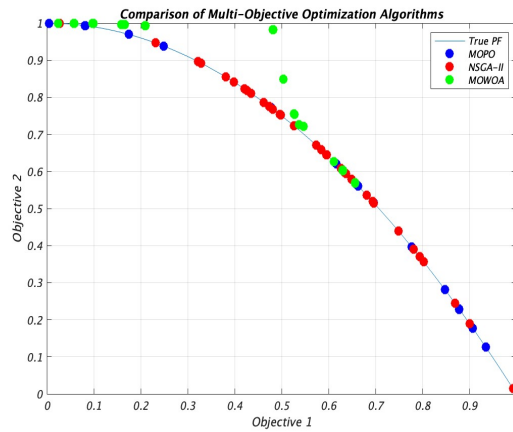
[b]0.45

Figure 5.9: 700 iterations



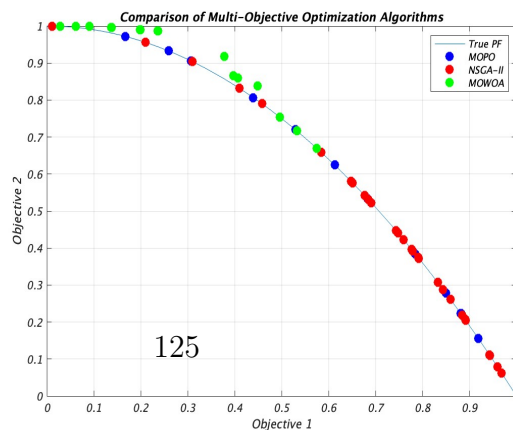
[b]0.45

Figure 5.10: 800 iterations



[b]0.45

Figure 5.11: 900 iterations



125

[b]0.45

Visible Light Communication (VLC) has emerged as a promising wireless communication technology, offering high-speed data transmission, energy efficiency, and enhanced security compared to traditional Radio Frequency (RF)-based systems. However, optimizing LED placement in VLC systems remains a significant challenge, requiring the balance of illumination, coverage, throughput, and energy efficiency. The complexity of this NP-hard problem necessitates the use of advanced optimization techniques, including metaheuristic, hybrid, and multi-objective approaches.

This thesis explored various optimization techniques to address LED placement challenges in indoor VLC systems. Our work is structured into five main chapters, each contributing to different aspects of VLC optimization.

The first chapter provided a comprehensive review of VLC technology, covering its architecture, modulation schemes, advantages, limitations, and real-world applications. We discussed key research challenges, including multi-user interference, shadowing, mobility, and illumination constraints. Furthermore, we examined existing optimization techniques applied to VLC, highlighting the need for more efficient LED placement strategies.

Chapter 2 explored optimization methodologies, focusing on classical, heuristic, and metaheuristic algorithms. We analyzed their mathematical foundations, classification, and computational complexity. The chapter also discussed single-objective vs. multi-objective optimization approaches and emphasized the growing role of bio-inspired metaheuristic algorithms in solving complex NP-hard problems such as LED placement in VLC.

In chapter 3, we introduced an enhanced metaheuristic approach, Whale Optimization Algorithm (EWOA), to improve search efficiency and convergence speed. By integrating chaotic maps and Opposition-Based Learning (OBL). Simulation results showed that EWOA outperforms the classical WOA and several baseline algorithms in terms of coverage and throughput. For instance, EWOA achieved up to 12% higher average SINR compared to WOA, CHIO, PSO, and other standard algorithms in most scenarios.

In chapter 4, recognizing the limitations of single metaheuristic algorithms, we proposed an hybrid approach, ICHIO-FA (Improved Coronavirus Herd Immunity Optimizer with Firefly Algorithm), incorporating OBL and chaotic maps to enhance solution diversity and accelerate convergence. This hybrid methods demonstrated significant improvements in optimization performance, efficiently balancing exploration and exploitation, leading to more precise LED placement solutions compared to standard metaheuristic approaches.

Chapter 5 introduced a multi-objective version of the Puma Optimizer Algorithm (MOPO) to optimize LED placement while balancing multiple conflicting objectives. This approach leveraged non-dominated sorting, ranking-based selection, and crowding distance mechanisms to ensure a diverse set of Pareto-optimal solutions. Our simulations demonstrated that MOPO outperformed NSGA-II and MOWOA, achieving better trade-offs between coverage and throughput while maintaining solution diversity and faster convergence.

While this thesis has provided significant advancements in LED placement optimization for VLC systems, several promising avenues for future research remain Extending multi-objective optimization to additional VLC parameters.

Future work could integrate power control, interference management, and security constraints into multi-objective optimization frameworks. Exploring machine learning-driven optimization approaches. Deep learning and reinforcement learning could be incorporated into metaheuristic algorithms to adapt LED placement strategies dynamically. Investigating real-time, adaptive VLC optimization. The integration of real-time optimization techniques to adapt LED placement based on user mobility and environmental changes could enhance system adaptability. Expanding optimization techniques to broader wireless communication challenges. The proposed methods could be extended to other domains, such as mesh router placement in Wi-Fi networks, UAV-assisted VLC, and smart city lighting networks.

- [1] Georges Dossin. Signaux lumineux au pays de mari. *Revue d'Assyriologie et d'archéologie orientale*, 35(3/4):174–186, 1938.
- [2] Alexander Graham Bell. Upon the production and reproduction of sound by light. *Journal of the Society of Telegraph Engineers*, 9(34):404–426, 1880.
- [3] DH Sliney. What is light? the visible spectrum and beyond. *Eye*, 30(2):222–229, 2016.
- [4] Sanjeev Kumar and Preeti Singh. A comprehensive survey of visible light communication: potential and challenges. *Wireless Personal Communications*, 109:1357–1375, 2019.
- [5] IEEE Standard Association et al. Ieee standard for local and metropolitan area networks-part 15.7: short-range wireless optical communication using visible light. *IEEE: Piscataway, NZ, USA*, pages 1–309, 2011.
- [6] Alin Cailean. *Etude et réalisation d'un système de communications par lumière visible (VLC/LiFi). Application au domaine automobile*. PhD thesis, Université de Versailles Saint-Quentin en Yvelines, 2014.
- [7] Subrato Bharati, Mohammad Atikur Rahman, and Prajoy Podder. Implementation of ask, fsk and psk with ber vs. snr comparison over awgn channel. *arXiv preprint arXiv:2002.03601*, 2020.
- [8] Peter J Winzer and Rene-Jean Essiambre. Advanced optical modulation formats. In *Optical Fiber Telecommunications VB*, pages 23–93. Elsevier, 2008.
- [9] R Karthika and S Balakrishnan. Wireless communication using li-fi technology. *SSRG International Journal of Electronics and Communication Engineering (SSRG-IJECE)*, 2(3):32–40, 2015.

- [10] Hassan M Oubei, Chao Shen, Abla Kammoun, Emna Zedini, Ki-Hong Park, Xiaobin Sun, Guangyu Liu, Chun Hong Kang, Tien Khee Ng, Mohamed-Slim Alouini, et al. Light based underwater wireless communications. *Japanese Journal of applied physics*, 57(8S2):08PA06, 2018.
- [11] Alin-Mihai Cailean, Barthélemy Cagneau, Luc Chassagne, Valentin Popa, and Mihai Dimian. A survey on the usage of dsrc and vlc in communication-based vehicle safety applications. In *2014 IEEE 21st Symposium on Communications and Vehicular Technology in the Benelux (SCVT)*, pages 69–74. IEEE, 2014.
- [12] Peng Deng and Mohsen Kavehrad. Adaptive real-time software defined mimo visible light communications using spatial multiplexing and spatial diversity. In *2016 IEEE International Conference on Wireless for Space and Extreme Environments (WiSEE)*, pages 111–116. IEEE, 2016.
- [13] Guilherme Ferreira Gomes, Fabricio Alves de Almeida, Patricia da Silva Lopes Alexandrino, Sebastiao Simões da Cunha, Bruno Silva de Sousa, and Antonio Carlos Ancelotti. A multiobjective sensor placement optimization for shm systems considering fisher information matrix and mode shape interpolation. *Engineering with Computers*, 35:519–535, 2019.
- [14] Mohaiminul Islam and Shangzhu Jin. An overview research on wireless communication network. *Networks*, 5(1):19–28, 2019.
- [15] Cem Sahin, Danh Nguyen, Simon Begashaw, Brandon Katz, James Chacko, Logan Henderson, Jennifer Stanford, and Kapil R Dandekar. Wireless communications engineering education via augmented reality. In *2016 IEEE frontiers in education conference (FIE)*, pages 1–7. IEEE, 2016.
- [16] <https://www.itu.int/en/ITU-D/Statistics/Documents/facts/FactsFigures2021.pdf>. [Accessed: June 4, 2025].
- [17] Zabih Ghassemlooy, Shlomi Arnon, Murat Uysal, Zhengyuan Xu, and Julian Cheng. Emerging optical wireless communications—advances and challenges. *IEEE journal on selected areas in communications*, 33(9):1738–1749, 2015.
- [18] Toshihiko Komine and Masao Nakagawa. Fundamental analysis for visible-light communication system using led lights. *IEEE transactions on Consumer Electronics*, 50(1):100–107, 2004.
- [19] Svilen Dimitrov and Harald Haas. *Principles of LED light communications: towards networked Li-Fi*. Cambridge University Press, 2015.

- [20] Zahra Nazari Chaleshtori, Zabih Ghassemlooy, Hossien B. Eldeeb, Murat Uysal, and Stanislav Zvanovec. Utilization of an OLED-based VLC system in office, corridor, and semi-open corridor environments. *Sensors*, 20(23), 2020.
- [21] Hossien B Eldeeb, Mohamed Al-Nahhal, Hossam AI Selmy, and Fathi E Abd El-Samie. Continuous phase modulation with chaotic interleaving for visible light communication systems based on orthogonal frequency division multiplexing. *Transactions on Emerging Telecommunications Technologies*, 31(10):e4100, 2020.
- [22] Lifang Feng, Rose Qingyang Hu, Jianping Wang, Peng Xu, and Yi Qian. Applying VLC in 5G networks: Architectures and key technologies. *IEEE Network*, 30(6):77–83, 2016.
- [23] Hossien B. Eldeeb, Hossam A. I. Selmy, Hany M. Elsayed, Ragia I. Badr, and Murat Uysal. Efficient resource allocation scheme for multi-user hybrid VLC/IR networks. In *2019 IEEE Photon. Conf. (IPC)*, pages 1–2, 2019.
- [24] Murat Uysal, Zabih Ghassemlooy, Abdelmoula Bekkali, Abdullah Kadri, and Hamid Menouar. Visible light communication for vehicular networking: Performance study of a V2V system using a measured headlamp beam pattern model. *IEEE Veh. Technol. Mag.*, 10(4):45–53, 2015.
- [25] David N Amanor, William W Edmonson, and Fatemeh Afghah. Intersatellite communication system based on visible light. *IEEE Transactions on Aerospace and Electronic Systems*, 54(6):2888–2899, 2018.
- [26] K Mahalakshmi, K Shantha Kumari, D Yuvaraj, R Keerthika, et al. Healthcare visible light communication. *International Journal of Pure and Applied Mathematics*, 118(11):345–348, 2018.
- [27] Mohammed Elamassie, Farshad Miramirkhani, and Murat Uysal. Performance characterization of underwater visible light communication. *IEEE Trans. Commun.*, 67(1):543–552, 2018.
- [28] Ishwar Ram Kumawat, Satyasai Jagannath Nanda, and Ravi Kumar Maddila. Positioning led panel for uniform illuminance in indoor vlc system using whale optimization. In *Optical and Wireless Technologies: Proceedings of OWT 2017*, pages 131–139. Springer, 2018.
- [29] Jupeng Ding, Zhitong Huang, and Yuefeng Ji. Evolutionary algorithm based power coverage optimization for visible light communications. *IEEE communications letters*, 16(4):439–441, 2012.

- [30] Lang Wang, Chunyue Wang, Xuefen Chi, Linlin Zhao, and Xiaoli Dong. Optimizing snr for indoor visible light communication via selecting communicating leds. *Optics communications*, 387:174–181, 2017.
- [31] Ram Sharma, A Charan Kumari, Mona Aggarwal, and Swaran Ahuja. Optimal led deployment for mobile indoor visible light communication system: Performance analysis. *AEU-International Journal of Electronics and Communications*, 83:427–432, 2018.
- [32] Irina Stefan and Harald Haas. Analysis of optimal placement of led arrays for visible light communication. In *2013 IEEE 77th Vehicular Technology Conference (VTC Spring)*, pages 1–5. IEEE, 2013.
- [33] Rui Guan, Jin-Yuan Wang, Yun-Peng Wen, Jun-Bo Wang, and Ming Chen. Pso-based led deployment optimization for visible light communications. In *2013 International Conference on Wireless Communications and Signal Processing*, pages 1–6. IEEE, 2013.
- [34] Ye Cai, Weipeng Guan, Yuxiang Wu, Canyu Xie, Yirong Chen, and Liangtao Fang. Indoor high precision three-dimensional positioning system based on visible light communication using particle swarm optimization. *IEEE Photonics Journal*, 9(6):1–20, 2017.
- [35] Geng Sun, Yanheng Liu, Ming Yang, Aimin Wang, Shuang Liang, and Ying Zhang. Coverage optimization of vlc in smart homes based on improved cuckoo search algorithm. *Computer Networks*, 116:63–78, 2017.
- [36] Jia Chaochuan, Yang Ting, Wang Chuanjiang, and Sun Mengli. High-accuracy 3d indoor visible light positioning method based on the improved adaptive cuckoo search algorithm. *Arabian Journal for Science and Engineering*, 47(2):2479–2498, 2022.
- [37] Xianmeng Meng, Chaochuan Jia, Cuicui Cai, Fugui He, and Qing Wang. Indoor high-precision 3d positioning system based on visible-light communication using improved whale optimization algorithm. In *Photonics*, volume 9, page 93. MDPI, 2022.
- [38] Shangsheng Wen, Xiaoge Cai, Weipeng Guan, Jiajia Jiang, Bangdong Chen, and Mouxiao Huang. High-precision indoor three-dimensional positioning system based on visible light communication using modified artificial fish swarm algorithm. *Optical Engineering*, 57(10):106102–106102, 2018.

- [39] Selma Yahia, Yassine Meraihi, Nesrine Sadeki, Mohamed Tellache, Sylia Mekhmoukh Taleb, Souad Refas, and Asma Benmessaoud Gabis. Manta ray foraging optimization algorithm for solving the leds placement problem in indoor vlc systems. In *2022 3rd International Conference on Human-Centric Smart Environments for Health and Well-being (IHSH)*, pages 43–48. IEEE, 2022.
- [40] Wesley Costa, Higor Camporez, Maria Pontes, Marcelo Segatto, Helder Rocha, Jair Silva, Malte Hinrichs, Anagnostis Paraskevopoulos, Volker Jungnickel, and Ronald Freund. Increasing the power and spectral efficiencies of an ofdm-based vlc system through multi-objective optimization. *J. Opt. Soc. Am. A*, 40(6):1268–1275, Jun 2023.
- [41] Abdelbaki Benayad, Amel Boustil, Yassine Meraihi, Seyedali Mirjalili, Selma Yahia, and Sylia Mekhmoukh Taleb. An enhanced whale optimization algorithm with opposition-based learning for leds placement in indoor vlc systems. In *Handbook of Whale Optimization Algorithm*, pages 279–289. Elsevier, 2024.
- [42] Abdelbaki Benayad, Amel Boustil, Yassine Meraihi, Selma Yahia, Sylia Mekhmoukh Taleb, Amylia Ait Saadi, and Amar Ramdane-Cherif. Solving the leds placement problem in indoor vlc system using a hybrid coronavirus herd immunity optimizer. *Journal of Optics*, pages 1–32, 2024.
- [43] Shinichiro Haruyama. Visible light communication using sustainable led lights. In *2013 Proceedings of ITU Kaleidoscope: Building Sustainable Communities*, pages 1–6. IEEE, 2013.
- [44] Harald Haas. High-speed wireless networking using visible light. *Spie Newsroom*, 1(1):1–3, 2013.
- [45] Gerard J Holzmann and William Slattery Lieberman. *Design and validation of computer protocols*, volume 512. Prentice hall Englewood Cliffs, 1991.
- [46] Yuichi Tanaka, Toshihiko Komine, Shinichiro Haruyama, and Masao Nakagawa. Indoor visible light data transmission system utilizing white led lights. *IEICE transactions on communications*, 86(8):2440–2454, 2003.
- [47] Don M Boroson, Bryan S Robinson, Dennis A Burianek, Daniel V Murphy, and Abhijit Biswas. Overview and status of the lunar laser communications demonstration. In *Free-Space Laser Communication Technologies XXIV*, volume 8246, pages 69–78. SPIE, 2012.
- [48] E Luzhanskiy, B Edwards, D Israel, D Cornwell, J Staren, N Cummings, T Roberts, and R Patschke. Overview and status of the laser communication relay demonstra-

- tion. In *Free-Space Laser Communication and Atmospheric Propagation XXVIII*, volume 9739, pages 100–113. SPIE, 2016.
- [49] Michael B Rahaim, Anna Maria Vegni, and Thomas DC Little. A hybrid radio frequency and broadcast visible light communication system. In *2011 IEEE GLOBECOM Workshops (GC Wkshps)*, pages 792–796. IEEE, 2011.
- [50] Dilukshan Karunatilaka, Fahad Zafar, Vineetha Kalavally, and Rajendran Parthiban. LED based indoor visible light communications: State of the art. *IEEE Communications Surveys & Tutorials*, 17(3):1649–1678, 2015.
- [51] Parth H Pathak, Xiaotao Feng, Pengfei Hu, and Prasant Mohapatra. Visible light communication, networking, and sensing: A survey, potential and challenges. *IEEE communications surveys & tutorials*, 17(4):2047–2077, 2015.
- [52] Kaiyun Cui, Gang Chen, Zhengyuan Xu, and Richard D Roberts. Traffic light to vehicle visible light communication channel characterization. *Appl. Opt.*, 51(27):6594–6605, 2012.
- [53] Carlos Medina, Mayteé Zambrano, and Kiara Navarro. Led based visible light communication: Technology, applications and challenges-a survey. *International Journal of Advances in Engineering & Technology*, 8(4):482, 2015.
- [54] Shlomi Arnon. *Visible light communication*. Cambridge University Press, 2015.
- [55] Richard D Roberts, Sridhar Rajagopal, and Sang-Kyu Lim. Ieee 802.15. 7 physical layer summary. In *2011 IEEE GLOBECOM Workshops (GC Wkshps)*, pages 772–776. IEEE, 2011.
- [56] Stefan Schmid, Theodoros Bourchas, Stefan Mangold, and Thomas R Gross. Linux light bulbs: Enabling internet protocol connectivity for light bulb networks. In *Proceedings of the 2nd International Workshop on Visible Light Communications Systems*, pages 3–8, 2015.
- [57] Hany Elgala, Raed Mesleh, and Harald Haas. Indoor optical wireless communication: potential and state-of-the-art. *IEEE Communications magazine*, 49(9):56–62, 2011.
- [58] Adriano JC Moreira, Rui T Valadas, and AM de Oliveira Duarte. Optical interference produced by artificial light. *Wireless Networks*, 3:131–140, 1997.
- [59] Aleksandar Jovicic, Junyi Li, and Tom Richardson. Visible light communication: opportunities, challenges and the path to market. *IEEE communications magazine*, 51(12):26–32, 2013.

- [60] Liqun Li, Pan Hu, Chunyi Peng, Guobin Shen, and Feng Zhao. Epsilon: A visible light based positioning system. In *11th USENIX Symposium on Networked Systems Design and Implementation (NSDI 14)*, pages 331–343, 2014.
- [61] Hongjia Wu, Qing Wang, Jie Xiong, and Marco Zuniga. Smartvlc: When smart lighting meets vlc. In *Proceedings of the 13th International Conference on emerging Networking Experiments and Technologies*, pages 212–223, 2017.
- [62] Deok-Rae Kim, Se-Hoon Yang, Hyun-Seung Kim, Yong-Hwan Son, and Sang-Kook Han. Outdoor visible light communication for inter-vehicle communication using controller area network. In *2012 Fourth International Conference on Communications and Electronics (ICCE)*, pages 31–34. IEEE, 2012.
- [63] Fernando Peres and Mauro Castelli. Combinatorial optimization problems and metaheuristics: Review, challenges, design, and development. *Applied Sciences*, 11(14):6449, 2021.
- [64] Alexander EI Brownlee, John R Woodward, and Jerry Swan. Metaheuristic design pattern: surrogate fitness functions. In *Proceedings of the Companion Publication of the 2015 Annual Conference on Genetic and Evolutionary Computation*, pages 1261–1264, 2015.
- [65] Dragan Savic. Single-objective vs. multiobjective optimisation for integrated decision support. 2002.
- [66] Carlos A Coello Coello. *Evolutionary algorithms for solving multi-objective problems*. Springer, 2007.
- [67] Gilles Brassard and Paul Bratley. *Algorithmics: theory & practice*. Prentice-Hall, Inc., 1988.
- [68] E David. Goldberg/1989/genetic algorithm in search, optimization and machine learning.
- [69] Alan R Parkinson, R Balling, and John D Hedengren. Optimization methods for engineering design. *Brigham Young University*, 5(11), 2013.
- [70] Seyedeh Zahra Mirjalili, Seyedali Mirjalili, Shahrzad Saremi, Hossam Faris, and Ibrahim Aljarah. Grasshopper optimization algorithm for multi-objective optimization problems. *Applied Intelligence*, 48:805–820, 2018.
- [71] Ali Asghar Heidari, Seyedali Mirjalili, Hossam Faris, Ibrahim Aljarah, Majdi Mafarja, and Huiling Chen. Harris hawks optimization: Algorithm and applications. *Future generation computer systems*, 97:849–872, 2019.

- [72] Xin-She Yang. *Nature-inspired optimization algorithms*. Academic Press, 2020.
- [73] Yassine Meraihi, Asma Benmessaoud Gabis, Seyedali Mirjalili, and Amar Ramdane-Cherif. Grasshopper optimization algorithm: theory, variants, and applications. *IEEE Access*, 9:50001–50024, 2021.
- [74] Giorgio Chiandussi, Marco Codegone, Simone Ferrero, and Federico Erminio Varese. Comparison of multi-objective optimization methodologies for engineering applications. *Computers & Mathematics with Applications*, 63(5):912–942, 2012.
- [75] Chantal Baril, Soumaya Yacout, and Bernard Clément. Design for six sigma through collaborative multiobjective optimization. *Computers & Industrial Engineering*, 60(1):43–55, 2011.
- [76] José Henrique de Freitas GOMES. Método dos polinômios canônicos e misturas para otimização multi-objetivo. 2013.
- [77] Singiresu S Rao. *Engineering optimization: theory and practice*. John Wiley & Sons, 2019.
- [78] Indraneel Das and John E Dennis. Normal-boundary intersection: A new method for generating the pareto surface in nonlinear multicriteria optimization problems. *SIAM journal on optimization*, 8(3):631–657, 1998.
- [79] Olusegun Olorunda and Andries P Engelbrecht. Measuring exploration/exploitation in particle swarms using swarm diversity. In *2008 IEEE congress on evolutionary computation (IEEE world congress on computational intelligence)*, pages 1128–1134. IEEE, 2008.
- [80] Jared L Cohon and David H Marks. A review and evaluation of multiobjective programming techniques. *Water resources research*, 11(2):208–220, 1975.
- [81] Lothar Thiele, Kaisa Miettinen, Pekka J Korhonen, and Julian Molina. A preference-based evolutionary algorithm for multi-objective optimization. *Evolutionary computation*, 17(3):411–436, 2009.
- [82] Achille Messac and Christopher A Mattson. Generating well-distributed sets of pareto points for engineering design using physical programming. *Optimization and Engineering*, 3:431–450, 2002.
- [83] R Venkata Rao, Dhiraj P Rai, and Joze Balic. Multi-objective optimization of machining and micro-machining processes using non-dominated sorting teaching-learning-based optimization algorithm. *Journal of Intelligent Manufacturing*, 29:1715–1737, 2018.

- [84] Lucien Duckstein. Multiobjective optimization in structural design- the model choice problem. *New directions in optimum structural design(A 85-48701 24-39)*. Chichester, England and New York, Wiley-Interscience, 1984,, pages 459–481, 1984.
- [85] Andrzej Osyczka. An approach to multicriterion optimization problems for engineering design. *Computer Methods in Applied Mechanics and Engineering*, 15(3):309–333, 1978.
- [86] John Von Neumann and Oscar Morgenstern. Theory of games and economic behaviour princeton univ. Press, Princeton, page 44, 1944.
- [87] Raphael Benayoun, Bernard Roy, and Barry Sussman. Electre: Une méthode pour guider le choix en présence de points de vue multiples. *Note de travail*, 49:2–120, 1966.
- [88] Jean-Pierre Brans, Ph Vincke, and Bertrand Mareschal. How to select and how to rank projects: The promethee method. *European journal of operational research*, 24(2):228–238, 1986.
- [89] Carlos M Fonseca, Peter J Fleming, et al. Genetic algorithms for multiobjective optimization: formulationdiscussion and generalization. In *Icga*, volume 93, pages 416–423. Citeseer, 1993.
- [90] Yaochu Jin and Bernhard Sendhoff. Incorporation of fuzzy preferences into evolutionary multiobjective optimization. In *GECCO*, volume 2, page 683, 2002.
- [91] Seyedali Mirjalili, Pradeep Jangir, and Shahrzad Saremi. Multi-objective ant lion optimizer: a multi-objective optimization algorithm for solving engineering problems. *Applied Intelligence*, 46:79–95, 2017.
- [92] Yacov Haimes. On a bicriterion formulation of the problems of integrated system identification and system optimization. *IEEE transactions on systems, man, and cybernetics*, (3):296–297, 1971.
- [93] Ching-Lai Hwang, Kwangsun Yoon, Ching-Lai Hwang, and Kwangsun Yoon. Methods for multiple attribute decision making. *Multiple attribute decision making: methods and applications a state-of-the-art survey*, pages 58–191, 1981.
- [94] Kalyanmoy Deb, Amrit Pratap, Sameer Agarwal, and TAMT Meyarivan. A fast and elitist multiobjective genetic algorithm: Nsga-ii. *IEEE transactions on evolutionary computation*, 6(2):182–197, 2002.
- [95] J David Schaffer. Multiple objective optimization with vector evaluated genetic algorithms. In *Proceedings of the first international conference on genetic algorithms and their applications*, pages 93–100. Psychology Press, 2014.

- [96] Sanaz Mostaghim and Jürgen Teich. Strategies for finding good local guides in multi-objective particle swarm optimization (mopso). In *Proceedings of the 2003 IEEE Swarm Intelligence Symposium. SIS'03 (Cat. No. 03EX706)*, pages 26–33. IEEE, 2003.
- [97] Carlos E Mariano and Eduardo M Morales. Moaq an ant-q algorithm for multiple objective optimization problems. In *Proceedings of the 1st Annual Conference on Genetic and Evolutionary Computation-Volume 1*, pages 894–901, 1999.
- [98] Gaurav Dhiman, Krishna Kant Singh, Mukesh Soni, Atulya Nagar, Mohammad Dehghani, Adam Slowik, Amandeep Kaur, Ashutosh Sharma, Essam H Houssein, and Korhan Cengiz. Mosoa: A new multi-objective seagull optimization algorithm. *Expert Systems with Applications*, 167:114150, 2021.
- [99] Paolo Serafini. Simulated annealing for multi objective optimization problems. In *Multiple Criteria Decision Making: Proceedings of the Tenth International Conference: Expand and Enrich the Domains of Thinking and Application*, pages 283–292. Springer, 1994.
- [100] Xavier Gandibleux, Nazik Mezdaoui, and Arnaud Fréville. A tabu search procedure to solve multiobjective combinatorial optimization problems. In *Advances in Multiple Objective and Goal Programming: Proceedings of the Second International Conference on Multi-Objective Programming and Goal Programming, Torremolinos, Spain, May 16–18, 1996*, pages 291–300. Springer, 1997.
- [101] Carlos A Coello Coello and Nareli Cruz Cortés. Solving multiobjective optimization problems using an artificial immune system. *Genetic programming and evolvable machines*, 6:163–190, 2005.
- [102] João Luiz Junho Pereira, Guilherme Antônio Oliver, Matheus Brendon Francisco, Sebastiao Simoes Cunha Jr, and Guilherme Ferreira Gomes. A review of multi-objective optimization: methods and algorithms in mechanical engineering problems. *Archives of Computational Methods in Engineering*, 29(4):2285–2308, 2022.
- [103] Mohamed A Tawhid and Vimal Savsani. Multi-objective sine-cosine algorithm (mosca) for multi-objective engineering design problems. *Neural Computing and Applications*, 31:915–929, 2019.
- [104] Yassine Meraihi, Dalila Acheli, and Amar Ramdane-Cherif. Qos multicast routing for wireless mesh network based on a modified binary bat algorithm. *Neural Computing and Applications*, 31(7):3057–3073, 2019.
- [105] Shahrzad Saremi, Seyedali Mirjalili, and Andrew Lewis. Biogeography-based optimisation with chaos. *Neural Computing and Applications*, 25:1077–1097, 2014.

- [106] Hamid R Tizhoosh. Opposition-based learning: a new scheme for machine intelligence. In *International conference on computational intelligence for modelling, control and automation and international conference on intelligent agents, web technologies and internet commerce (CIMCA-IAWTIC'06)*, volume 1, pages 695–701. IEEE, 2005.
- [107] Selma Yahia, Yassine Meraihi, Amar Ramdane-Cherif, Asma Benmessaoud Gabis, Dalila Acheli, and Hongyu Guan. A survey of channel modeling techniques for visible light communications. *Journal of Network and Computer Applications*, 194:103206, 2021.
- [108] Selma Yahia, Yassine Meraihi, Amar Ramdane-Cherif, Asma Benmessaoud Gabis, and Hossien B Eldeeb. Performance evaluation of vehicular visible light communication based on angle-oriented receiver. *Computer Communications*, 191:500–509, 2022.
- [109] Seyedali Mirjalili and Andrew Lewis. The whale optimization algorithm. *Advances in engineering software*, 95:51–67, 2016.
- [110] Gaganpreet Kaur and Sankalop Arora. Chaotic whale optimization algorithm. *Journal of Computational Design and Engineering*, 5(3):275–284, 2018.
- [111] Mohammed Azmi Al-Betar, Zaid Abdi Alkareem Alyasseri, Mohammed A Awadallah, and Iyad Abu Doush. Coronavirus herd immunity optimizer (chio). *Neural Computing and Applications*, 33(10):5011–5042, 2021.
- [112] Amir H Gandomi, X-S Yang, Siamak Talatahari, and Amir Hossein Alavi. Firefly algorithm with chaos. *Communications in Nonlinear Science and Numerical Simulation*, 18(1):89–98, 2013.
- [113] Xin-She Yang and Xingshi He. Firefly algorithm: recent advances and applications. *International journal of swarm intelligence*, 1(1):36–50, 2013.
- [114] Yassine Meraihi, Dalila Acheli, and Amar Ramdane-Cherif. Qos multicast routing for wireless mesh network based on a modified binary bat algorithm. *Neural Computing and Applications*, 31(7):3057–3073, 2019.
- [115] Hamid R Tizhoosh. Opposition-based learning: a new scheme for machine intelligence. In *International conference on computational intelligence for modelling, control and automation and international conference on intelligent agents, web technologies and internet commerce (CIMCA-IAWTIC'06)*, volume 1, pages 695–701. IEEE, 2005.

- [116] J Ajith, Satyasai Jagannath Nanda, and Ravi Kumar Maddila. A multi-objective natural aggregation algorithm for optimizing user allocation matrix in visible light communication. *Optik*, 267:169692, 2022.
- [117] Bo Fan, Hui Tian, and Shufei Liang. Energy efficient illumination optimization for indoor visible light communication. In *2016 19th International Symposium on Wireless Personal Multimedia Communications (WPMC)*, pages 183–187. IEEE, 2016.
- [118] Trong-Hop Do and Myungsik Yoo. Optimization for link quality and power consumption of visible light communication system. *Photonic Network Communications*, 27:99–105, 2014.
- [119] Lingling Liu, Aimin Wang, Jing Wu, Jiao Lu, Jiahui Li, and Geng Sun. Secure and energy-efficient unmanned aerial vehicle-enabled visible light communication via a multi-objective optimization approach. *arXiv preprint arXiv:2403.15410*, 2024.
- [120] Julian Solis, Pablo Palacios Játiva, Cesar A Azurdia Meza, Francisco Castillo Soria, Carlos Gutiérrez, Shaharyar Kamal, and Alberto Castro. Spatial multiplexing mimo underground mining visible light communication optimization using multi-objective particle swarm optimization. In *2023 IEEE CHILEAN Conference on Electrical, Electronics Engineering, Information and Communication Technologies (CHILECON)*, pages 1–6. IEEE, 2023.
- [121] David N Amanor, William W Edmonson, and Fatemeh Afghah. Link performance improvement via design variables optimization in led-based vlc system for inter-satellite communication. In *2017 IEEE International Conference on Wireless for Space and Extreme Environments (WiSEE)*, pages 7–12. IEEE, 2017.